INTERNAL STRATIGRAPHY, COMPOSITION, AND DEPOSITIONAL SETTING OF THE WOODFORD SHALE IN SOUTHERN SEMINOLE COUNTY, OKLAHOMA

By

BRITNI PAIGE WATSON

Bachelor of Science in Geology

Oklahoma State University

Stillwater, Oklahoma

2005

Submitted to the Faculty of the
Graduate College of the
Oklahoma State University
in partial fulfillment of
the requirements for
the Degree of
MASTER OF SCIENCE
December, 2008

INTERNAL STRATIGRAPHY, COMPOSITION, AND DEPOSITIONAL SETTING OF THE WOODFORD SHALE IN SOUTHERN SEMINOLE COUNTY, OKLAHOMA

Thesis Approved:

Dr. Jim Puckette

Thesis Adviser

Dr. Alex Simms

Dr. Anna Cruse

Dr. A. Gordon Emslie

Dean of the Graduate College

ACKNOWLEDGMENTS

I would like to express my gratitude to the faculty of the Boone Pickens School of Geology; in particular to my thesis adviser, Dr. Jim Puckette, for the time and energy he spent on this project. I would also like to thank the other members of my committee, Dr. Alex Simms and Dr. Anna Cruse, for their time and suggestions. I am also very grateful to Devon Energy Corporation for the generous fellowship awarded to me during my graduate studies.

I am extremely appreciative of Chesapeake Energy Corporation. Not only did they provide me with all of the data and resources for this project, they also afforded me an internship, which gave me the opportunity to learn a great deal about the industry. I would like to thank the entire Arkoma Oklahoma team for their technical help and encouragement. In particular, I am thankful to my mentor, Ken Rechlin, who provided me with ideas, guidance, and support throughout the process. I would also like to express my appreciation to Rick Urash and others at the Reservoir Technology Center (RTC).

I am so grateful for my Mom and Dad who have always had high expectations for me to live up to. Thank you for always supporting me even though there were many detours along the way.

To my husband, Rob, thank you so much for helping me keep it all in perspective. At times, I was beyond overwhelmed; your support and encouragement got me through it.

TABLE OF CONTENTS

Chapter **Page**

LIST OF TABLES

Table **Page**

LIST OF FIGURES

Figure **Page**

LIST OF PLATES

Plate

CHAPTER I

INTRODUCTION

Preface

The rising cost of energy and the increased demand for oil and gas has facilitated the petroleum industry's search for fossil fuels in unlikely places. Increased exploration and development of unconventional shale-gas reservoirs is a growing trend (King, 1993). The Barnett Shale of the Ft. Worth Basin of Texas, Fayetteville Shale in Arkansas, and the Woodford Shale in the Arkoma Basin of Oklahoma are three important shale-gas reservoirs in the central U.S. However, shale production is not limited to gas. A shale-oil play in the Bakken Shale of the Williston Basin in North Dakota and Montana has recently commanded much attention. This thesis will examine the detrital and authigenic composition of the Woodford Shale in southern Seminole County, Oklahoma. Composition, in particular silica content, is believed to be a major influence on reservoir properties and oil and gas production from shale. The results of the study will be used to help evaluate the potential for oil production from the Woodford Shale within the study area. This study will use a host of scientific data including (but not limited to): core, wire-line log signatures, spectral gamma-ray curves, total organic carbon measurements, and thin-section, x-ray diffraction, and scanning electron microscope analyses to determine lithology and rock constituents.

Woodford Shale composition and productivity have not been examined in Seminole County due to its location outside the Woodford gas play in the Arkoma Basin. Previous work on shale gas plays has demonstrated that understanding the role lithologic heterogeneity and composition plays in influencing production is essential for reservoir characterization (Bohacs and Lazar, 2008; Bustin et al., 2008). An in-depth examination of the Woodford in the study area will lead to a better understanding of the shale's internal litho-stratigraphy and rock properties. The relative amounts of silica-rich minerals or other brittle materials such as calcite are believed to have a significant effect on shale productivity (Fertl and Chilingarian, 1989). If the Woodford Shale in Seminole County is siliceous, brittle, and prone to fracturing, it could produce oil and gas in commercial volumes. This information will undoubtedly be beneficial for both those in the energy industry and those in academia whose interests include the origin and oil and gas productivity of shales and other unconventional reservoirs.

Location of Study Area

The name Woodford Shale is applied to Mississippian-Devonian dark shales in parts of Oklahoma and Texas. Equivalent age shales are recognized across the continental U.S. and include the Antrim, Bakken, Chattanooga, New Albany, Noel, and Ohio Shales. This study focuses on four townships in southern Seminole County, Oklahoma (Figure 1). In these townships (T.6N., R.6E.; T.6N., R.7E.; T.7N., R.6E.; and T.7N., R.7E.), the Woodford occurs at depths ranging from 2,700' to 4,700' measured depth (MD) (1,750'-3,800' subsea (SS)) with depths between 3,500' and 4,500' MD (2,000-3,000'SS) being more common. The Woodford Shale is greater than 150 feet thick in roughly 97% of the study area. In some locations, thicknesses of over 300 feet were penetrated by vertical wells. The area of study was chosen for data availability including core, wire-line logs, and seismic lines.

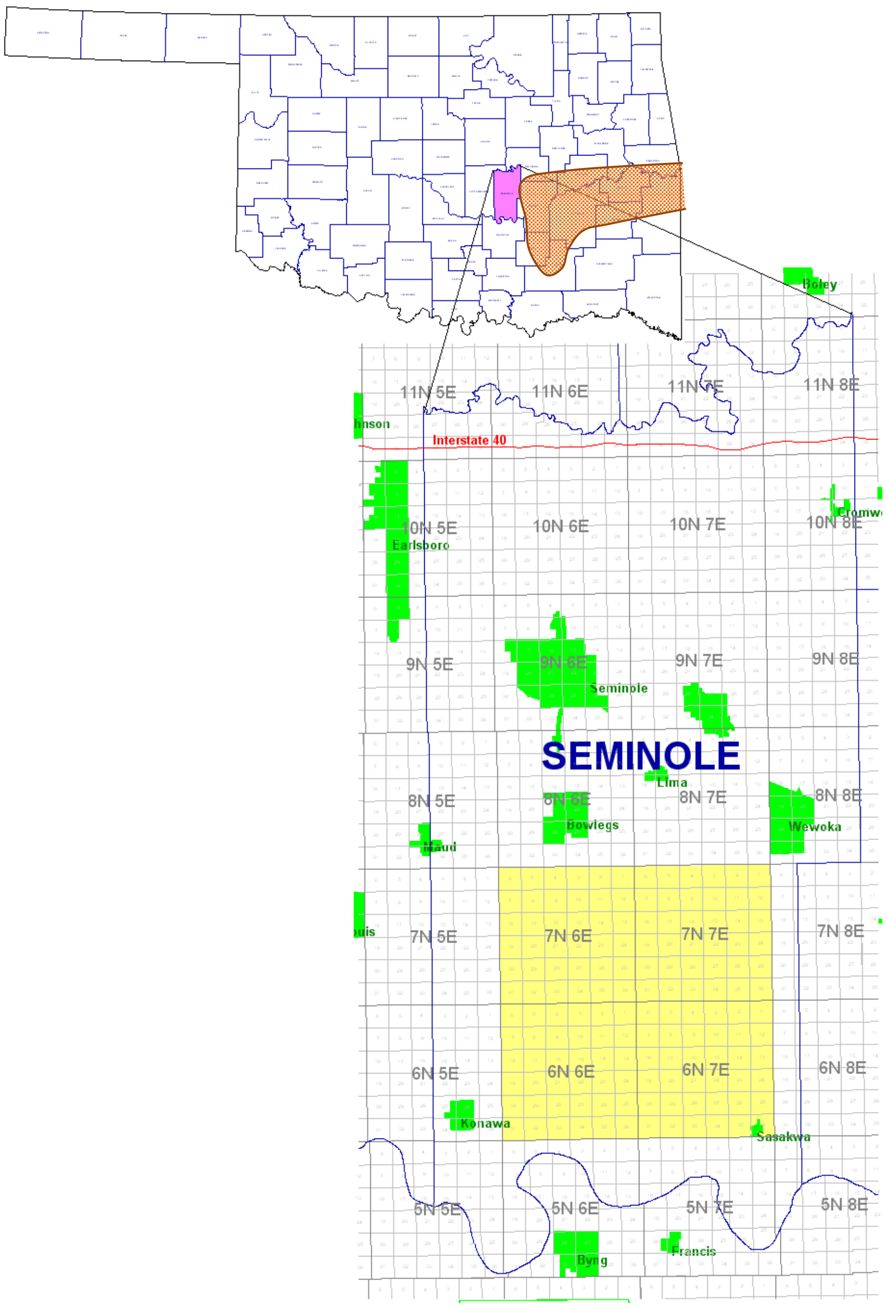

Figure 1. Study area shown in yellow, southern Seminole County, Oklahoma; nearby towns shown in green; general location of Arkoma Basin shown in orange

Overview of Woodford Shale Gas Play

In recent years, the oil and gas industry has devoted considerable economic resources to develop shales as unconventional gas reservoirs. The Woodford Shale gas play expanded greatly in 2004 with 24 wells being drilled in the Arkoma Basin of eastern Oklahoma and adjacent areas (T.12N., R.4E. to T.4S., R.27E.) (Figure 1). For the twenty years prior to 2004, only five Woodford-producing wells were drilled. Between January 2004 and August 2007, 282 Woodford-producing wells were drilled. Total production of oil and gas from these wells is 80.4 billion cubic feet equivalent (BCFE); 12.7 BCFE from wells with commingled production and 67.7 BCFE from Woodford only completions (IHS, 2007). The heart of the Woodford Shale gas play is in the Arkoma Basin in Hughes, Coal, and Pittsburg counties (Figures 1 and 2).

Of the nearly 500 Woodford-producing wells drilled in the Arkoma Basin and adjacent areas (T.12N., R.4E. to T.4S., R.27E.), roughly 200 are horizontal (IHS, 2007). Horizontal drilling has increased in popularity as a means of producing gas from shale reservoirs. This method of drilling increases the surface area of the well-bore exposed to the reservoir, thereby improving productivity. Two advantages of horizontal wells are increased production rate and a larger drainage area (Joshi, 1991). Zones in shale that are rich in silica or chert are postulated to be more favorable for production as they contain more natural fractures than clay-rich zones (Fertl and Chilingarian, 1989). Fractures are hydraulically induced during completion to provide pathways for hydrocarbon migration from the rock to the well-bore. Whereas cost is 2-3 times greater for a horizontal well than a vertical one, the increase in production and return on investment are typically significantly greater (King, 1993).

In addition to the Woodford Shale gas play, the potential exists for a Woodford Shale oil play in southern Seminole County. In this area, vertical wells that were completed in the Woodford Shale produced both gas and oil. Thermal maturation studies by Cardott (2001) indicate that vitrinite reflectance values for the Woodford in this area are within the oil window (Figure 2). The Adams Petroleum Swashbuckler #1, a vertical well in Section 7, T.6N., R.8E., was perforated and fracture-stimulated in a 7 feet thick interval in the Woodford Shale and produced over 33,000 barrels of oil between April 1979 and December 2006. It is possible for horizontal drilling technology to result in a 3 to 7 fold increase in production over vertical wells (King, 1993). That said, an oil play in the Woodford Shale could be viable and economically attractive at today's oil prices if horizontal drilling is successful.

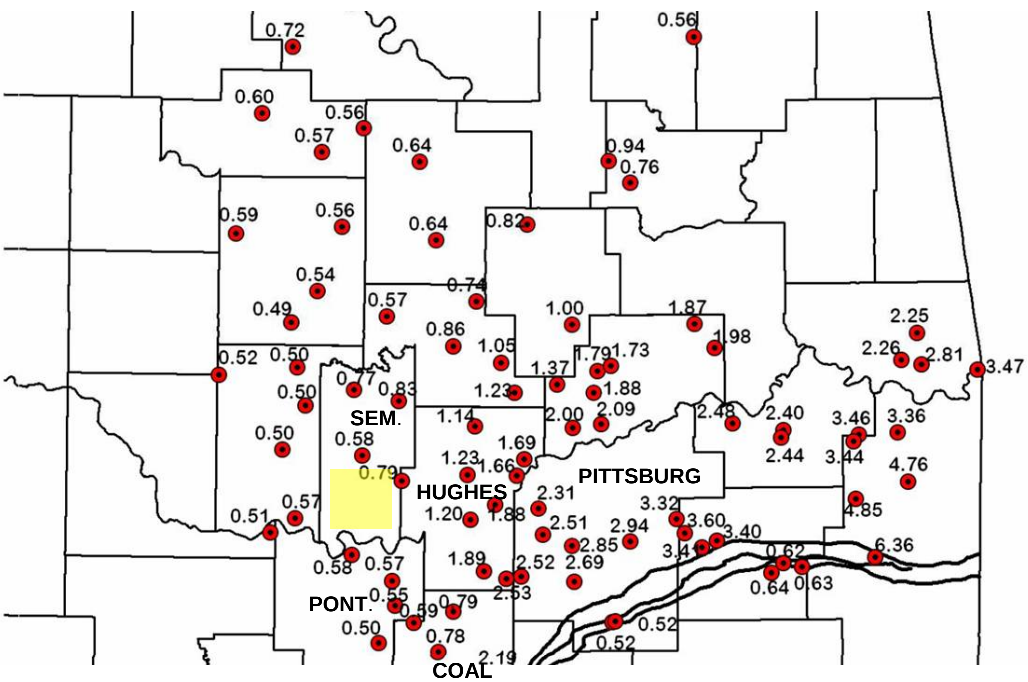

Figure 2. Vitrinite Reflectance (VRo) values for the Woodford Shale from east-central Oklahoma (after Cardott, 2007). The study area is highlighted in yellow.

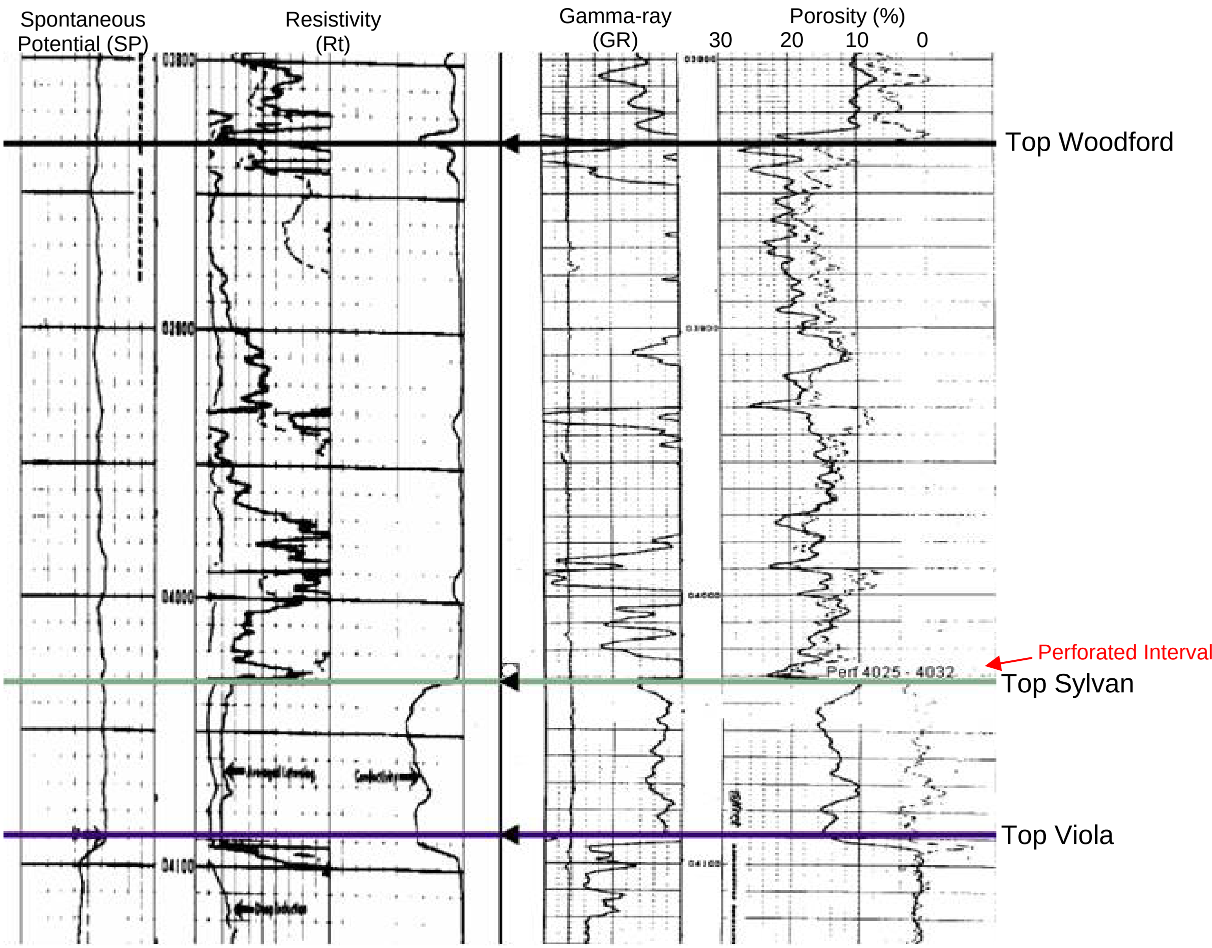

Figure 3. Portion of Adams Petroleum, Swashbuckler #1 well-log showing the wire-line log signature across the Woodford Shale, Sylvan Shale, and upper part of the Viola Group. The reported perforated interval in the base of the Woodford Shale is indicated by the red arrow.

Objective

Two basic questions were considered: 1) What does the informal internal electro-stratigraphy utilized by the petroleum industry represent? and 2) What was the depositional setting of the Woodford Shale in southern Seminole County? In an attempt to answer these questions, two hypotheses were developed: 1) distinct wire-line log signatures of the Woodford Shale are the result of compositional heterogeneity, and 2) the Woodford Shale lithofacies in Seminole County are the result of deposition in a mid-shelf setting. This setting is located between the proposed inner shelf setting in the

Ozarks (Noel Shale) and the distal shelf/slope of the Arbuckle Region (Puckette et al., 2008).

The purpose of this study is to develop a better understanding of the origin and nature of compositional heterogeneities within the Woodford Shale. Integrating core, petrophysical, wire-line log, and seismic data will facilitate characterization of the Woodford Shale and improve the understanding of its potential for oil and gas production.

Core analysis will allow the determination of lithology and improve our interpretation of depositional and diagenetic processes. Examination of thin sections will confirm micro-fabrics, cements, and fracturing. X-ray diffraction data will yield weight percent of constituents. Scanning electron microscopy is used to characterize and describe detrital and authigenic constituents. Spectral gamma-ray curves will provide data concerning depositional rates and bottom-water or pore geochemistry.

Normal faults are common in the study area and may present problems in the drilling and completion of shale wells. A database of over 675 wire-line logs was used to create thickness maps of Woodford Shale, Hunton Group, and Sylvan Shale in the study area. In addition, the Woodford Shale was subdivided into four electrofacies, for which thickness maps were also created. A Viola Group structure map was also created using wire-line logs to identify faults and define structural grain. To confirm the structural interpretation, which was determined by mapping, a loose 2-D seismic grid was used.

Stratigraphy

J.A. Taff (1904) introduced the name Woodford Chert for outcrops near the town of Woodford in Carter County, Oklahoma. The Woodford Shale is cherty in many locations including along I-35 in the Arbuckle Mountains, on the Tishomingo Uplift and in the subsurface of the Arkoma Basin. The stratigraphy of the study area is shown in Figure 4. The Woodford is a Late Devonian-Early Mississippian siliceous black shale, which records a transition from primarily carbonate deposition in the early Paleozoic to predominately clastic deposition in the late Paleozoic (Ham and Wilson, 1967). The majority of the Woodford is Famennian; the formation contains the Frasnian-Famennian extinction (Over, 1992). However, the uppermost portion is early Mississippian (Tournaisian/Kinderhookian) (Cardott, 2007). The Woodford Formation is composed of the Woodford Shale and often contains a basal sandstone, the Misener Sandstone. Where present, the Misener Sandstone is typically less than 10 feet thick (Lambert, 1993). Typically, the Woodford Formation unconformably overlies the Ordovician-Devonian carbonates of the Hunton Group. Where the Hunton Group is absent, the Woodford Formation unconformably overlies the Sylvan Shale or, in rare occurrences, the Viola Group. In the study area, the Woodford Shale is overlain by the Mississippian Caney Shale, which includes the basal, silty Mayes Formation (Maughan, 2006). In a majority (~90%) of the study area, the Hunton Group is less than 25 feet thick or absent altogether, and the Woodford Shale rests on the Sylvan Shale. In a few wells (~1%), the Woodford Shale directly overlies the Viola Group.

The distinct wire-line log signature of the Woodford Shale allows it to be typically divided into three informal members: upper, middle and lower. These are distinguished based on geochemistry as well as log signature (Cardott, 2007). The lower and middle members show higher gamma-ray intensity and higher resistivity. The upper member has lower gamma ray counts, lower resistivity, and consists of interbedded chert layers (Krystyniak, 2005). This thesis will not focus on separating the three members as has been done in the past (Hester, 1988; Lambert, 1993; Blackford, 2007). For the purpose of this study, the Woodford is divided into four subunits recognized in electric logs, which can be correlated to changes in core.

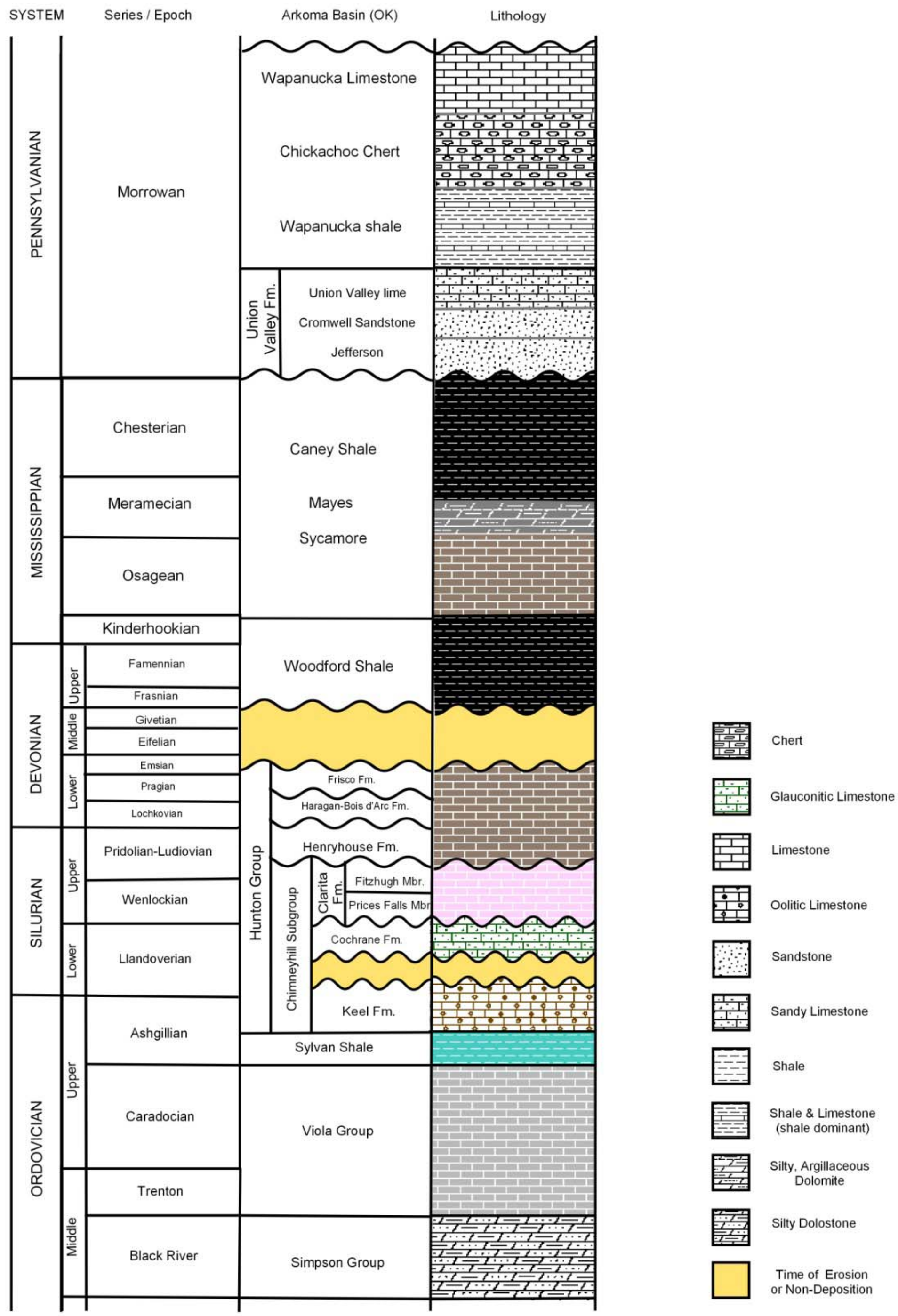

Figure 4. Stratigraphic Column of Middle Ordovician through Lower Pennsylvanian Strata in Central and Southern Oklahoma after Johnson (1988), Amsden (1989) and Rechlin (2003)

Methodology

Two cores were described and analyzed at the Chesapeake Energy Corporation Reservoir Technology Center (RTC) in Oklahoma City. The cored wells are the Ingram Exploration, Circle Creek #1 and the Chesapeake, Nancy 1-17H, located in Section 13, T.6N., R.6E. and Section 17, T.10N., R.5E., respectively. The Circle Creek #1 is located within the four township study area, whereas the Nancy 1-17H is located about twenty-five miles northwest in Pottawatomie County. Since it is located outside the study area, the Nancy 1-17H is discussed in less detail.

Spectral gamma-ray data, total organic carbon (TOC) data, thin sections, X-ray diffraction (XRD) data, scanning electron microscope (SEM) images, and a tight rock analysis (TRA) provided by Chesapeake Energy were used as methods of investigation. The TRA provides such petrophysical characteristics as: bulk density, grain density, porosity, effective porosity, fluid saturation, permeability and total organic carbon. Due to the proprietary nature of data acquisition used for the tight rock analysis, methods are not discussed in detail.

The XRD data were gathered using a Bruker D4 X-ray diffraction system, which allowed the determination of bulk mineralogy, relative clay abundance, and expandability of clay species. To prepare the samples, a small portion of each sample (~1.6 g) was mixed with 1.0-µm corundum (Al_2O_3) in the ratio 80% sample to 20% corundum by weight. Each sample was then ground under acetone in a McCrone Micronizing mill for approximately ten minutes. The samples produced were an average of 5µm in size, in order to ensure adequate particle statistics. Mineral abundances were determined using FULLPAT, a quantitative X-ray powder diffraction (QXRD) program.

The SEM data, obtained with a Jeol JSM-6390 LV scanning electron microscope, were used to determine matrix composition and texture, porosity types, pore shape and size, and nature of the organic component. Samples were cut using a Buelher Isomet saw and then prepared using an argon-ion polishing technique.

Thin-section analysis was completed for the Circle Creek #1 core to determine rock fabric, rock texture, general composition, cement types, and fossil identification. Thirteen thin sections were analyzed and photographed with a Zeiss AxioCam MRc5 camera and AxioVision Rel 4.6 software using 10X objective. Detailed images, photographed with an increased magnification of 20X, were also taken for seven of these thin sections.

Total and spectral gamma-ray curves were analyzed across the Woodford Shale in the two cored wells. Uranium/Thorium ratios were compared to lithology and the total API gamma-ray signature. This data was obtained using a spectral core gamma logger which collected data at approximately one inch intervals. Readings are listed at six inch intervals for each core.

Total Organic Carbon data was obtained for both the Circle Creek #1 and the Nancy 1-17H using a LECO carbon/sulfur analyzer. Carbonate was dissolved out of the sample using 5% hydrochloric acid (HCl) and then put into the analyzer, which heated the sample and measured the amount of carbon dioxide (CO_2) released. This method assumes that once carbonates are gone, the only source of carbon is organic material.

A color annotated depth-correlated chart with XRD and lithology was constructed for the Circle Creek #1 core. This chart contains the description of the lithology, color, sedimentary structures, and comments (Plate 1). A second chart combines lithology and

TRA data (Plate 2). Chert index and fracture intensity graphs were also created after chert layers and fractures were measured and counted in both cores (Plate 5). Similar charts (Plates 3 and 4) were created for the Nancy 1-17H core. Detailed lithologies are not known as thin sections are not yet available for the Nancy 1-17H core; however, general lithologies are discussed later in the petrographic analysis chapter.

Based on the petrophysical characteristics of the two cores, as well as data from outcrop investigations and cores in other areas, a depositional model was created for the Woodford Shale in Seminole County.

Subsurface structure and thickness maps were constructed utilizing wire-line log and 2-D seismic data available. A structure map of the top of the Viola Limestone (Plate 6) was created by picking tops in Geographix X-Section, then gridding and contouring the sub-sea (SS) depth values in GeoAtlas using a minimum curvature algorithm. Fault location and interpretation were aided by over thirty 2-D seismic lines, spanning 121 line miles. Post-Hunton erosion removed the Hunton Group in some areas, which limits the usefulness of the unit as a marker horizon for structural mapping. For seismic mapping, the Viola Group carbonates were the chosen horizon as the Woodford Shale reflector has a weak contrast with the overlying Caney Shale and is not a consistent, recognizable reflector. The Viola Group reflector is easily picked since it shows up as a sharp contrast from surrounding horizons. Along this reflector, abrupt fault terminations are evident.

Thickness maps created for the Woodford Shale and Hunton Group (Plate 7) are based on data from approximately 675 vertical wells in the study area and adjacent sections. Litho-stratigraphic unit tops were selected based on log signature and thicknesses were calculated for each formation using Geographix X-Section software. In addition, the Woodford Shale was divided into four subunits and tops were picked for a subset of 535 wells. Thickness values were posted for each unit of interest on the maps, which were then printed and contoured by hand. After hand contouring, the maps were digitized. Thickness maps for each of the four subunits are available in Plate 8.

CHAPTER II

PREVIOUS INVESTIGATIONS

Historically, the Woodford Shale has been of great interest; studied initially for its role as a source rock and more recently for its reservoir potential.

The Woodford Shale is a Late Devonian-Early Mississippian siliceous black shale. Woodford sediments accumulated in a shallow to deep, sometimes euxinic, epicontinental sea on the southern margin of the North American craton (Roberts and Mitterer, 1992). Deeper portions of the sea were in the position of the former Southern Oklahoma Aulacogen. The stratified nature of the Woodford Sea was favorable for accumulation and preservation of large amounts of organic carbon (Comer, 2008). The Woodford Shale serves as an important source rock in the southern Mid-continent of the U.S. and is stratigraphically equivalent to the Antrim, Bakken, Chattanooga, New Albany, Noel, and Ohio shales (Cardott and Lambert, 1985). Together, these shales indicate the presence of widespread anoxic conditions over the North American craton during the Late Devonian and Early Mississippian.

Roberts and Mitterer (1992) discuss the bedded chert cyclicity in the Woodford, hypothesizing that the cherty beds were most likely deposited during relatively short periods of siliceous productivity as organic-carbon-rich siliceous oozes. Laminated mud deposition probably occurred over a much longer period of time during lower levels of silica production; as a result, there was less dilution of clays and organic matter.

Lambert (1993) investigated the internal stratigraphy and organic facies of the Chattanooga (Woodford) in Oklahoma and Kansas. During the Late Devonian, North America was located in the tropics, likely in low southerly latitudes. Lambert divides the formation into lower, middle and upper shale members. The distribution and geochemistry of these members suggest that the middle member was deposited during the maximum transgression, since it has the highest total organic carbon (TOC), greatest areal extent and thickness, and contains hydrogen-rich organic matter of marine origin. Since it has the greatest component of hydrogen-rich types I and II organic matter (Lambert, 1993), it is the member that is most likely to generate hydrocarbons where thermally mature.

The Woodford Shale is bounded on the top and bottom by unconformities. The lower member is considered transgressive systems tract deposits; the middle member, early-highstand deposits; and the upper member, late-highstand systems tract deposition (Lambert, 1993).

Blackford (2007) mapped the Woodford Shale in the Arkoma Basin and assessed the Woodford gas play. He used hundreds of well logs to create structure maps of the Woodford and isopach maps of each of the three members. Blackford (2007) also created an isopach map of the Hunton in the Arkoma Basin and discussed the significance of the Hunton Group to Woodford Shale completions and production. If the Woodford is fracture-stimulated, these fractures can spread into the underlying Hunton, which can be detrimental to production if the Hunton contains significant volumes of water. Blackford

(2007) suggests targeting areas where the Hunton is entirely removed, particularly where the Woodford overlies the Sylvan Shale, which would serve as a barrier to fracture propagation.

Over (1992) determined the age of the Woodford using conodont fauna. According to his study, the basal Woodford was deposited unconformably over lower Paleozoic carbonate strata as a south-north transgressive unit during the Frasnian and early Famennian. The sparsity of preserved fauna in the upper Woodford, along with the lack of bioturbation, indicates an offshore, quiet water depositional environment, void of benthic fauna (Over, 1992). The Woodford contains an abundant and diverse conodont fauna, which Over (1992) describes in detail. He describes disconformities within the shale sequence based on gaps in the conodont succession; however, these disconformities are not well-defined by lithologic changes (Over, 1992).

Cardott and Lambert (1985) mapped the thermal maturation of the Woodford Shale based on vitrinite reflectance (Ro). They sampled the formation at depths ranging from 5,060’ to 25,115’ and observed a systematic increase in R_0 with depth. Cardott and Lambert (1985) state that the Woodford consists of shales and cherts with a range of thermal maturities from marginally mature in outcrop to metamorphic in the deep Anadarko Basin. Based on the vitrinite reflectance measurements, they make predictions on the occurrence of oil and gas.

Comer and Hinch (1987) studied the Woodford and Chattanooga shales, as well as the middle unit of the Arkansas Novaculite in an attempt to recognize and quantify oil expulsion. Comer and Hinch (1987) estimate that 27%-33% of the oil generated in these source rocks was expelled. Analyzing 300 samples from 16 cores and 43 outcrops, they calculate the total organic carbon (TOC) content to be 5.4 +/- 6.9% by weight. TOC values ranged from 0.1% in some chert beds to 26% in a highly compacted black shale bed. Comer and Hinch (1987) report that oil-filled fractures occur within the Woodford throughout Oklahoma and Arkansas, indicating that fractures are the principal avenues of expulsion.

Fertl and Chilingarian (1989) evaluated hydrocarbon resources in the Woodford Shale using well logs. They state that in southern and central Oklahoma, the Woodford Shale is carbonaceous, dark brown to black in color, with locally interbedded thin intervals of chert, siliceous shales, and siltstones. In the main oil-producing region of central and southern Oklahoma, 22 billion barrels of bitumen and 16 billion barrels of hydrocarbons have been expelled from the Woodford (Fertl and Chilingarian, 1989). In this area, hydrocarbon production occurs directly from the Woodford section and is controlled by natural fractures, which are particularly common in intervals with high carbonate, silt, or chert content. Well-log responses of the Woodford in southern and central Oklahoma consist of excessively high gamma ray, high formation resistivity, and low bulk density.

Fertl and Chilingarian (1989) also discuss various case studies, including two wells from Caddo and Carter counties, Oklahoma, in which there is evidence of oil migration. Oil residues or accumulations were found in fractures, stylolites, chert nodules and sandstone lenses embedded in the organic rich, mature source rock beds.

SHALE OIL PLAYS

Bakken Oil Production

The Bakken Formation is age-equivalent to the Woodford Formation, and produces oil in the Williston Basin of North Dakota, Montana, and Saskatchewan. It is arguably the most successful shale oil play in the U.S. The USGS estimate of recoverable oil from the Bakken Formation is larger than all other USGS oil assessments of the lower 48 states and is the largest continuous oil accumulation ever assessed by the USGS (http://www.usgs.gov/; accessed July 8, 2008).

There are many similarities between the Bakken and Woodford Formations. The Bakken Formation is also commonly divided into three members: an upper shale, a middle siltstone, and a lower shale (Meissner, 1978). Both formations contain oil-generative Type II kerogen (Williams, 1974; Comer, 1992) and both average about 10 weight-percent organic carbon (Dow, 1974; Krystyniak, 2005).

Meissner (1978) found that effective matrix porosities and permeabilities within the upper and lower members of the Bakken Formation are very low to nonexistent. However, the middle siltstone member has an average porosity of 5.5 percent and permeability ranging from 0.1 to 57 millidarcies. The Bakken oil play is focused in this middle member.

Williams and Dow (1974) suggested 10 billion barrels of oil could potentially be generated from the Bakken Shale. Webster (1984) suggested that potential hydrocarbon generation could be closer to 92 BBbls. Recently, Flannery and Kraus (2006) used a newer computer model to estimate potential oil generation of 300 BBbls.

Like the Woodford, the Bakken Formation is now regarded as an unconventional reservoir play due to improvements in horizontal drilling, completion, and fracturing technology. Flannery and Kraus (2006) state that operators are recovering oil at impressive rates of 500 barrels per day on average from the middle siltstone member. Companies have extended exploration to other parts of the Williston Basin, including down-dip from the current siltstone play, where the middle member becomes thicker and sandier. Flannery and Kraus (2006) created a 3-D thermal and fluid flow model using geochemical, thermal and rock property data available to aid their interpretation of the play.

According to the North Dakota Department of Mineral Resources, oil production from the Bakken Formation in 2006 (Table 1) was 2,245,411 barrels, accounting for nearly 6% of total state production from 300 wells. In 2007 (Table 2), that number jumped to a total of 7,382,025 barrels of oil, roughly 16.5% of the state's total oil production, from 457 wells (https://www.dmr.nd.gov/, accessed February 8, 2008). Oil is also produced from the Bakken Formation in Montana and Saskatchewan, and that production is not accounted for here. The success of the Bakken oil play in recent years may be reassuring to those interested in a potential Woodford oil play.

Formation	Barrels of Oil Produced	Percent	Wells
BAKKEN	2245411	5.6740	300
BIRDBEAR	1242060	3.1386	109
CAMBRO/ORDOVICIAN	15754	0.0398	2
DAWSON BAY	34061	0.0861	3
DEVONIAN	962058	2.4311	59
DUPEROW	901638	2.2784	121
GUNTON	18822	0.0476	1
HEATH	220369	0.5569	40
LODGEPOLE	1596325	4.0338	29
MADISON	11680192	29.5151	2107
MIDALE/NESSON	155200	0.3922	30
MISSION CANYON	2213	0.0056	1
ORDOVICIAN	533782	1.3488	55
RATCLIFFE	11876	0.0300	4
RED RIVER	1871889	4.7301	203
RED RIVER B	15706913	39.6903	269
SANISH	67118	0.1696	13
SILURIAN	593657	1.5001	55
SPEARFISH	15465	0.0391	9
SPEARFISH/CHARLES	416980	1.0537	106
SPEARFISH/MADISON	63128	0.1595	36
STONEWALL	463033	1.1701	51
TYLER	433896	1.0964	45
TYLER A	31035	0.0784	4
WINNIPEG/DEADWOOD	1267	0.0032	2
WINNIPEGOSIS	289508	0.7316	16
2006 Total	39573650	100.0000	3670

Table 1. Oil production by formation, North Dakota, 2006 (North Dakota Department of Mineral Resources; https://www.dmr.nd.gov/, accessed February 8, 2008)

Formation	Barrels of Oil Produced	Percent	Wells
BAKKEN	7382025	16.5139	457
BIRDBEAR	1153949	2.5814	111
CAMBRO/ORDOVICIAN	12489	0.0279	2
DAWSON BAY	31178	0.0697	3
DEVONIAN	992888	2.2211	62
DUPEROW	806651	1.8045	121
GUNTON	16729	0.0374	1
HEATH	180224	0.4032	40
LODGEPOLE	1331618	2.9789	29
MADISON	11352593	25.3962	2123
MIDALE/NESSON	178634	0.3996	28
MISSION CANYON	1967	0.0044	1
ORDOVICIAN	471503	1.0548	54
RATCLIFFE	10512	0.0235	4
RED RIVER	1891163	4.2306	209
RED RIVER B	16722579	37.4091	278
RIVAL	17291	0.0387	4
SANISH	61987	0.1387	13
SILURIAN	576815	1.2904	56
SPEARFISH	21612	0.0483	13
SPEARFISH/CHARLES	374252	0.8372	109
SPEARFISH/MADISON	53579	0.1199	36
STONEWALL	417206	0.9333	50
TYLER	374096	0.8369	42
TYLER A	29680	0.0664	4
WINNIPEG/DEADWOOD	1371	0.0031	3
WINNIPEGOSIS	237343	0.5309	19
2007 Total	44701934	100.0000	3872

Table 2. Oil production by formation, North Dakota, 2007 (North Dakota Department of Mineral Resources; https://www.dmr.nd.gov/, accessed February 8, 2008)

Woodford Oil Production

Significant, but spatially limited, oil production from the Woodford Shale exists in Oklahoma. Fertl and Chilingarian (1989) present two case studies in which wells in Carter and Caddo counties produced oil**.** The Carter County well produced at an initial rate of 50 barrels of oil per day (BOPD), and sustained a rate of 23 barrels per day. The Caddo County well was put on production at 240 barrels per day after the cleanest intervals were perforated (Fertl and Chilingarian,1989).

Bramlett (1981) also discusses Woodford oil production in Oklahoma. He states that the Woodford Formation had produced from fractured cherts in the upper Woodford Shale, as well as a basal detrital zone, in several locations in southern Oklahoma. In a well in Caddo County, the Woodford Formation produced 215 BOPD initially. He reports that two other wells from Marshall County produced between 29 and 195 BOPD and 9 and 269 BOPD from the Woodford Formation, however this production is commingled with other zones (Bramlett, 1981).

These wells lend credence to the proposal that a large Woodford Shale oil-production potential exists in Oklahoma. As with the Bakken Shale, the development of new technology, including horizontal drilling and large multi-stage hydraulic stimulations may be necessary to develop the Woodford Shale oil reserves.

CHAPTER III

GEOLOGIC HISTORY

The depositional history of the Mid-Continent began with the rifting and formation of the Southern Oklahoma Aulacogen (SOA) during the Cambrian (Figure 5A). This fault-bounded trough was first partially filled with as much as 20,000 feet of igneous rocks (Johnson, 1989). During late Cambrian to early Mississippian time, the SOA was in its slow subsidence stage (Figure 5B). At this time, a broad epicontinental sea existed with its depocenter over the SOA. This episode of long-term subsidence resulted in a large accumulation of sediments, dominantly carbonates, with lesser amounts of siliciclastics. These became the early Paleozoic Cambrian Timbered Hills Group, Cambrian-Ordovician Arbuckle Group, Ordovician Simpson and Viola Groups, Ordovician Sylvan Shale, and Ordovician-Devonian Hunton Group. The carbonate in the sequence accumulated as a result of relatively shallow water depths and continued slow subsidence of the basin. Carbonate deposition was continuous and kept pace with slow subsidence (Rechlin, 2003).

Sea level fluctuated throughout lower Paleozoic carbonate deposition. This is evidenced by depositional cycles in the Arbuckle Group (Franseen and others, 2004) and unconformities within the Hunton (Kuykendall and Fritz, 2001). These unconformities most likely formed due to cyclic drops in sea level, which resulted in subaerial exposure and erosion. An unconformity at the base of the Frisco Formation, the uppermost member of the Hunton Group, represents a period of significant erosion. During the Devonian, relative sea level was at its lowest point to Frisco deposition, leading to the belief that much of the Hunton was eroded prior to that time (Kuykendall and Fritz, 2001). A significant drop in sea level was responsible for the unconformity at the top of the Hunton Group that separates it from the overlying Woodford Shale (Figure 5C). Where more extensive erosion occurred, the Hunton Group is absent. Subsequent widespread flooding in the late Paleozoic is recorded by deposition of the sediments that became the organic-rich Woodford Shale.

An epicontinental sea covered most of the North American craton during Woodford deposition. The deepest portions of the sea existed within the SOA (Roberts, 1992). This sometimes anoxic environment allowed for accumulation and preservation of large amounts of organic carbon in both shales and cherts of the Woodford. The siliceous sediments were deposited during relatively short periods of high siliceous productivity as organic carbon-rich siliceous oozes. Mud deposition, on the other hand, occurred over longer periods of time, which had lower levels of silica productivity and less dilution of organic carbon by siliceous sediments. Roberts (1992) suggests sedimentation rates for cherts to be 2.5 times faster than shales and estimates that Woodford deposition would have occurred over a time span of 10 to 15 million years.

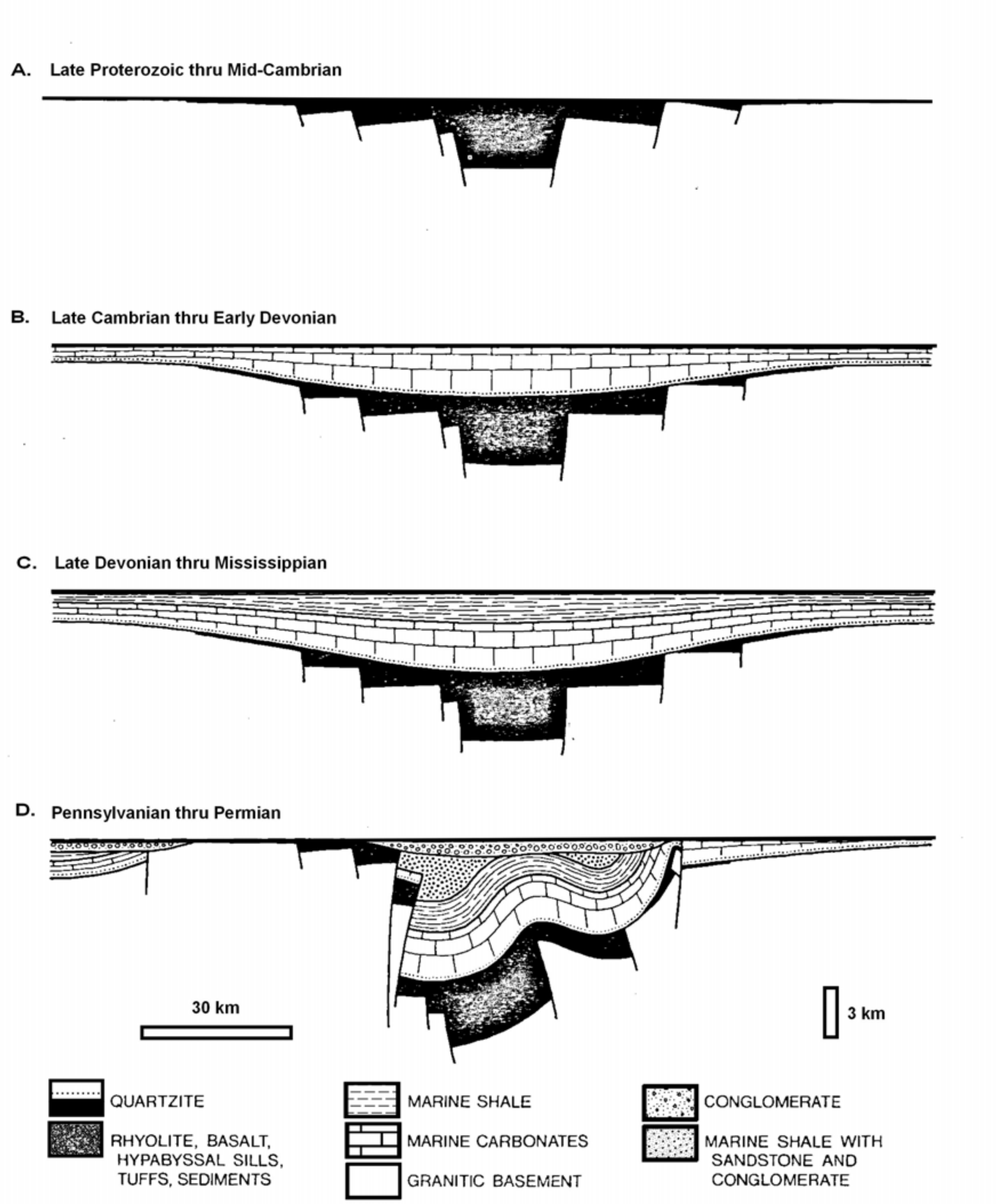

Figure 5. Evolution of the Southern Oklahoma Aulacogen (after Hoffman et al., 1974).

During Woodford deposition, the southern margin of North America was in the tropics. Figures 6 and 7 are paleogeographic maps of North America during the Late-Devonian (Frasnian-Famennian) and early Mississippian (Tournaisian) (Blakey, 2008). Woodford sediments were deposited as a marine transgression from south to north (Over and Barrick, 1990) in low southerly latitudes. Over and Barrick (1990) suggest a stratified water column and anoxic bottom waters developed as water deepened after initial Woodford sedimentation based on conodont biofacies. Water depth is estimated to have been between 50 and 400 meters during Woodford deposition (Over and Barrick, 1990).

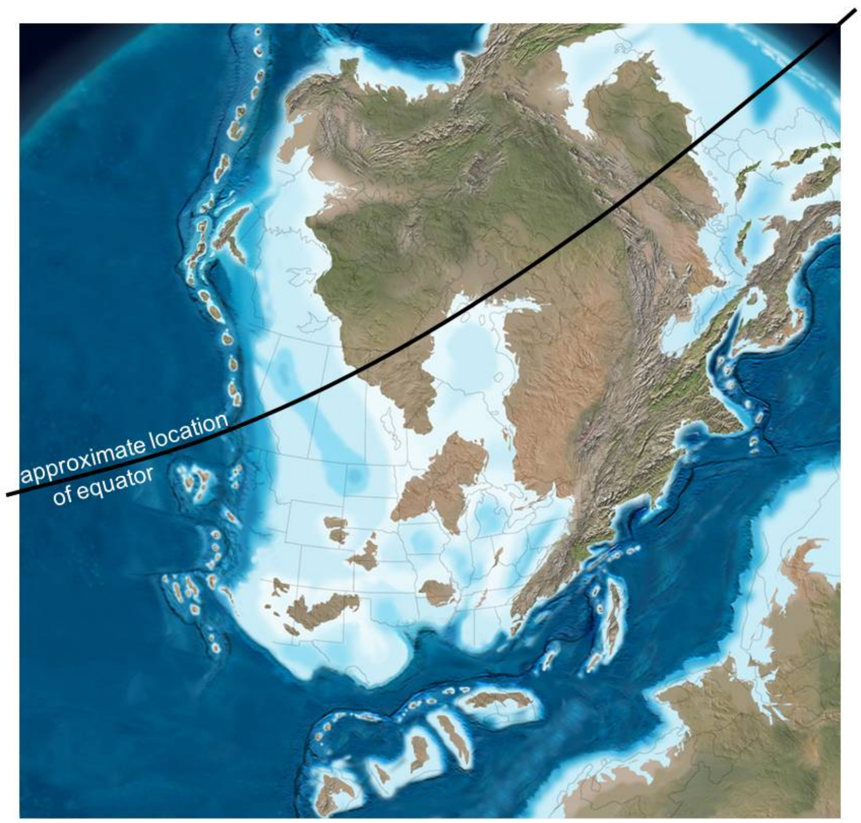

Figure 6. Late-Devonian Paleogeography (modified from Blakey (2008); http://www2.nau.edu/rcb7/namD360.jpg, accessed February 8, 2008)

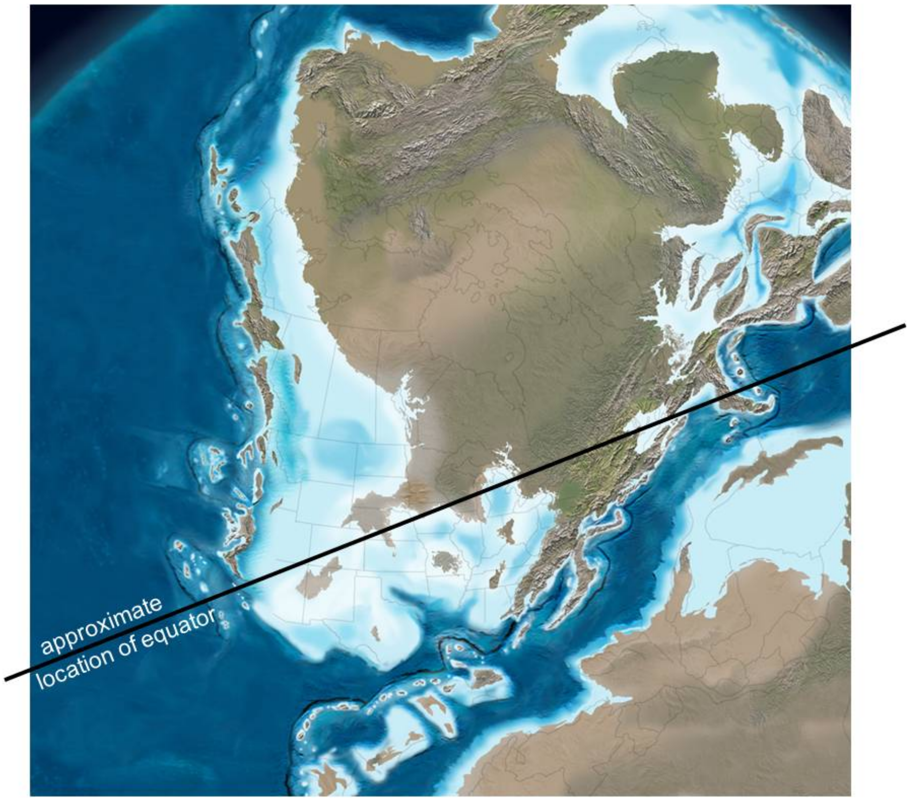

Figure 7. Early-Mississippian Paleogeography (modified from Blakey (2008); http://www2.nau.edu/rcb7/namM345.jpg, accessed February 8, 2008)

Topographically positive areas during the Late Devonian were the central Kansas uplift (part of the Transcontinental Arch), the Chautauqua Arch, the St. Francois Mountains, and the Texas Arch (Johnson, 1989). Negative areas included the Ouachita Trough in southeast Oklahoma and the Oklahoma Basin of southwestern Kansas and Oklahoma. The Southern Oklahoma Aulacogen was the depocenter of the Oklahoma Basin at that time (Lambert, 1993). Figure 8 shows these Late Devonian positive structures from which Woodford sediments were derived and negative features in which the sediments were deposited.

The Frasnian-Famennian extinction is one of the five major Phanerozoic extinction events and is entirely contained within the Woodford Shale (Over, 2002). There is no evidence of a rapid fall in sea level or interruption of mud deposition. Pyrite, phosphatic nodules, and conodont concentration are suggestive of sea-level rise at the F/F boundary in the Mid-Continent region of North America (Over, 2002).

The deformation stage of the Southern Oklahoma Aulacogen began during the Pennsylvanian (Morrowan) (Figure 5D). Intense crustal shortening occurred associated with late Paleozoic continental collision which created the Ouachita orogenic belt. The Oklahoma Basin was partitioned into the Arkoma, Ardmore, and Anadarko proto-basins during the Pennsylvanian orogenic episode (Johnson, 1989). Folds and faults were produced in the frontal Wichita fault zone and Anadarko Basin, with less intense activity to the north (Amsden, 1975). The study area in Seminole County, Oklahoma, is located in the area outside the region of intense deformation.

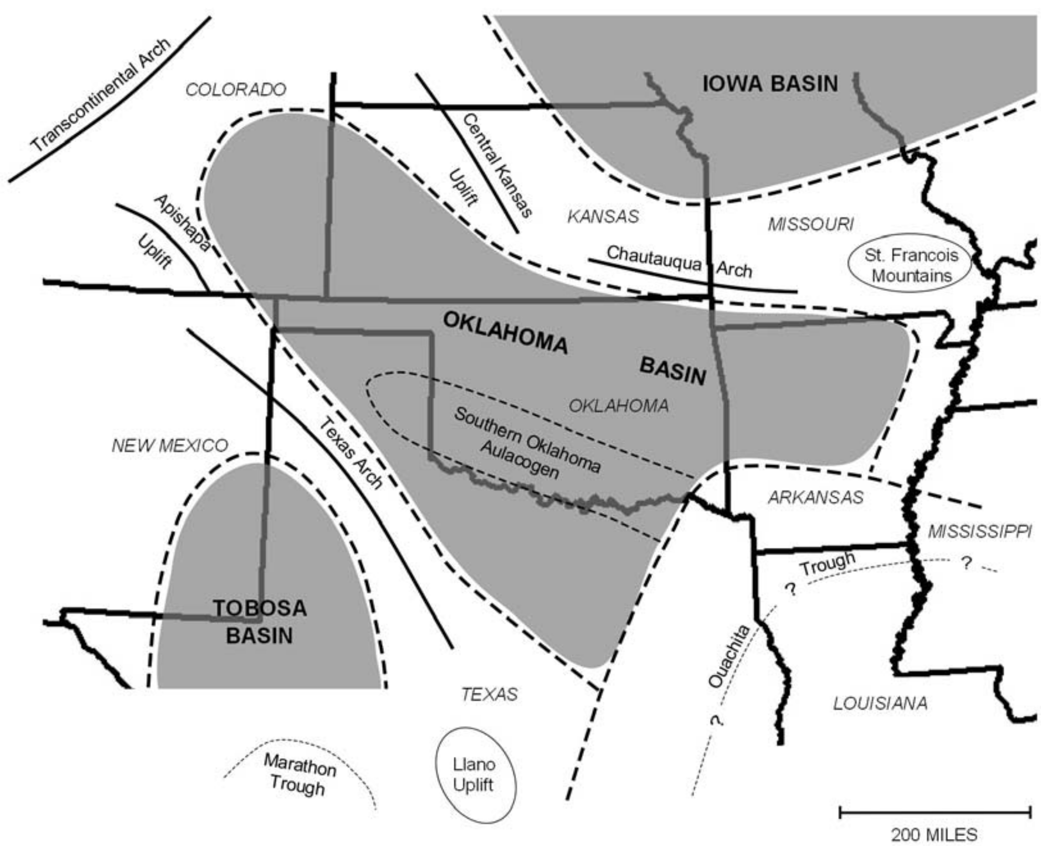

Figure 8. Map of south-central United States, showing approximate boundary of the Oklahoma basin and other major features that existed in early and middle Paleozoic time (after Johnson, 1989)

CHAPTER IV

WIRE-LINE LOG MAPPING

Wire-line Log Characteristics

The study area contains many old oil fields, with production dating back to the early and mid 20th century. As a result, there were more than 675 wire-line electric logs available for examination. Most of these were vintage wire-line logs from the late 1930s to the mid 1970s. Spontaneous Potential (SP) and resistivity logs are common; the availability of gamma-ray (GR) logs is limited. When the GR curve is not available, resistivity logs are key for picking lithostratigraphic boundaries and informal mapping units. Resistivity logs are also an invaluable tool for identifying and distinguishing the four Woodford Shale subunits. Plate 11 contains a cross-section in which the correlation between GR and resistivity is illustrated. When GR is not available, resistivity alone can be used with confidence to identify electric-log based subunits.

SP logs can be used to identify the top and bottom of the Hunton Group as well as the top of the Viola Group. In both cases, the curve distinguishes somewhat permeable carbonate zones from adjacent impermeable to low permeability shales. Since shales are not easily discriminated with the SP curve, this tool cannot be used to separate the Woodford Shale from the overlying Caney Shale or the subjacent Sylvan Shale when the Hunton is absent due to erosion. For the same reason, the SP curve does not allow differentiation of the four subunits. Because resistivity is effective for distinguishing these intervals and it correlates to the gamma-ray, it was used throughout the study area to establish correlations using vintage and recent well logs.

The Woodford Shale is rich in radioactive minerals and reads very high, or "hot", on the gamma-ray curve. This distinct log signature is due primarily to the presence of uranium, which causes it to exceed 150 API units, which is the industry convention for classifying shales as radioactive. This "hot" signature allows for it to be easily picked on a GR curve. The top of the Woodford Shale represents a sharp contact with the overlying Mississippian rocks. Since there are also "hot" streaks in these rocks, the contact between the Mississippian and Woodford can be difficult to establish using the GR curve alone. Therefore, this contact is typically picked based on a downward decrease in bulk density into the Woodford Shale, where this curve is available, or a downward decrease in resistivity. Using resistivity, SP, and GR curves on newer wells, a stratigraphic framework was established that ensured all tops picked in the study area are consistent.

Previous studies (including Hester, 1988; Lambert, 1993; and Blackford, 2007) have divided the Woodford Shale into three informal members: upper, middle, and lower. In this study, the Woodford Shale is divided into four subunits based on observations from well logs and core analysis. These intervals were delineated based on gamma-ray and resistivity curves, which were correlated with lithologic changes observed in the Circle Creek #1 core. A typical example of the division of subunits is shown in Figure 9.

Figure 9 is a wire-line log from the Ingram Exploration, Circle Creek #1 well in section 13, T.6N., R.6E., which shows the Woodford Shale divided into four subunits. In this well, the Woodford Shale overlies roughly 70 feet of Sylvan Shale, which overlies the Viola Group. The Hunton Group is absent and, as with other well logs lacking the Hunton Group, it appears that the upper portion of the Sylvan Shale is missing and presumed to have been eroded. The porosity increase across the Woodford Shale compared to the underlying and overlying units that is apparent in this well is also evident in other well logs. This interval of the Woodford Shale is marked accordingly by "Top Woodford" and "Top Sylvan" lines. In addition, the wire-line log characteristics of S1, S2, S3, and S4 are apparent. These subunits within the Woodford Shale are marked accordingly.

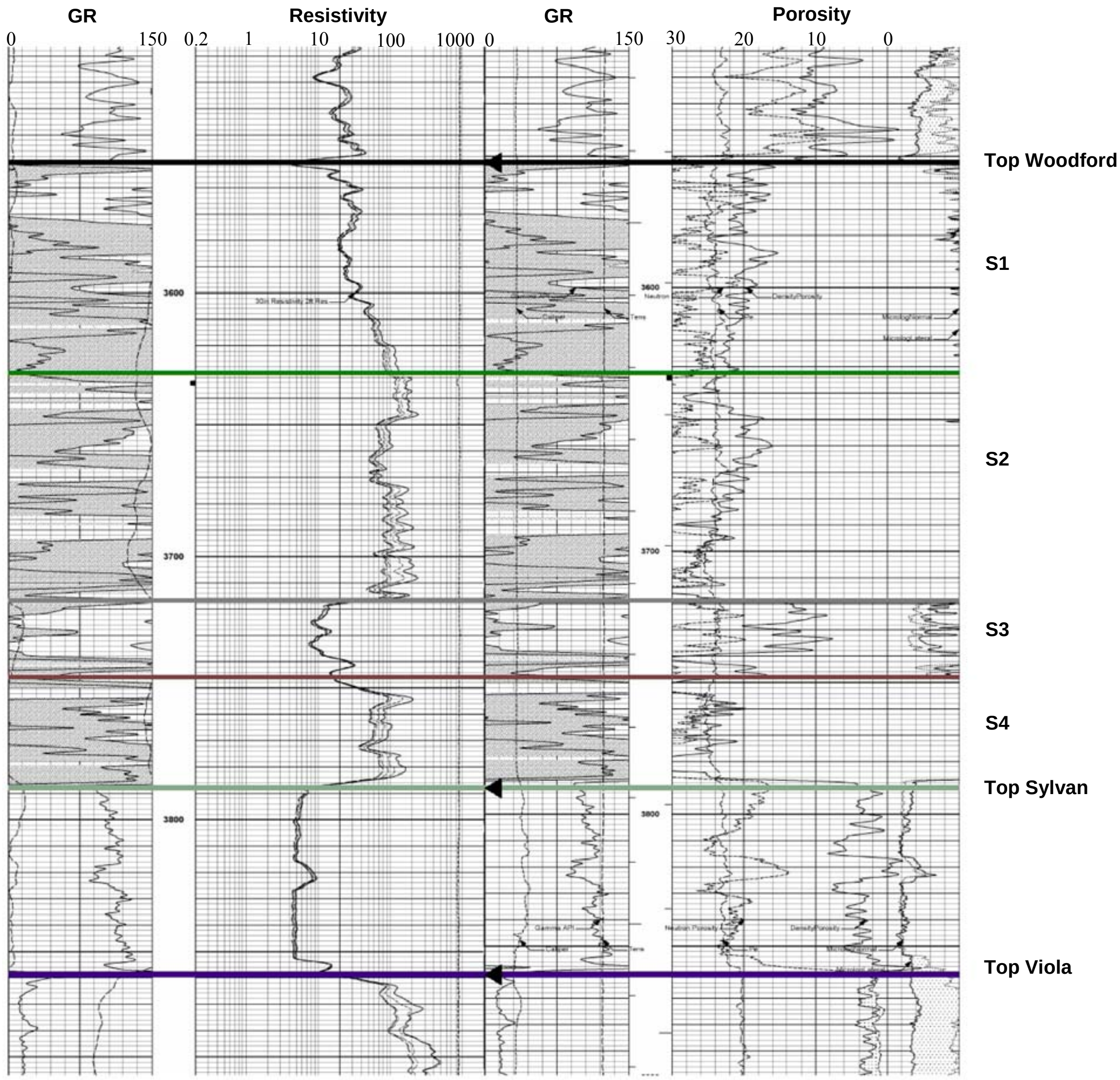

Figure 9. Woodford Shale divided into four subunits, Ingram Exploration Circle Creek #1, Section 13, T.6N., R.6E., Seminole County.

Subunit 1 (S1) is the uppermost zone. Resistivity values range from less than 10 ohm-m near the top (which marks the pick for the top of the Woodford Shale) to 100 ohm-m at the base. The majority of the interval has resistivity values between 20 and 40 ohm-m. Thicknesses of S1 range from 40 to 130 feet with an average of 85 feet for the study area.

The base of S1 is marked by an increase in resistivity, which represents the top of subunit 2. Typical resistivities are approximately 100 ohm-m, but values can vary between 80 ohm-m to spikes over 1000 ohm-m near the base. Near the top and base of S2, resistivity values are typically 100 to 200 ohm-m, but in some locations read 300 to 400 ohm-m. The average thickness of S2 is 70 feet, and ranges from less than 10 feet in the northeastern part of the study area to greater than 110 feet in the south and southeastern areas.

The top of S3 is picked where a significant decrease in resistivity occurs. Resistivities range from 20 to 40 ohm-m, but can increase sharply to over 100 ohm-m in places. On average, the thickness of S3 is 20 feet, but can range from less than 5 feet in the northeastern area to about 40 feet in the southwestern area.

The top of S4 is marked by an increase in resistivity. This interval is similar to S2. It has resistivities ranging from 100 to 200 ohm-m, but commonly has sharp increases up to 800 ohm-m. The base of S4 coincides with the top of the subjacent formation, which may be the Hunton Group, Sylvan Shale, or Viola Group. The average thickness of S4 is 35 feet, but can be less than 10 feet in areas. Thin S4 coincides with a thick underlying Hunton Group. Paleo-highs on the Hunton surface represented topographic highs during Woodford deposition. S4 is up to 70’ thick in a few places within the southern portion of the study area. These areas likely represent paleo-lows on the eroded Hunton surface.

In the study area, resistivity of the Sylvan Shale averages around 5 ohm-m, which distinguishes it from the underlying Viola Group that has resistivity readings over 100 ohm-m. Hunton Group resistivity values range between 10 and 100 ohm-m across the majority of the interval. However, near the base and the top of the Hunton Group, resistivity values can exceed 100 ohm-m. Outside the study area, where the Hunton Group is productive, resistivities are typically higher. Many wells produce from the Hunton Group in locations adjacent to the study area. These include in T.5N., R. 5 & 6E., T.6N., R.5E., T.8N., R.5, 6, 7, & 8E., the eastern part of T.5N., R.7E., western part of T.5N., R.8E., parts of T.7N., R.5E., and the northern part of T.7N., R.8E. (Figure 10). The Hunton Group is altogether absent or less than 25' thick in roughly 90% of the study area. In the northeast and southwest quadrants of the study area, the Hunton Group is significantly thicker, roughly 175 feet and 250 feet, respectively. The Sylvan Shale ranges in thickness from 0 to greater than 125 feet and averages 95 feet where the Hunton Group is present.

On most gamma-ray logs in this area, the gamma-ray curve in the Woodford Shale reads greater than 150 API units, and is arbitrarily truncated, which makes it impossible to determine the real API values. Based on the information gleaned from the spectral gamma-ray analysis of the Chesapeake Circle Creek #1 core, the average GR of the Woodford Shale is 241 API units in S1, 330 API units in S2, 175 API units in S3, and 309 API units in S4. However, some intervals have gamma-ray values exceeding 600 API units. The gamma-ray signature of the Woodford Shale in the Circle Creek #1 is discussed in greater detail in the petrographic analysis chapter.

The base of the Woodford Shale is marked by a sharp decrease in GR regardless of the underlying formation. The Hunton and Viola Groups are both relatively clean limestones with GR values averaging between 15 and 45 API units. The Sylvan Shale also has an average lower GR signature of 100 API units, which is significantly less than the Woodford Shale.

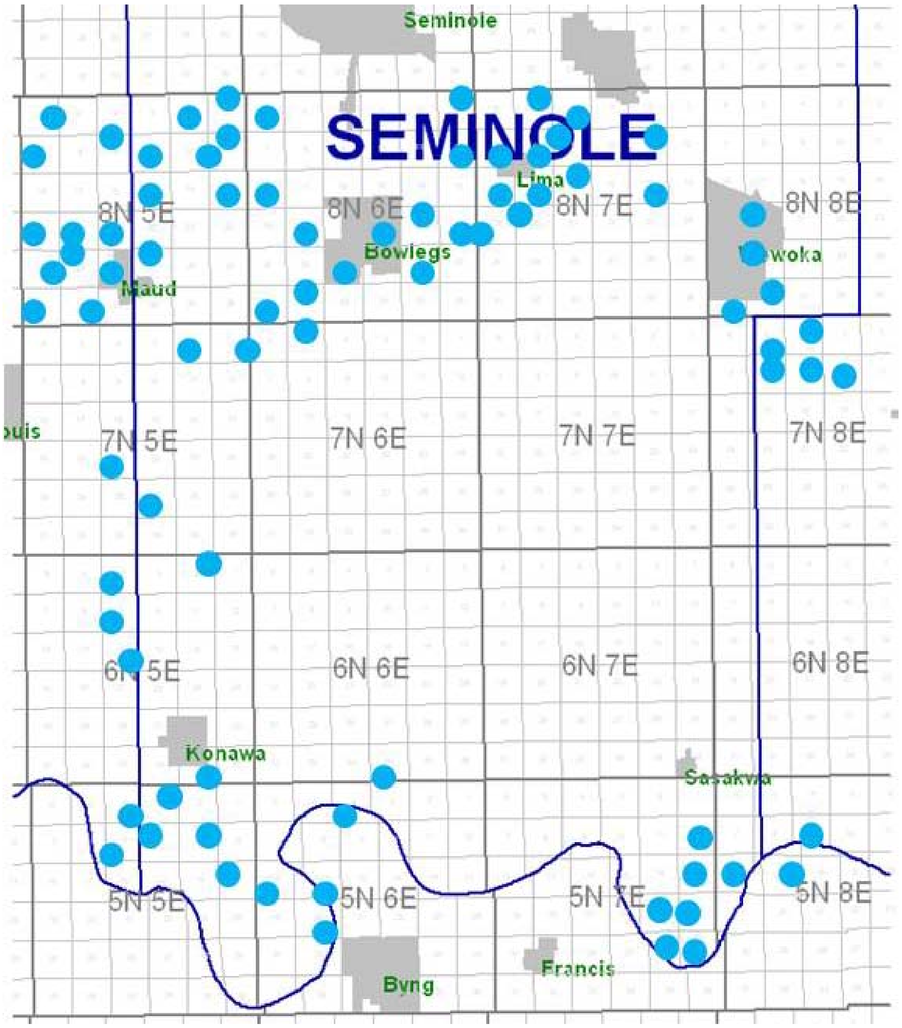

Figure 10. Map of Hunton production surrounding study area (Hunton producers indicated by ●).

Figures 11 and 12 are images of portions of other wire-line logs from wells within the study area. Figure 11 is from the TDR Exploration, Walton No. 1 in section 25, T.6N., R.6E. and shows the Woodford overlying a relatively thin Hunton Group (~20 feet). Beneath the Hunton Group is approximately 100 feet of Sylvan Shale, and the upper part of the Viola Group. Figure 12 is a log from the Shield Operating, Vamoosa No. 1 in section 15, T.6N., R.6E. This log indicates the Hunton Group is not present because of erosion prior to Woodford deposition. This log shows the Woodford Shale overlying roughly 60 feet of Sylvan Shale, before the well reached a total depth in the

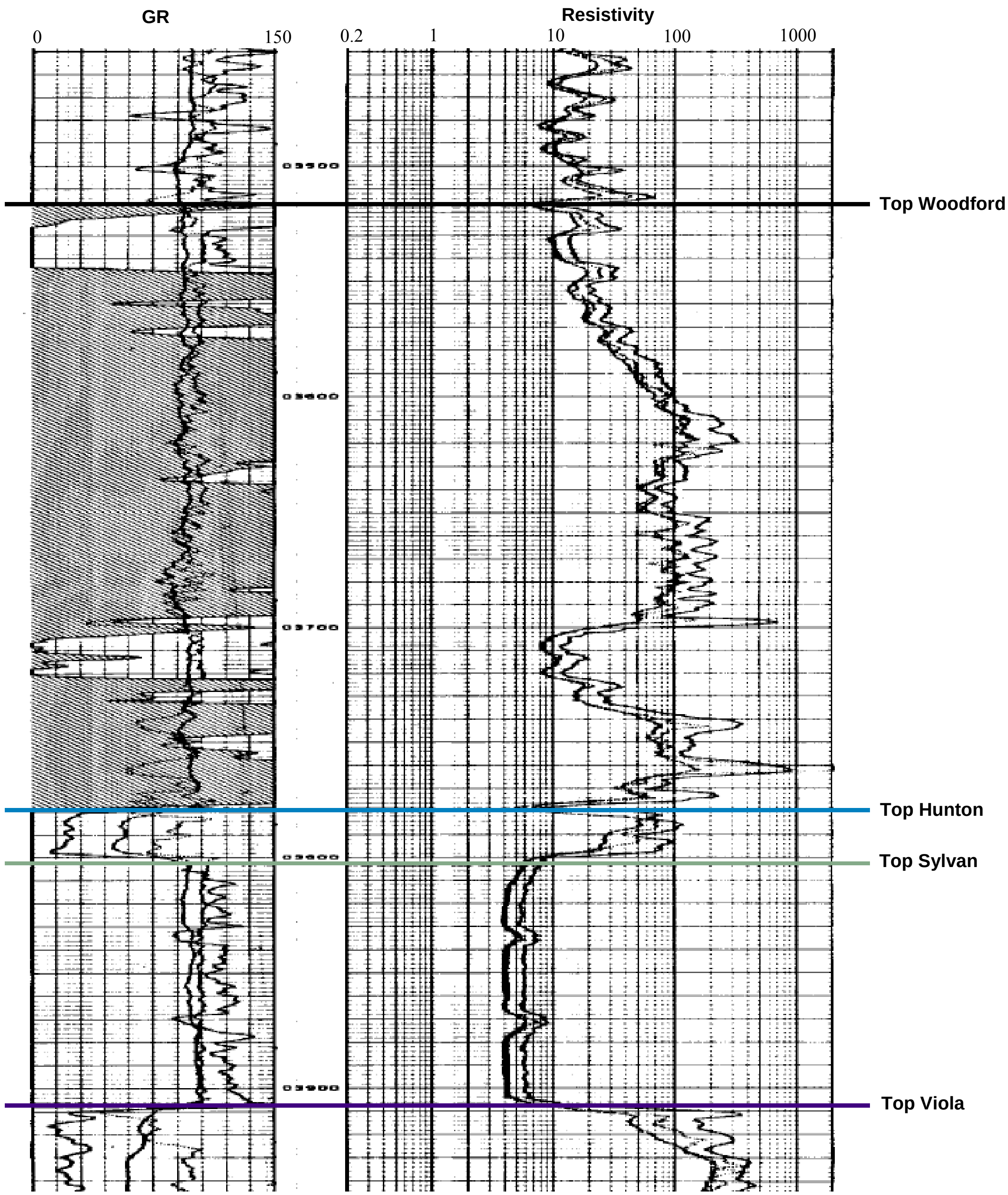

Figure 11. Woodford Shale overlying relatively thin Hunton Group, TDR Exploration Walton No. 1, Section 25, T.6N., R.6E., Seminole County

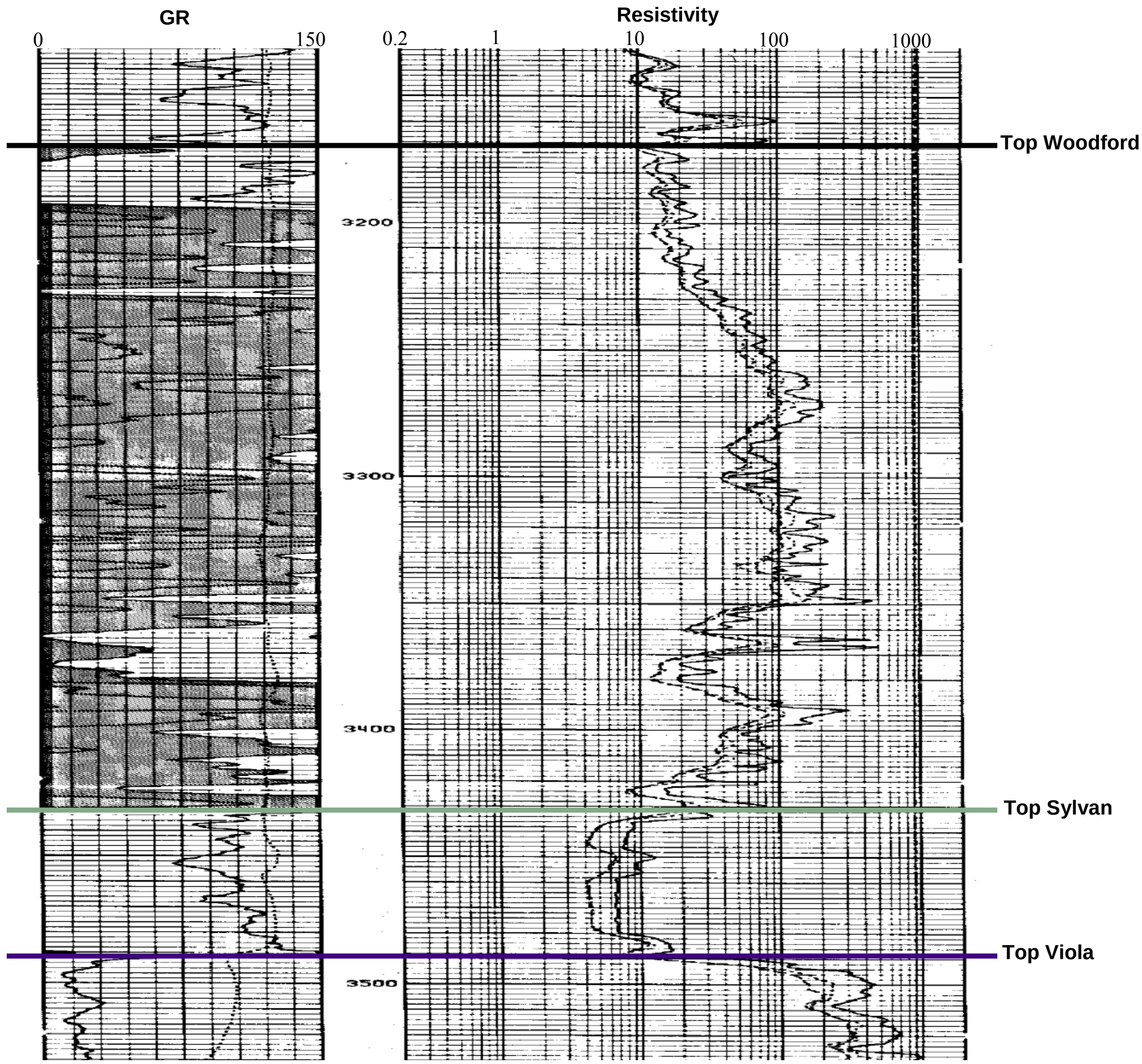

Figure 12. Woodford Shale overlying Sylvan Shale, Shield Operating Vamoosa No. 1, Section 15, T.6N., R.6E., Seminole County

Viola Group. It is likely that the uppermost Sylvan Shale was reduced by the same erosional event that removed the Hunton Group from this location. A second explanation for the missing Hunton Group and thinner Sylvan Shale is that this well encountered a normal fault resulting in missing section observed on wire-line log. Figure 13, a portion of the log from the Lindemuth and Associates, Davis “A” 10 in section 7, T.6N., R.8E., shows Woodford Shale overlying the Viola Group. Both the Hunton Group and the

Sylvan Shale are absent in this well. This could be explained by the presence of a fault, however, it is more likely that the Hunton Group and Sylvan Shale were eroded from this location prior to Woodford deposition.

Evidence for erosion is two-fold: (1) similar patterns of missing strata are evident over a relatively wide area and not confined to a linear trend, and (2) patterns in resistivity and gamma-ray indicate that the Hunton and Sylvan intervals lose the upper portions first, which is a characteristic of erosion. This is evident in Figures 11, 12, and 14, where resistivity signatures indicate that the lower portions of the Sylvan Shale remain in the logged intervals.

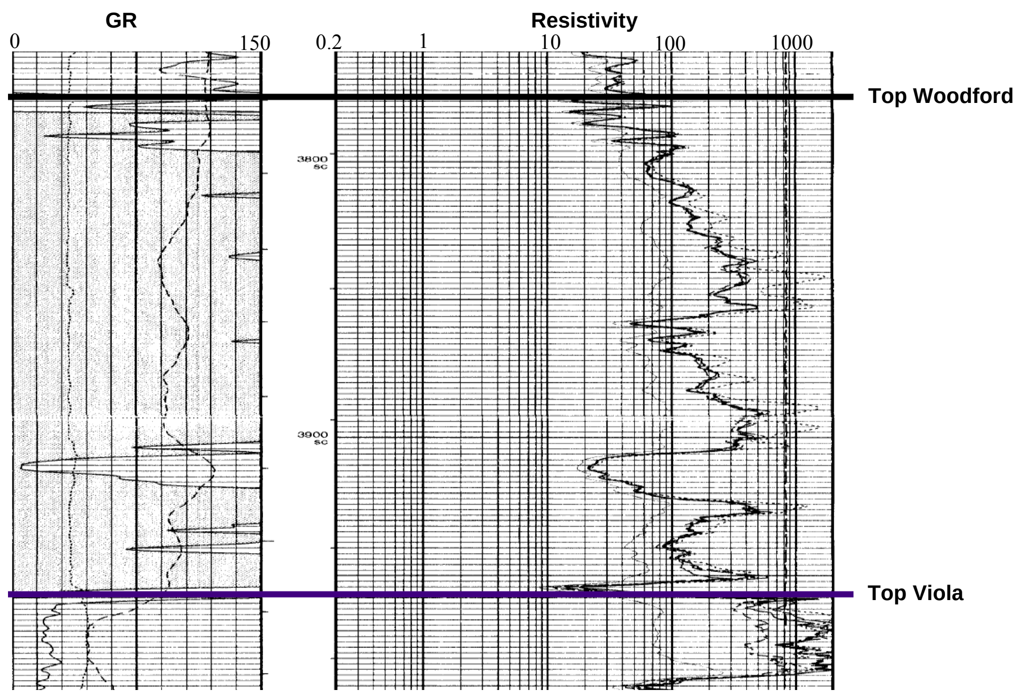

Figure 13. Woodford Shale overlying Viola Group, Lindemuth & Assoc., Davis 'A' 10, Section 7, T.6N., R.8E., Seminole County

Figure 14 shows the Woodford Shale overlying the Sylvan Shale in the Kewanee Oil Co., Amason 4 in section 15, T.6N., R.6E. Spontaneous potential, resistivity, gamma-ray, porosity, and bulk density logs are shown for this well. A notable feature is the decrease in bulk density as well as the increase in porosity and resistivity for the Woodford interval as compared to the overlying Mississippian Caney Shale and underlying Sylvan Shale.

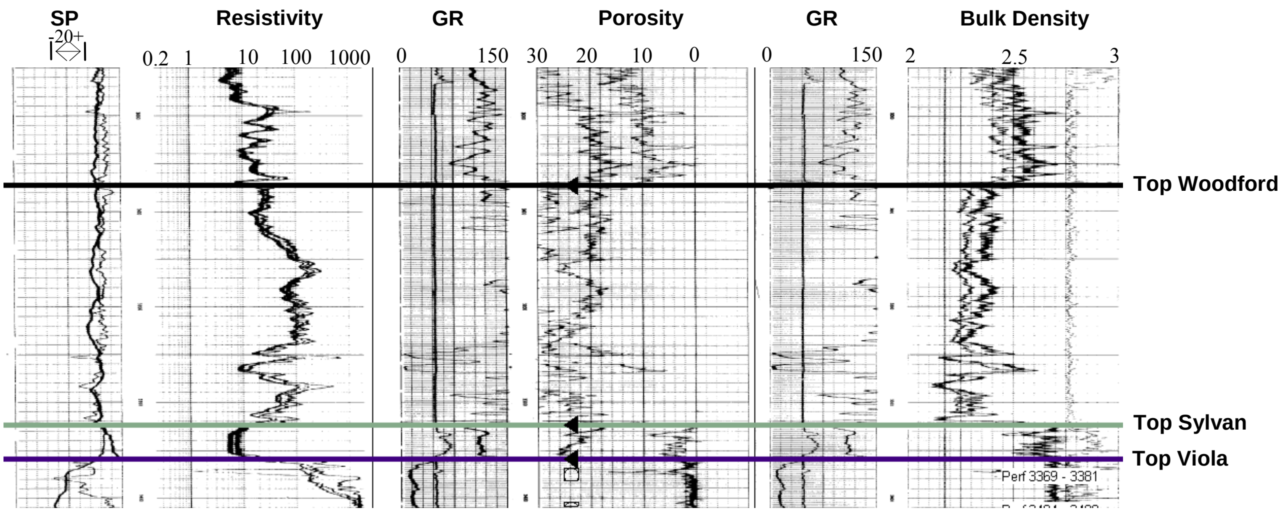

Figure 14. Woodford Shale overlying Sylvan Shale, from Kewanee Oil Co. Amason 4, Section 15, T.6N., R.6E., Seminole County

Other studies have noted that there is often an inverse relationship between the thicknesses of the Hunton Group and Woodford Shale. For example, Blackford (2007) found that a thin, highly eroded Hunton Group often corresponds to a thick accumulation of Woodford Shale although exceptions to this inverse proportionality were evident. As Woodford deposition progressed from the south, the lower Woodford Shale sediments were deposited in the deepest basinal settings and as onlap onto the shelf. In the northern portions of the Arkoma Basin, the Hunton Group experienced extensive erosion prior to the Woodford onlap. Therefore it is possible for thin Woodford Shale to overlie a thin or absent Hunton Group (Figures 11 and 12).

While no direct correlation (Figure 15) between Hunton thickness and overall Woodford thickness is observed in the study area, it is important to note that there is a relationship between Hunton thickness and presence of S3 and S4, as these subunits were not deposited in many areas where the Hunton Group is thickest. North of the study area, near the Nancy 1-17H core location in section 17, T.10N., R.5E. (Figure 16), there is 33 feet of Hunton Group and S3 and S4 are missing. It is most likely that these subunits were never deposited in this location because there is no evidence for intra-Woodford unconformities. These would be near impossible to identify without biostratigraphic data (Over, 1992). Since the Woodford was deposited as a S-N marine transgressive sequence, early Woodford sediments may not have onlapped over the Hunton Group paleo-high. Figure 22 is a map of Hunton Group thickness, which reflects paleo-topography.

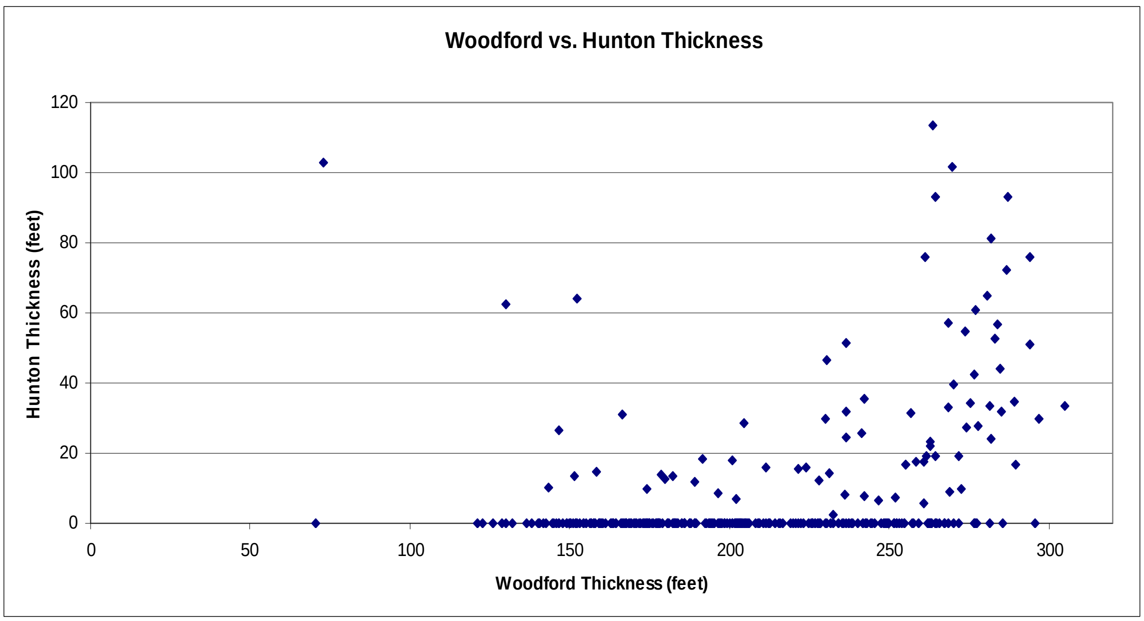

Figure 15. Study area comparison of gross Woodford Shale versus Hunton Group thickness

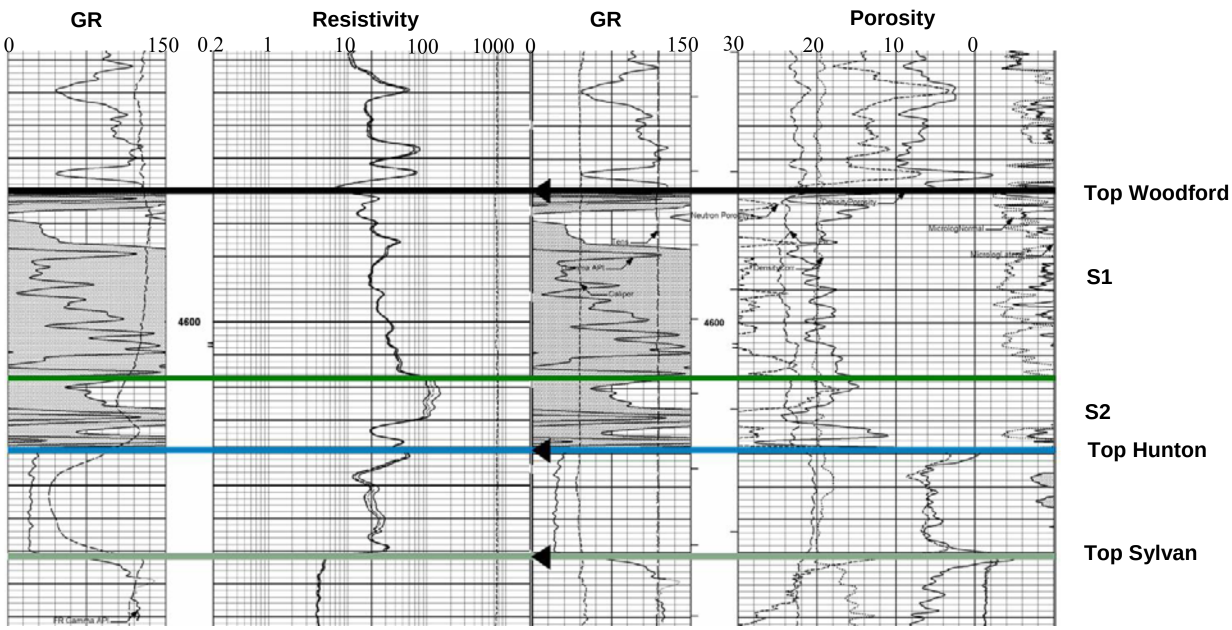

Figure 16. Woodford Shale divided into subunits, from the Chesapeake Nancy 1-17H, Section 17, T.10N., R.5E., Pottawatomie County

Mapping

Woodford Shale, Sylvan Shale, Hunton Group, and Viola Group tops were picked in 675 vertical wells in the study area and adjacent sections. In roughly 535 of those wells, it was possible to further subdivide the Woodford into four subunits. This data set was used to map the thicknesses of the total Woodford Shale (Figure 17, Plate 7) as well as the four subunits (Figures 18 through 21, Plate 8). A Hunton Group thickness map (Figure 22, Plate 7), and a structure map of the top of the Viola Group (Figure 23, Plate 6) were also constructed.

Measured depths (MD) were used for creating thickness maps, while sub-sea (SS) depths were used to create the structure map. As wells in the study area are essentially vertical, using MD for thickness is equivalent to using true vertical depth (TVD). Thicknesses are not corrected for dip, which is less than 5º.

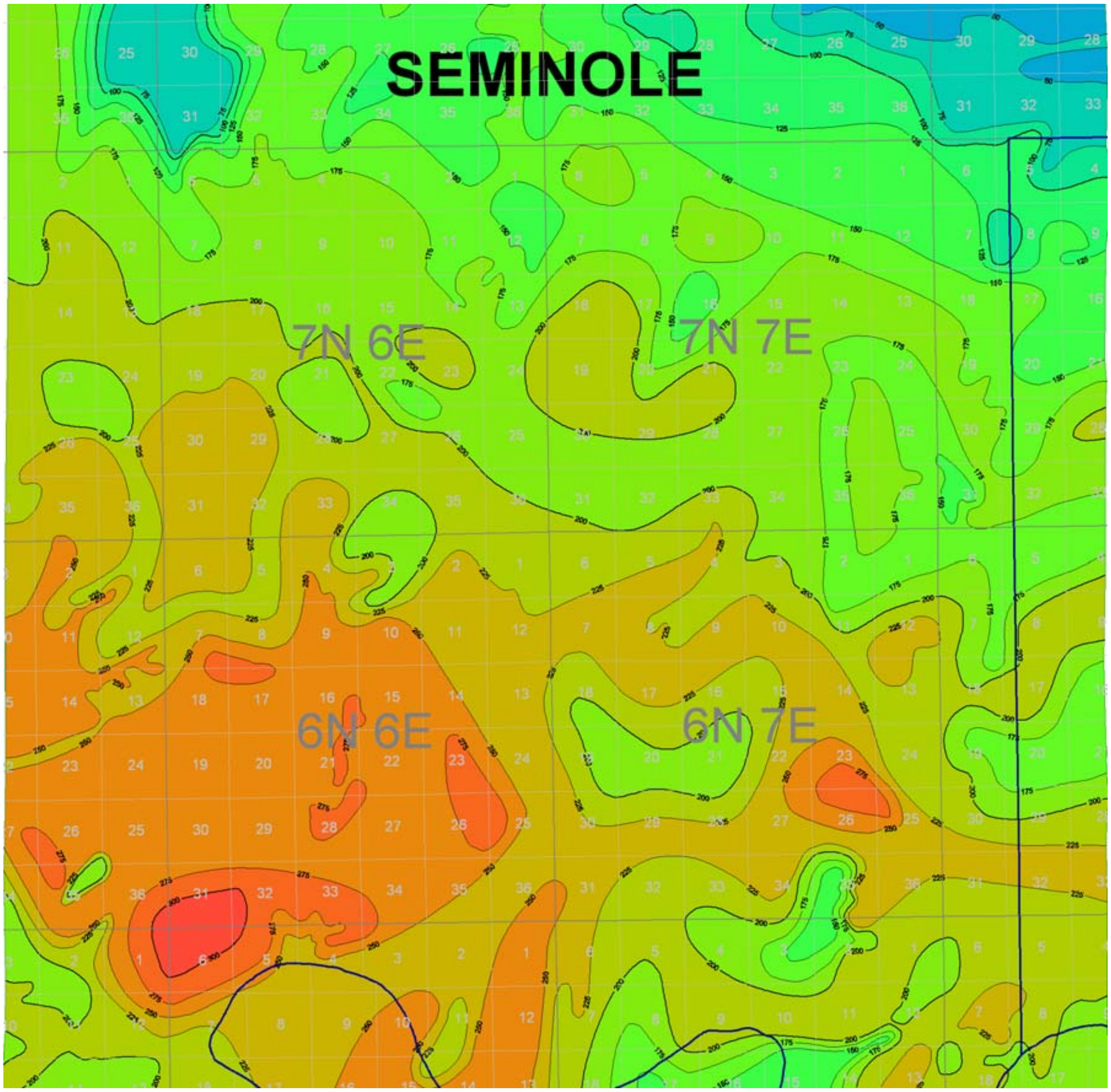

Figure 17. Study Area Map of Woodford Shale thickness, 25' contour interval. This figure is also found in Plate 7.

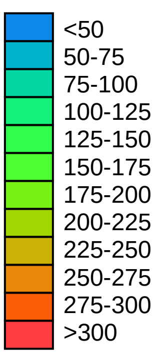

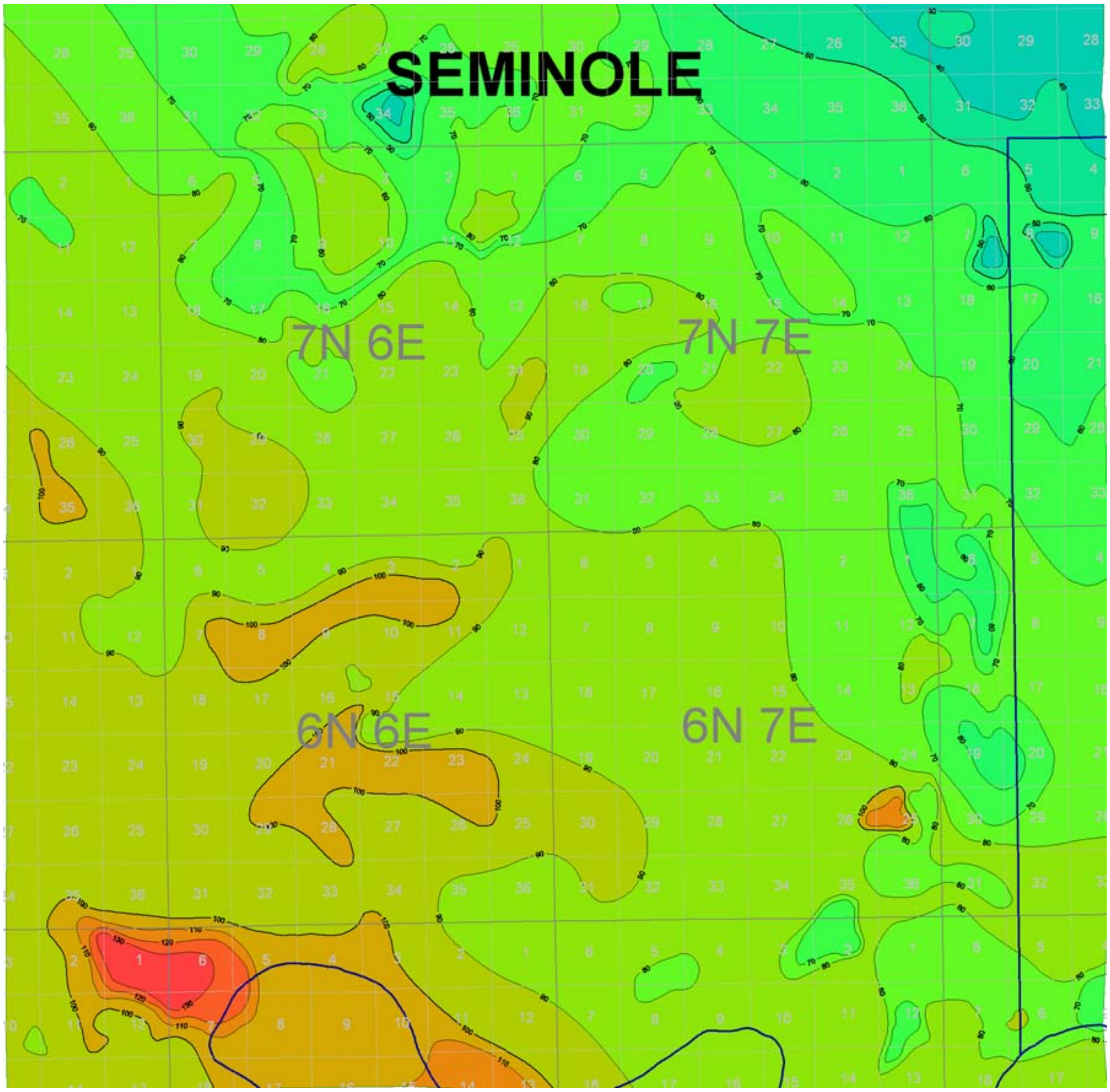

Figure 18. Study Area Map of S1 Thickness, 10’ contour interval (also found in Plate 8)

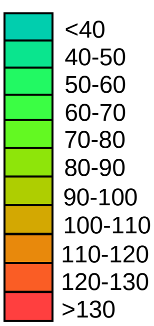

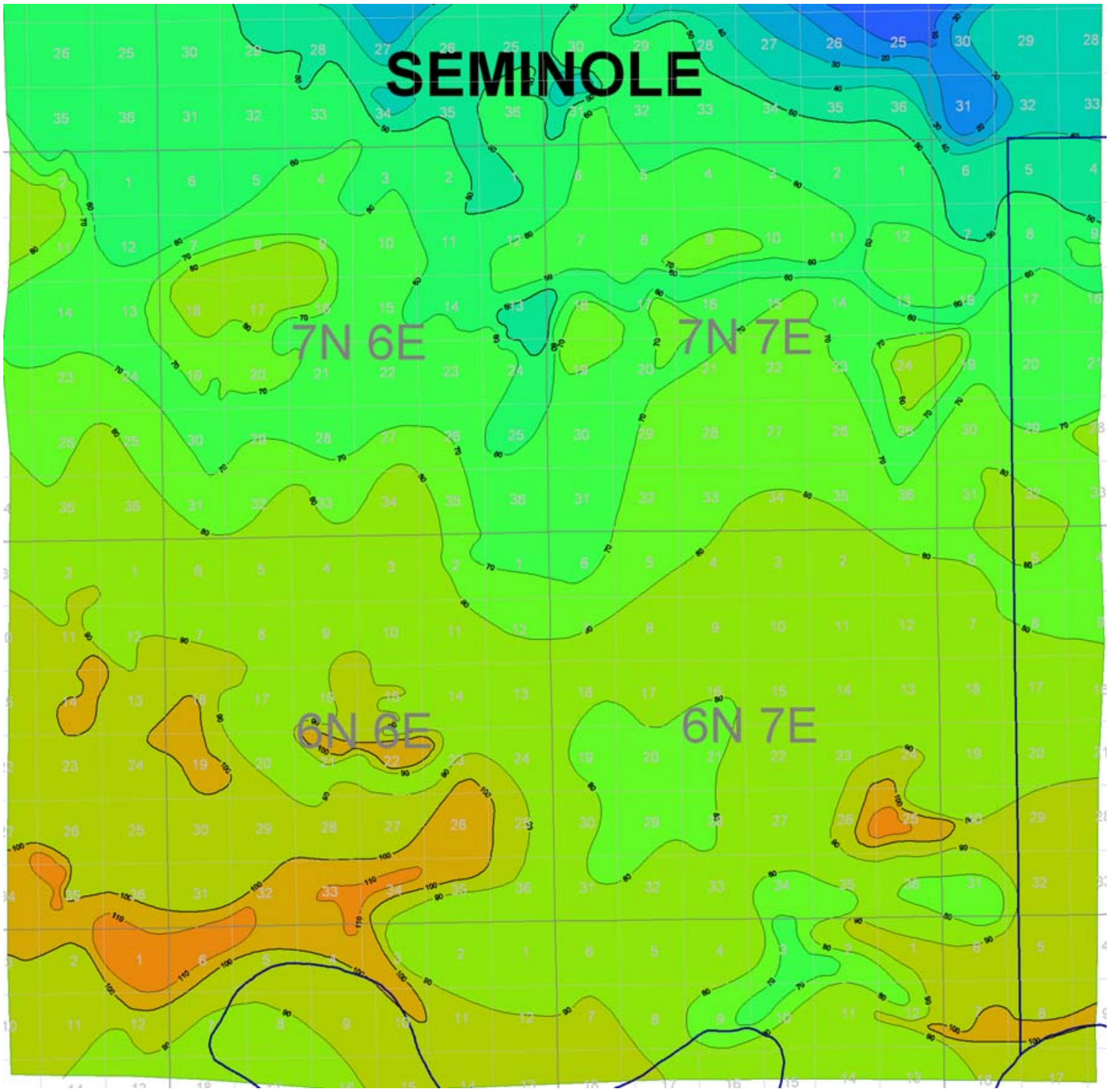

Figure 19. Study Area Map of S2 Thickness, 10’ contour interval (also found in Plate 8)

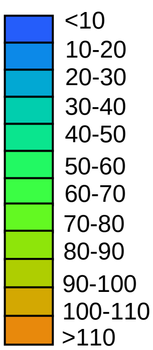

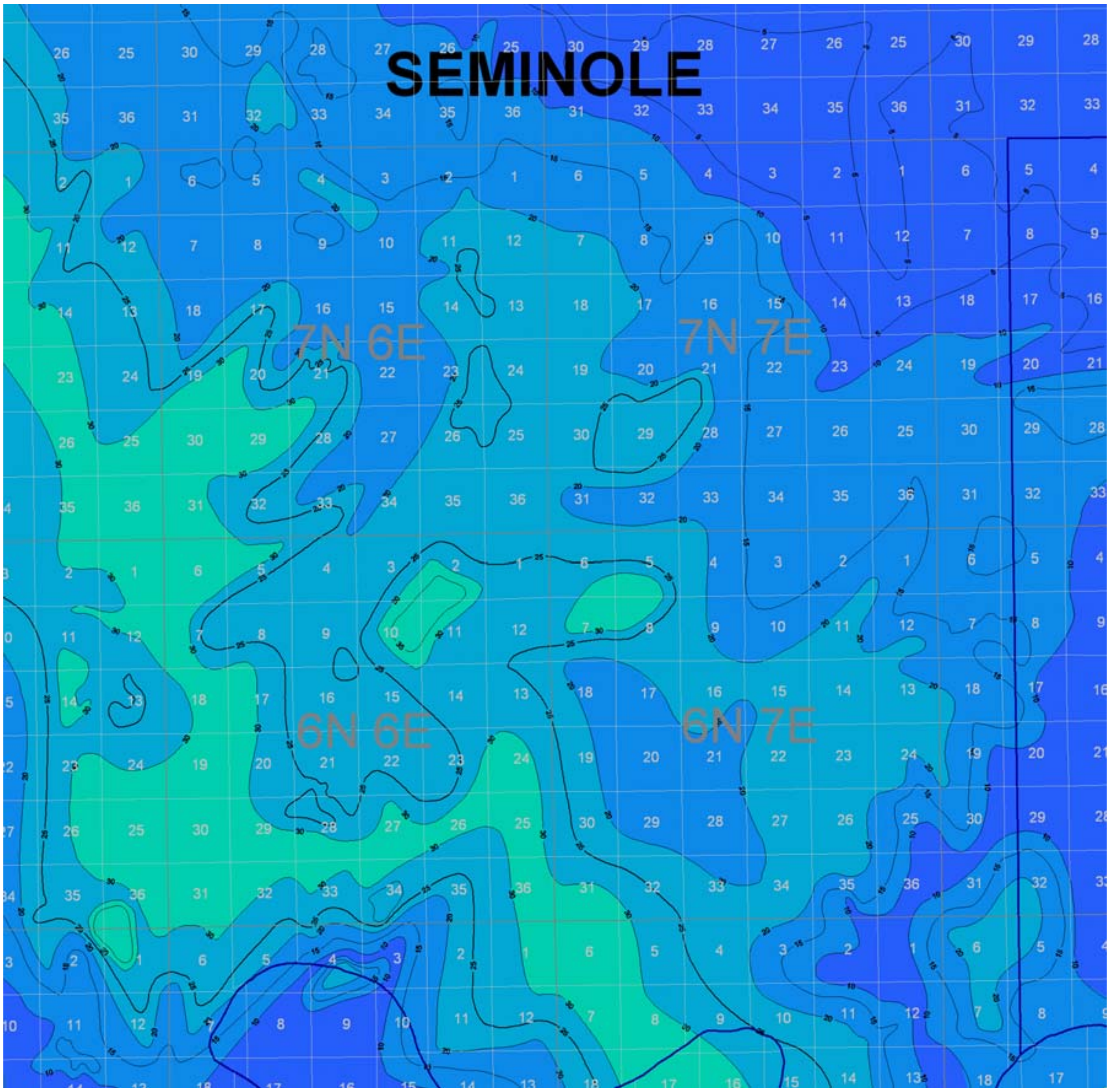

Figure 20. Study Area Map of S3 Thickness, 5' contour interval (also found in Plate 8)

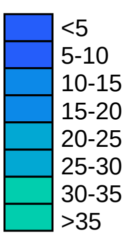

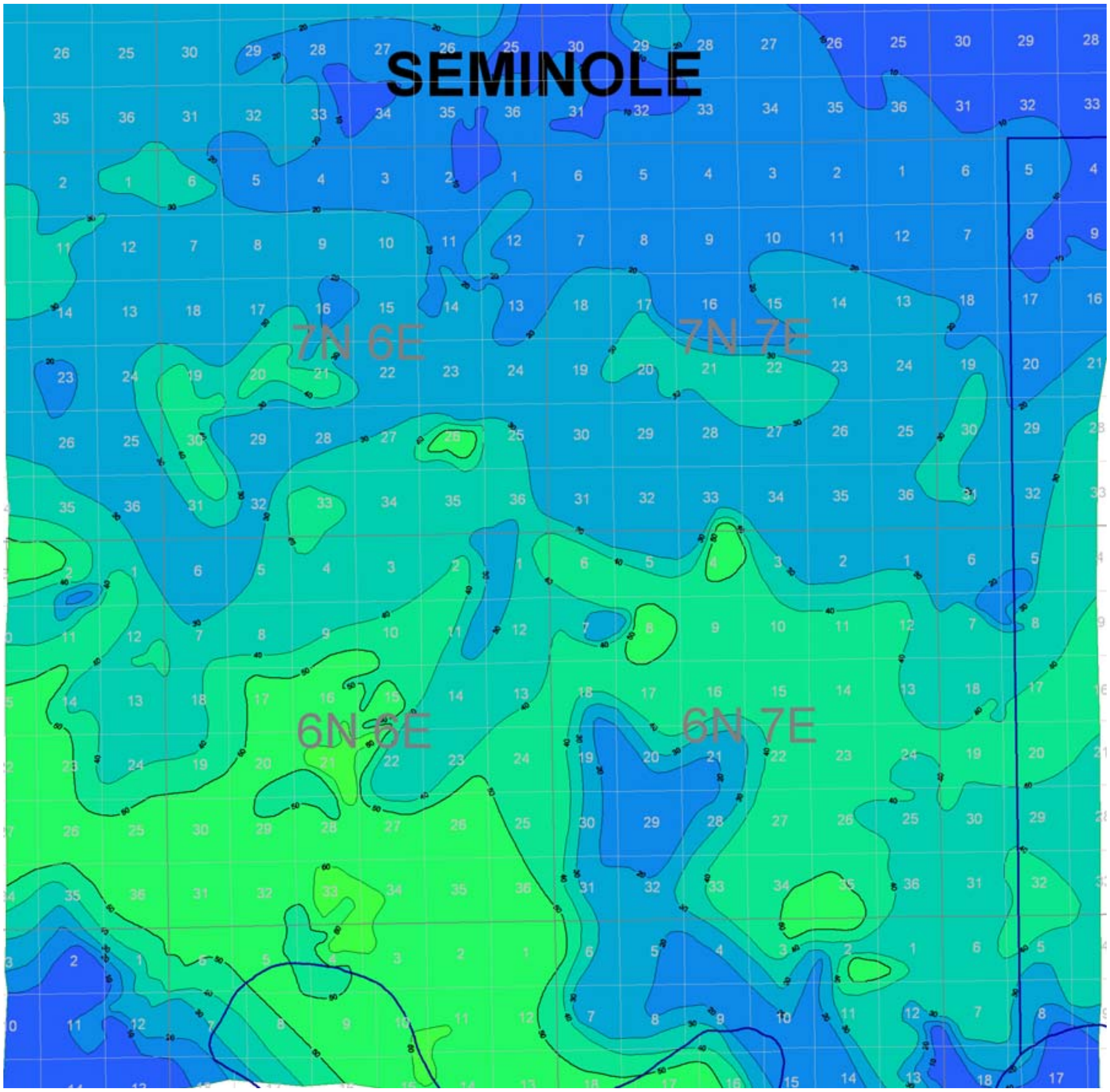

Figure 21. Study Area Map of S4 Thickness, 10’ contour interval (also found in Plate 8)

<10
10-20
20-30
30-40
40-50
50-60
>60

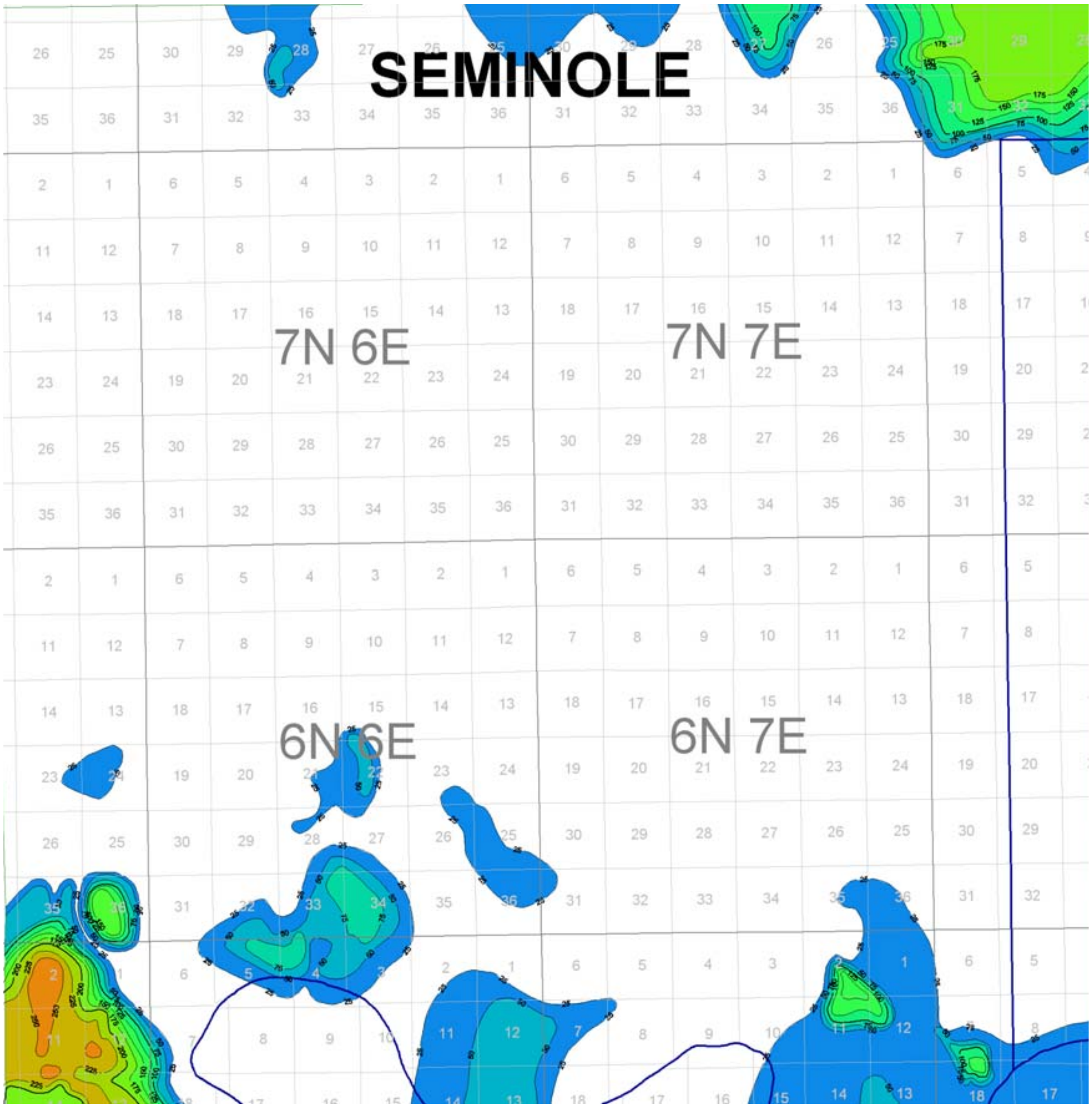

Figure 22. Study Area Map of Hunton Group thickness, 25' contour interval. This figure is also found in Plate 7.

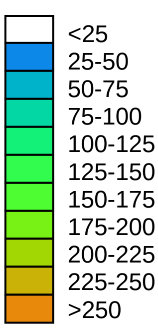

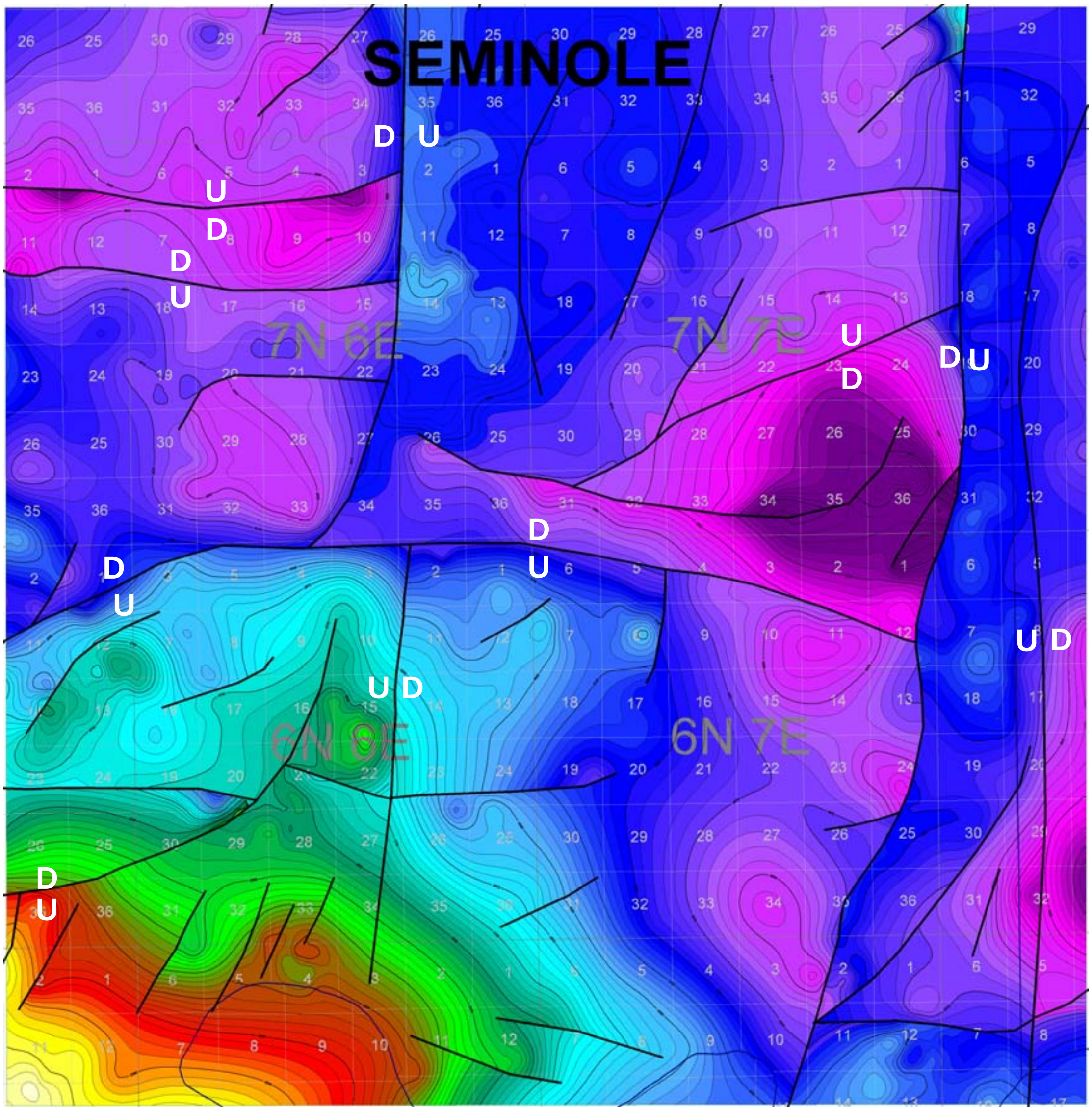

Figure 23. Map of study area showing faults and structural attitude of the top of the Viola Group relative to sea level datum. Cooler colors represent structurally lower portions of the study area, whereas warmer colors represent structurally higher areas. The contour interval is 25 feet. This figure is also found in Plate 6. Structural deformation is apparently post-Woodford as no relationship between present structural attitude and Woodford Shale thickness was evident.

A structure map of the top of the Viola Group (Figure 23, Plate 6) was created by gridding and contouring subsea Viola Group tops, using a minimum curvature algorithm. Fault placement and interpretation was aided by over thirty 2-D seismic lines, spanning 121 line miles (Figure 24). A sample line, OD-004, used to create the Viola Group structure map, is shown in Figure 25.

Normal faulting is common in the study area. The structural grain or attitude of the area is dominated by a series of north-south trending and east-west trending faults. Most production in the study area is controlled by the large N-S trending normal faults; hydrocarbons are generally found on the upthrown block as the faults are a component of the anticlinal traps. In the far eastern portion of T.7N., R.7E. and T.6N., R.7E., there is a large N-S fault with approximately 400-500’ of throw, down to the west. A large E-W fault with roughly 200-250’ of throw, down to the north, runs along the northern edge of townships T.6N., R.6E. and T.6N., R.7E., across the middle of the study area.

Some faults appear to terminate against others. Compressional structures, i.e. reverse faults, are found at the intersection of the N-S and the E-W faults. An example of an apparent reverse fault is seen on seismic line OD-004 through section 36 of T.7N., R.7E. and section 31 of T.7N., R.8E. (Figure 25).

In T.7N., R.6E., two E-W trending faults located in sections 3, 4, 5, and 6, and 15, 16, 17, and 18, respectively, terminate against a N-S trending fault that cuts across sections 3, 10, 15, 22, 27, and 34. This N-S fault terminates near the southern end of the township and has throw down to the west with roughly 350’ of offset. The western part of the study area, the N-S trend transitions into an E-W trend. In the southwest corner of the study area (T.6N., R.6E.), production appears to be controlled by small pop-up features. These features are predominately post-Woodford (Pennsylvanian Orogeny) and do not affect Woodford Shale thickness.

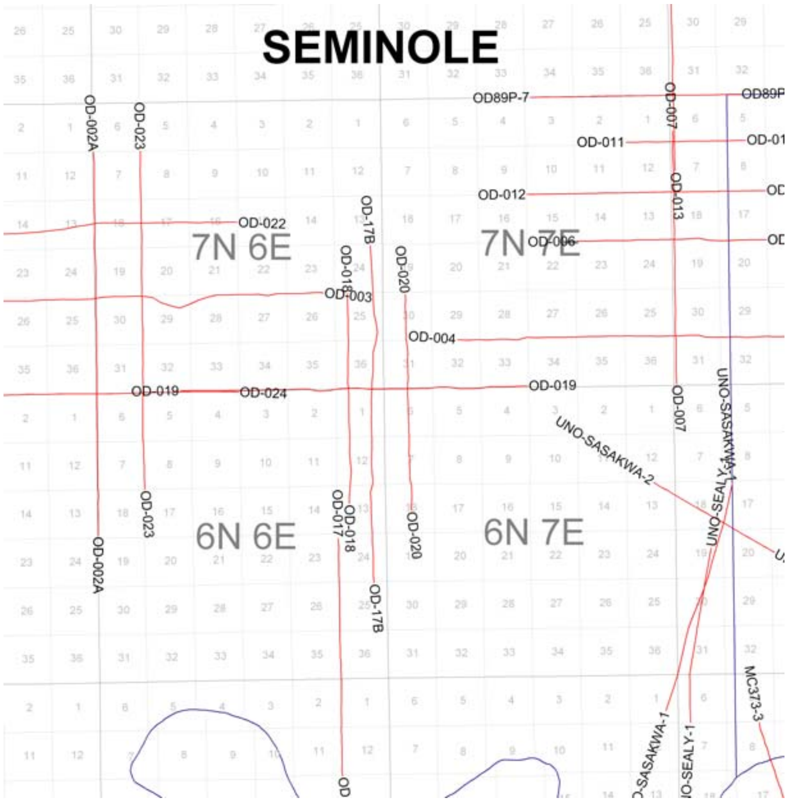

Figure 24. Map of Study Area showing location of available 2-D seismic lines.
This figure is also found in Plate 6.

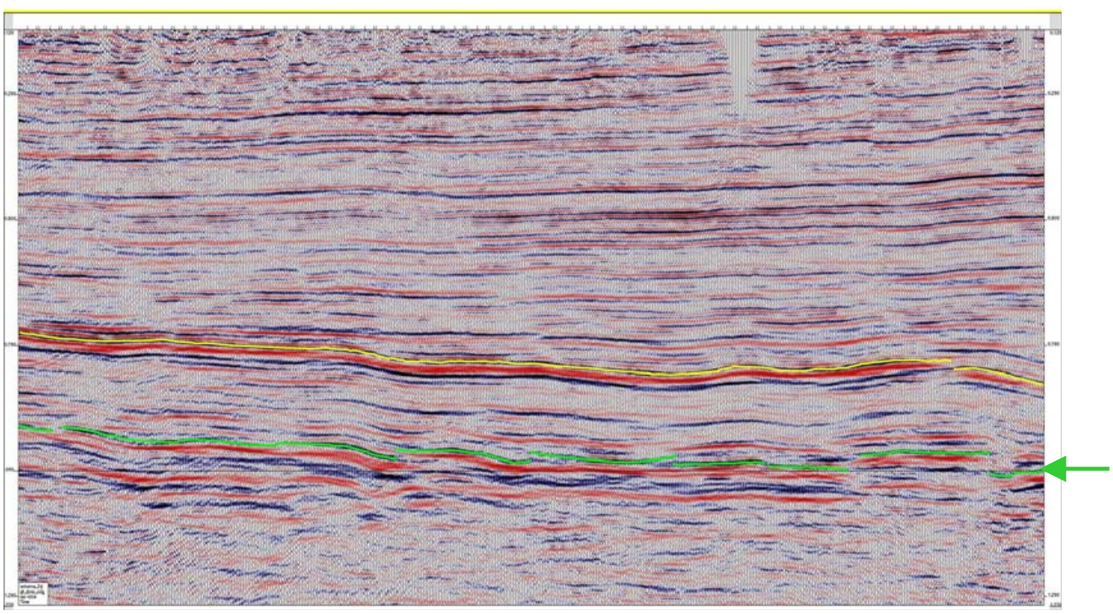

Figure 25. Interpreted seismic line (OD-004) showing the Viola Group (green arrow) reflector.
This figure is also found in Plate 6.

Woodford Shale depositional thickness is controlled by the presence of the Hunton Group. The Hunton Group is thickest in the northeast and southern portions with the majority of the study area having little or no Hunton Group (Figure 22, Plate 7).

Mapping of Subunits

The four subunits established using wire-line logs and calibrated with the Circle Creek #1 core (Figure 9), are S1, S2, S3, and S4. Mapping of these units was preferred over sequence stratigraphic mapping of cycles of transgression and regressions as these are not easily seen in logs or in core, and because there is not a full gamma-ray on most available logs. However, four subunits were defined and delineated based on changes in electric log responses/characteristics.

Wells in which S4 is present also contain the three other subunits. When S4 is absent, but S3 is present, S1 and S2 are also present. The Nancy 1-17H, which located outside the study area in section 17, T.10N., R5E. encountered only S1 and S2. However the Hunton Group is present in the well (Figure 22). This relationship is observed in several areas outside the study area, however, within the study area all subunits are present in all wells.

S1 is thickest to the southwest and thins to the northeast (Figure 18). The thickness map for S1 is similar to the overall Woodford thickness map. In general, S2, S3, and S4 (Figures 19-21) are also thicker to the southwest and thin to the northeast. In the far southwestern corner of the study area, S4 is thin. In this corner, and the northeast corner, thin S4 corresponds to the presence of a thicker Hunton Group. This relationship fits with the model of onlap deposition as the lower Woodford Shale subunits may not have been deposited on Hunton Group paleo-highs, but may thicken in paleo-lows.

CHAPTER V

PETROGRAPHIC ANALYSIS

Overview

Two cores were analyzed in the Chesapeake Energy Corporation Reservoir Technology Center (RTC) in Oklahoma City: the Ingram Exploration, Circle Creek #1, located in Section 13, T.6N., R.6E. and the Chesapeake Nancy 1-17H from Section 17, T.10N., R.5E. (Figure 26). Core photos are available in Appendices I and II. The Nancy 1-17H is located outside the four-township study area, roughly 25 miles northwest of the Circle Creek #1. As a result, it is analyzed in less detail, however, important observations were made in this core.

Lithologies of the cored intervals from the Circle Creek #1 were assigned based on thin-section analysis and abundance of constituents established by the X-ray diffraction (XRD) data (Plate 1). Additional petrographic analysis included imaging argon-ion polished wafers with a scanning electron microscope. XRD data is also available for the Nancy 1-17H (Plate 3); however, thin sections are not available for the Nancy 1-17H. No detailed lithologies have been assigned for the Nancy 1-17H; however, generalized lithologies are noted.

A Tight Rock Analysis (TRA), shown in Plates 2 and 4, was also completed for both cores. TRA examines bulk density, porosity, water saturation, gas saturation, mobile

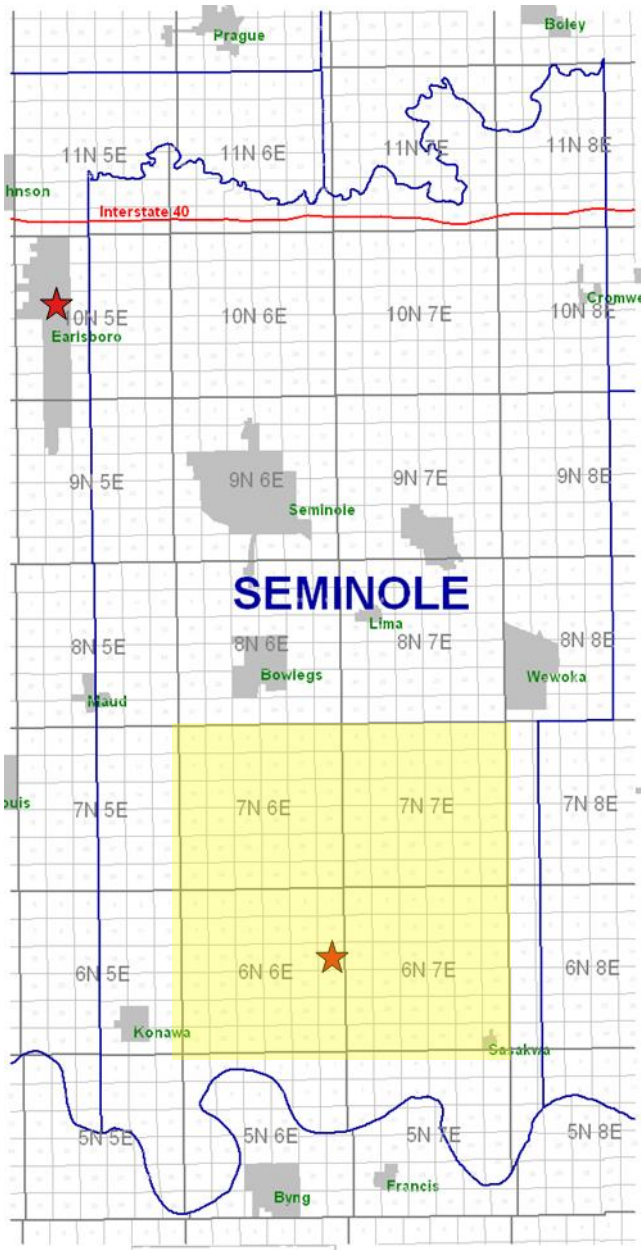

Figure 26. Map of Seminole County, Oklahoma, showing the study area in yellow and the locations of the two cores analyzed (core locations indicated by ★).

oil saturation, gas-filled porosity, expandable clay water, bound hydrocarbon saturation, bound clay water, pressure decay permeabilities, mobile oil porosity, and mobile oil and gas filled porosity as percentages of bulk volume. Permeability values are not yet available for the Nancy 1-17H. Portions of the TRA are not included in this thesis due to the proprietary nature of the data.

Thin-section images are shown in plane polarized light (PPL) as cross polarized light (XPL) yields a poor image (black-out). XPL is typically used for mineral identification in mudstones, however, due to the presence of organic matter (which is isotropic) XPL images tend to be very dark. This is also true to a degree in PPL. The finely disseminated organic matter can absorb a significant amount of light, particularly when the organic matter is mature, having vitrinite reflectance values greater than 1.5% (gas window). In the Circle Creek #1, as well as the Nancy 1-17H, the Woodford Shale contains oil; therefore, the organic matter is not as dark as is seen in gas shales. However, the organic matter still absorbs some light and as a result exposure time was increased to create these images.

Samples for scanning electron microscope (SEM) examination were made using an argon-ion polishing technique. Data gathered by SEM allows for the determination of matrix composition, texture, porosity types, pore shape/size, and nature of the organic component. Most SEM images are shown with secondary electron imaging (SEI) while others are shown with backscattered electron compositional imaging (BEC). SEI is used to image porosity in the organic material, as it reflects surface texture (Goldstein et al., 2003). BEC reflects differences in electron density- relative to quartz, clay, and dolomite. Constituents with higher electron density, i.e. pyrite, appear as the brightest components. Organic matter and empty space have very similar electron density; therefore, it is difficult to image porosity with BEC.

Spectral gamma-ray curves were generated by scanning the core using a spectral core gamma logger. Measurements are provided on six inch intervals. This data is available in Plate 9. Total organic carbon (TOC) curves were created by analyzing samples with a LECO carbon/sulfur analyzer at three to five feet intervals for both cores. This data is available in Plate 10.

Circle Creek #1

The Ingram Exploration, Circle Creek #1 was cored from 3,543 feet to 3,807 feet (core depth). The core includes the basal portion of the Mayes Limestone (3,543' to 3,558.5'), the Woodford Shale (3,558.5' to 3,800'- except for a missing section from 3,618.7' to 3,649' core depth), and the top of the Sylvan Shale (3,800' to 3,807'). The Circle Creek #1 recovered 15.5' of the Mayes Formation, a silty/argillaceous dolostone; 211.2' of the Woodford Shale; and roughly 7' of the Sylvan Shale, a silty/argillaceous mudstone. The lithotypes encountered by the Circle Creek #1 and their corresponding depths are shown in Plate 1, which also details the weight-percent of constituents determined from X-ray diffraction. These constituents include: total clay, quartz, potassium feldspar (k-spar), plagioclase, apatite, pyrite, marcasite, calcite, dolomite, illite/smectite, illite + mica, chlorite, and kaolinite, all of which are expressed as a normalized weight-percent totaling 100%.

In addition to the petrolog description, cherty layers were measured and summed in order to assign a decimal-percent index value for each foot (Figure 27, Plate 5). A zero value on Chert Index scale represents deposits that contain more silt and no chert. A value of one on the Chert Index scale represents a bed that is 100% chert, with no silt or clay-shale. A chert index is assigned to each foot of the core by counting the chert layers,

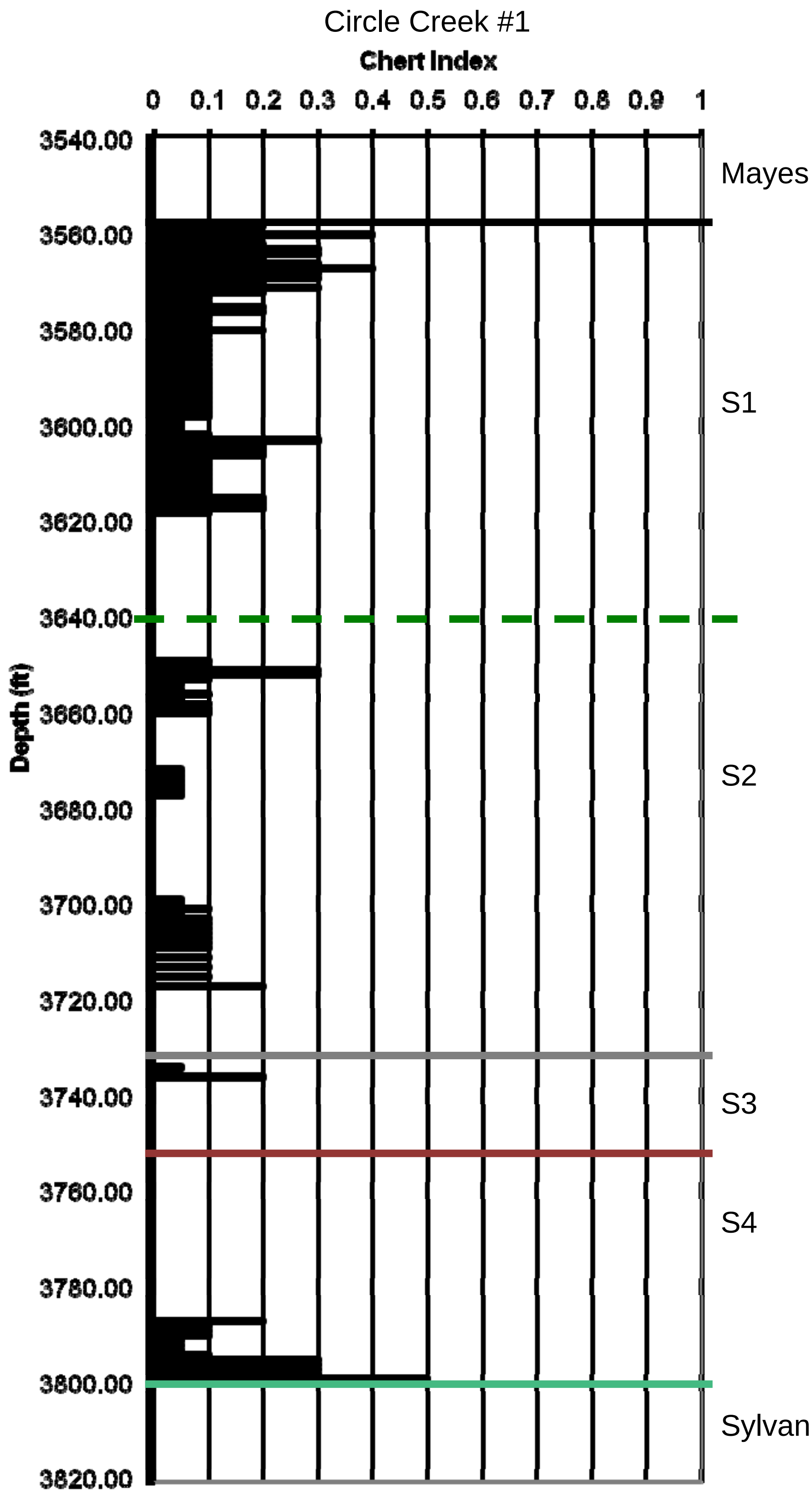

Figure 27. Chert Index Graph, decimal fraction of chert per foot, with intervals labeled (missing section from 3,618.7'-3,649'); (also available in Plate 5)

measuring their thickness, and assigning a decimal-fraction to each foot. The highest chert index observed in the Circle Creek #1 is 0.5 (indicating the one foot interval is ~50% chert), while the lowest is 0.0 (indicating the one foot interval is 0% chert). The richest chert intervals are found from 3,797'-3,800', where large chert nodules are observed. From 3,559'-3,661' core depth, cherty layers are found throughout the approximately 100' thick section, which has the most cherty laminations. There is very little to no chert observed from 3,543.5'-3,558', 3,661'-3,672', 3,678'-3,699', 3,718'-3,734', 3,737'-3,787', and 3,801'-3,807' core depth.

Natural fractures were counted to create a fracture frequency graph (Figure 28, Plate 5) to compare fracturing and lithotype. Most fractures are located between 3,687' and 3,698' core depth, where 1-2 natural fractures per foot were observed. Natural fractures are also found between 3,588'-3,596', 3,604'-3,606', 3,772'-3,784'. No natural fractures were observed during core analysis from 3,543'-3,588', 3,605'-3,686', 3,699'-3,771', and 3,784'-3,803' (end of core).

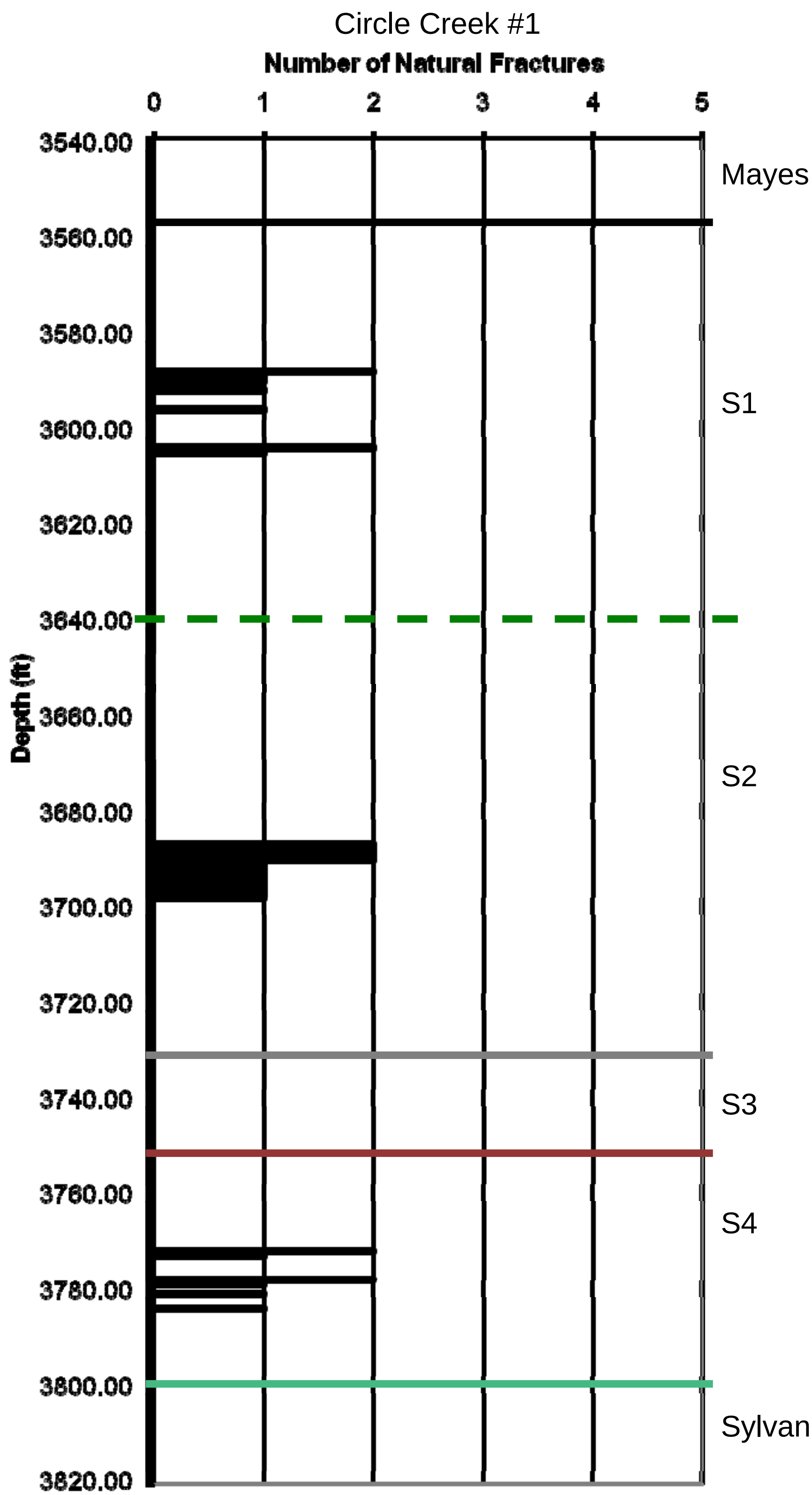

Figure 28. Fracture Intensity Graph, number of natural fractures per foot, with intervals Labeled (missing section from 3,618.7'-3,649'); (also available in Plate 5)

Thin-Section and SEM Analysis

The Mayes Formation, the majority of which is classified as a silty, argillaceous dolostone, was cored from 3,543’-3,558.5’ and consists of clay, sand, and silt detrital components as well as the authigenic minerals: dolomite, ferroan dolomite, pyrite, and chert (Figure 29). The clay matrix is predominately illite and authigenic dolomite is abundant. The approximate silt and sand content is 60%, and accessory grains include glauconite (which is common) and mica. Skeletal grains include shell and conodont fragments. Minor elongate, dark brown organic particles are also found. A bed with abundant glauconite begins at 3,555.4’ and extends to 3,556.8’. Figure 30 is a thin-section image from 3,555.9’, from the bed at the contact of the Mayes with the underlying Woodford Shale. Glauconite is a reliable indicator of slow sedimentation rate in marine settings and is found at the bases of transgressive/regressive cycles (Amorosi, 1995).

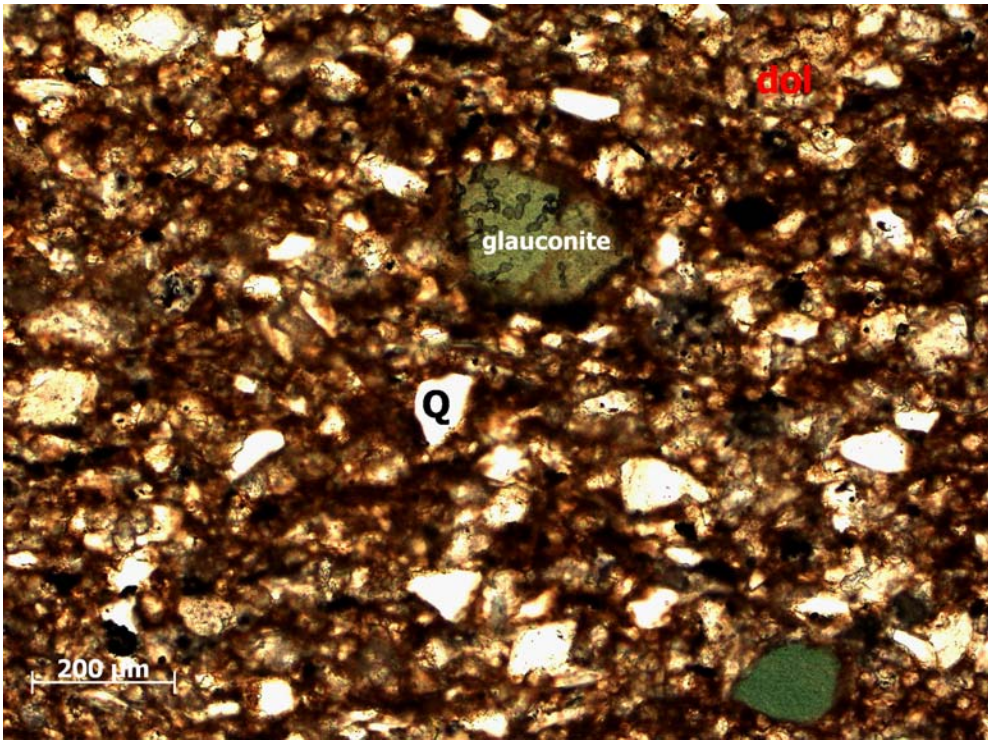

Figure 29. Thin section photomicrograph image from 3,554.1' core depth, showing dolomite (dol), quartz (Q), and glauconite (glauconite). This dolomitic, silty mudstone is located near the base of the Mayes Formation.

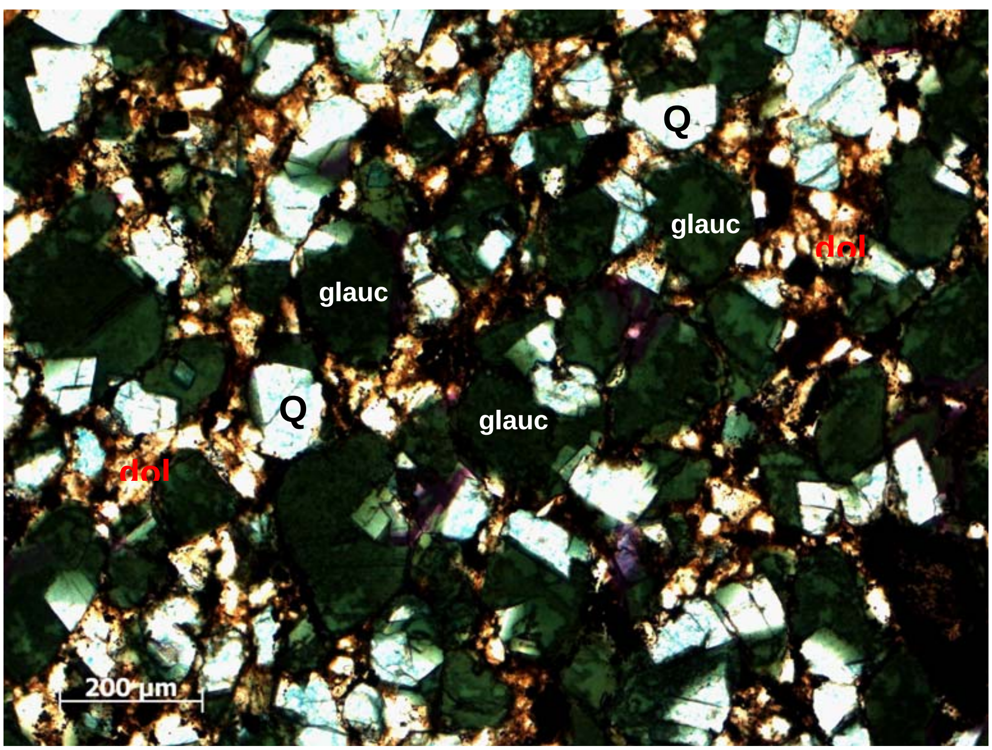

Figure 30. Photomicrograph image from 3,555.9' core depth showing abundant glauconite (glauc). This dolomitic, glauconitic sandstone, is found at the contact between the Woodford Shale and overlying Mayes Formation. Quartz (Q) and dolomite (light blue rhombs) are common.

The top of the Woodford Shale is located at 3,558.5 feet core depth. The uppermost subunit, S1, was cored from 3,558.5’ to 3,618’ and is classified as an organic-rich, siliceous mudrock. Authigenic minerals in this interval include silica cement (matrix), quartz, chert, pyrite and ferroan dolomite; there is also carbonate cement in the matrix. The silt and sand content is roughly 15-20%. The interval is dominated by a silica- and illite-rich matrix, and can be laminated or non-laminated. If present, laminations occur as a result of variation in silica content; they may be cherty or pyrite-rich. Accessory grains include mica and poorly preserved radiolarians. There are also abundant algal macerals, some of which are partially in-filled or replaced by authigenic quartz or chert. There are other organic particles, which are commonly brown, that are also often partially in-filled by pyrite.

Pyrite is black in thin-section due to its opaque nature. Round to sub-round chert grains that are 50-150 microns in diameter are likely radiolarians (Figures 31 and 32). Orange-brown, elongate grains are interpreted as algal macerals. In Figure 31, algal macerals are aligned with bedding, and pyrite is seen inside chert-replaced radiolarians as opaque masses with cubic morphology. Phosphate nodules are small and rare, but do occur in the upper 20 feet of the subunit. The dark color of the thin-section is the result of the high clay content.

Figure 32, contains abundant chert and is classified as a chert. The numerous radiolarians are in-filled with chert, in the form of chalcedony, and/or pyrite. Chalcedony is microfibrous (microcrystalline, fibrous) quartz. In general, it is observed that algal macerals and radiolarians are more compacted in muddy intervals than in siliceous intervals.

SEM images from 3,574.9’ (Figures 33 and 34) reveal the platy nature of the clays, “popcorn” appearance of silica cement, angular silt grains bounded by silica cement, and spongy appearance of organic matter, which contains porosity. Increased magnification reveals the platy nature of the illite lining the pore spaces as well as a better view of the organic matter. At 3602.3’ (Figures 35 and 36) framboidal pyrite, the elongate shape of mica grains, and spongy character of the porous organic matter are observed. Increased magnification (Figure 37) reveals pore space within the organic matter.

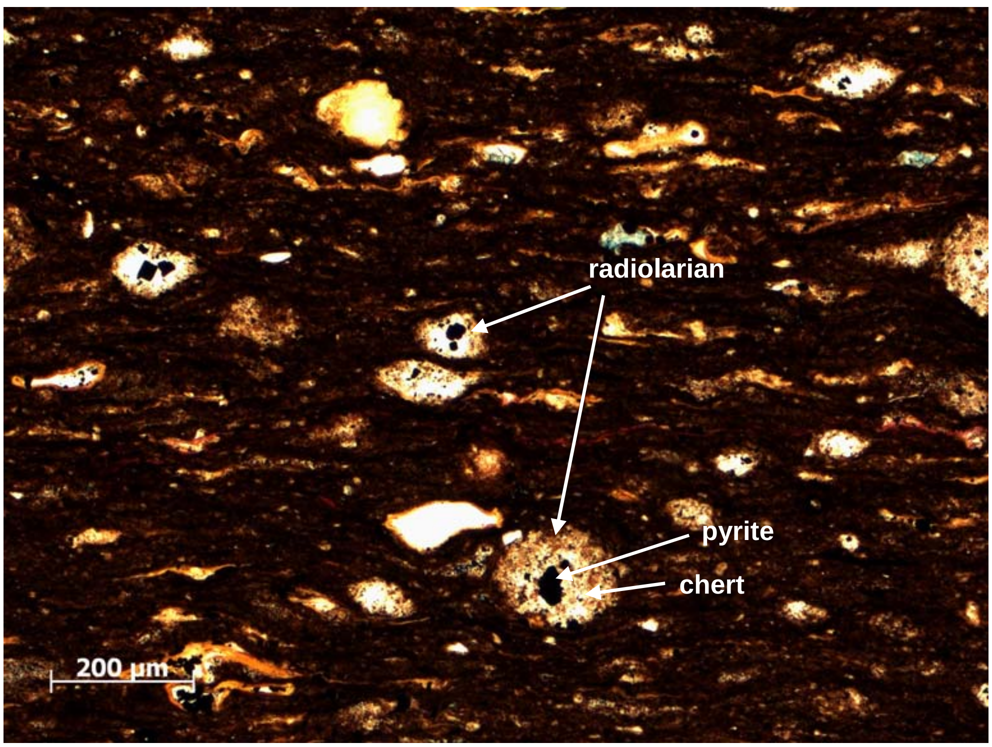

Figure 31. Photomicrograph from 3,575.8’ core depth, a siliceous argillaceous mudrock from S1. Constituents include radiolarians, abundant algal macerals, pyrite, quartz, and clay.

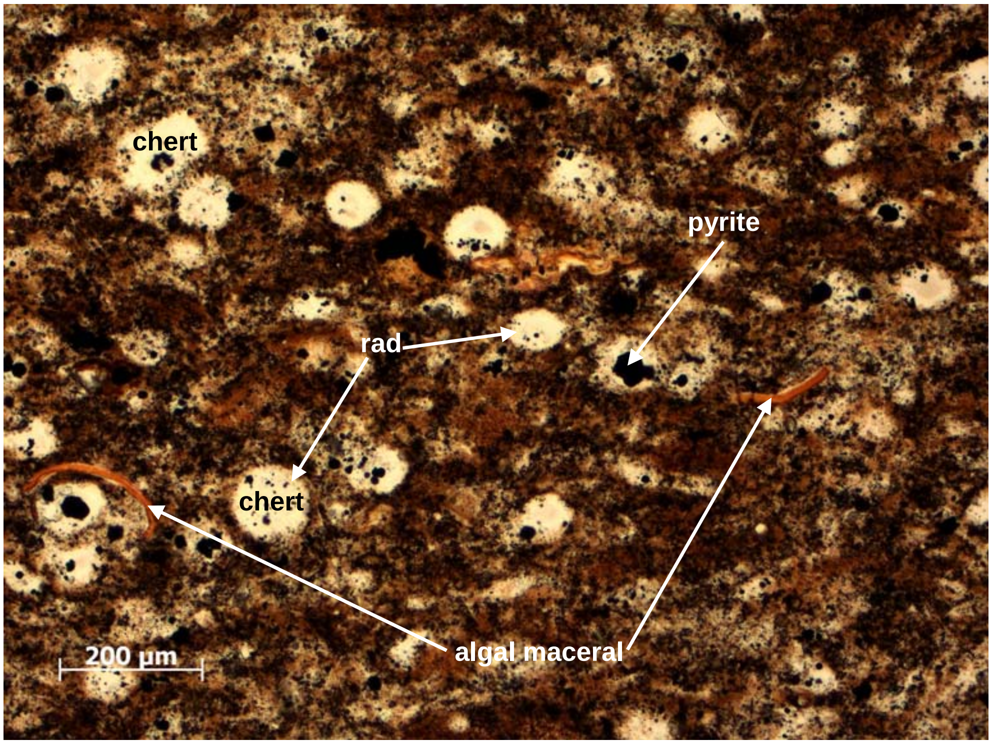

Figure 32. Photomicrograph of the Woodford Shale from 3,605.5’ core depth, a chert-rich bed within S1. This sample contains radiolarians (rad) replaced by chert (chert), algal macerals, and pyrite.

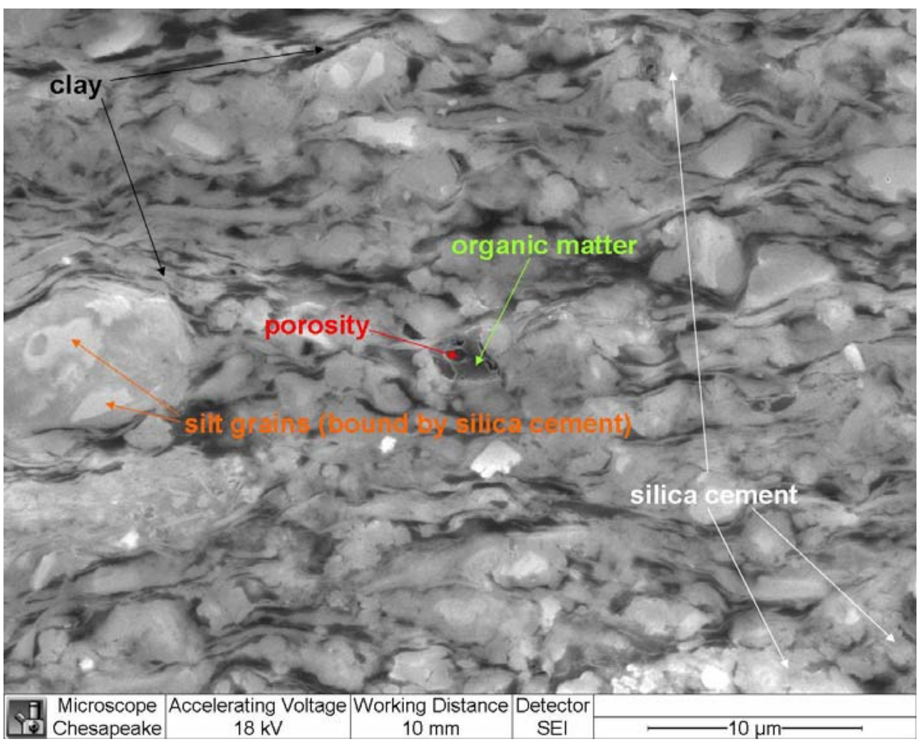

Figure 33. SEM image from 3,574.9’ core depth, a siliceous/argillaceous mudrock from S1, showing common constituents of the Woodford Shale. (Image taken by Rick Urash).

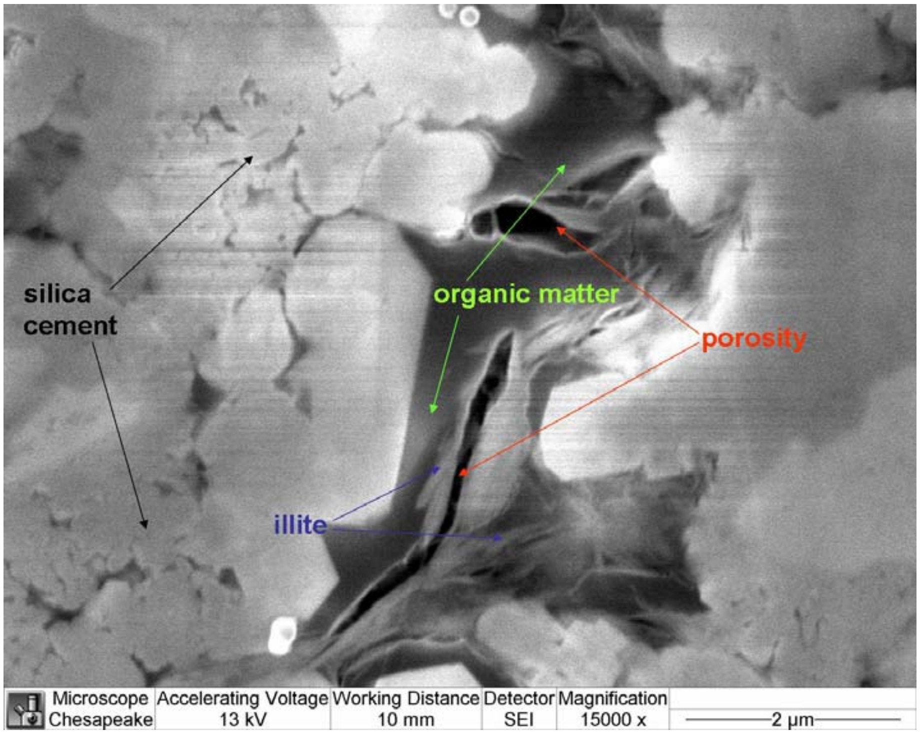

Figure 34. SEM image from 3,574.9' core depth, a siliceous/argillaceous mudrock from S1 of the Woodford Shale. Authigenic illite (illite) lines porosity developed in organic matter. (Image taken by Rick Urash).

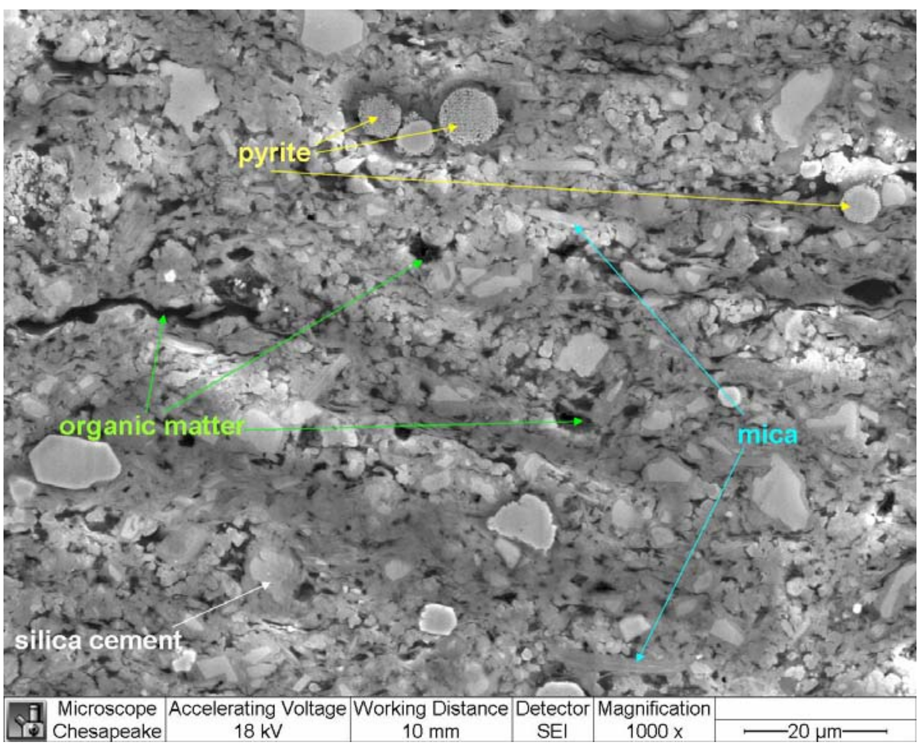

Figure 35. SEM image from S1 of the Woodford Shale showing silt grains, silica cement, pyrite, mica, and organic matter from the Ingram Exploration Circle Creek #1. Depth 3,602.3'. (Image taken by Rick Urash).

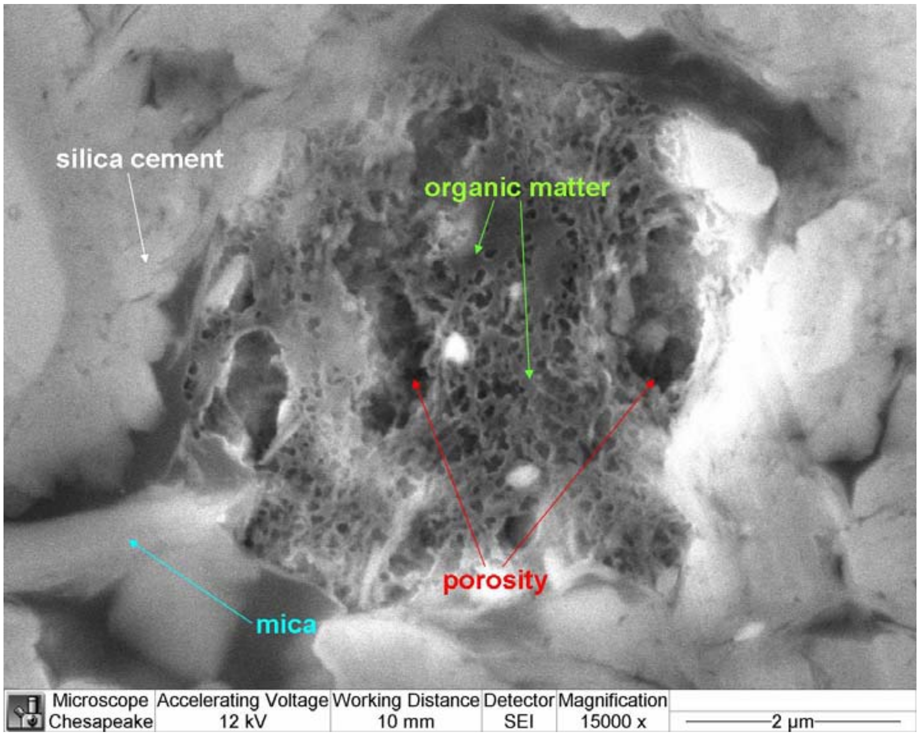

Figure 36. SEM image from S1 of the Woodford Shale showing spongy porosity developed In organic matter. Depth 3602.3 feet, Circle Creek #1. (Image taken by Rick Urash).

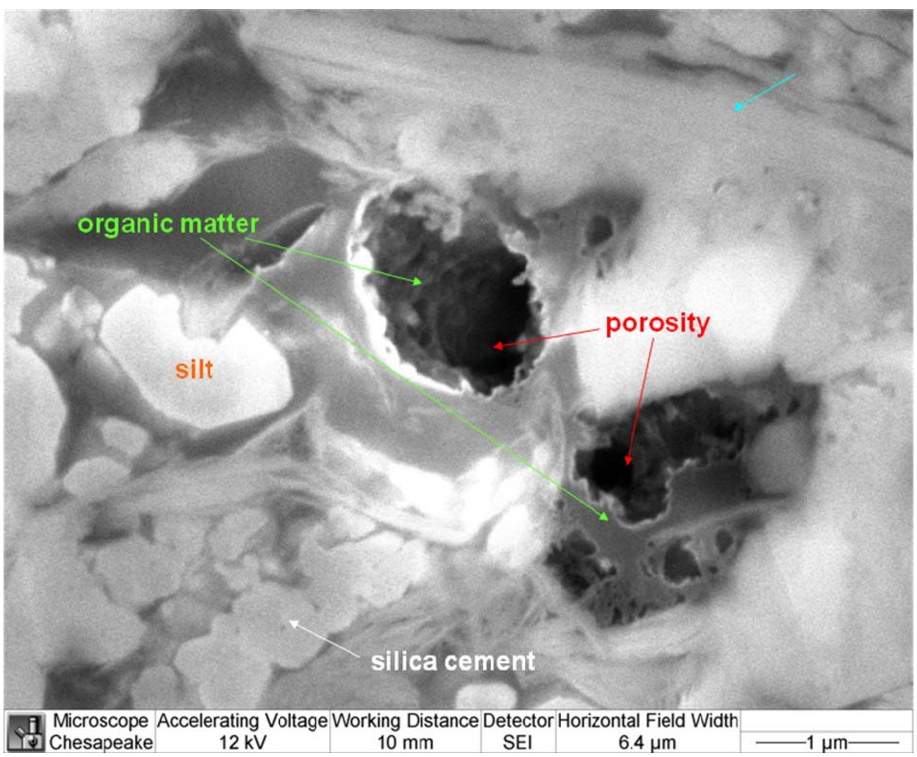

Figure 37. SEM image showing porosity within organic matter, Ingram Exploration Circle Creek #1 Depth 3.602.3’. (Image taken by Rick Urash).

Subunit 2 (3,650’-3,730’ core depth) consists of several lithotypes including muddy chert, siliceous clay-rich mudrock, organic-rich dolomitic siliceous silty mudrock, siliceous silty mudrock, and organic-rich muddy chert. The matrix is dominated by silica, illite, or a combination of both. The subunit transitions from laminated to faintly laminated at the top, to non-laminated at the base. Silt and sand content varies from 10-20%. Accessory grains include mica, with lenticular clay bodies and glauconite becoming more common with depth. Poorly preserved radiolarians are found near the top of the subunit, with conodont fragments and microfossils becoming more common with depth, however, these are still minor constituents. Authigenic minerals include silica cement, authigenic quartz, chert, pyrite, dolomite, and rare calcite and phosphate. Phosphate is more common with depth, but is still rare in this facies. Laminations are a result of variations in silica content.

In S2, algal macerals are less flattened in radiolarian/silica-rich beds (Figure 38) and more flattened in clay-rich zones (Figures 39 and 40). Pyrite is common and replaces chert, which in-filled radiolarians.

SEM images show silt grains, pyrite and an organic particle, likely an algal macerals (Figure 41). Authigenic quartz formed inside organic grains. The platy nature of the illite is evident in the enlarged image (Figure 42).

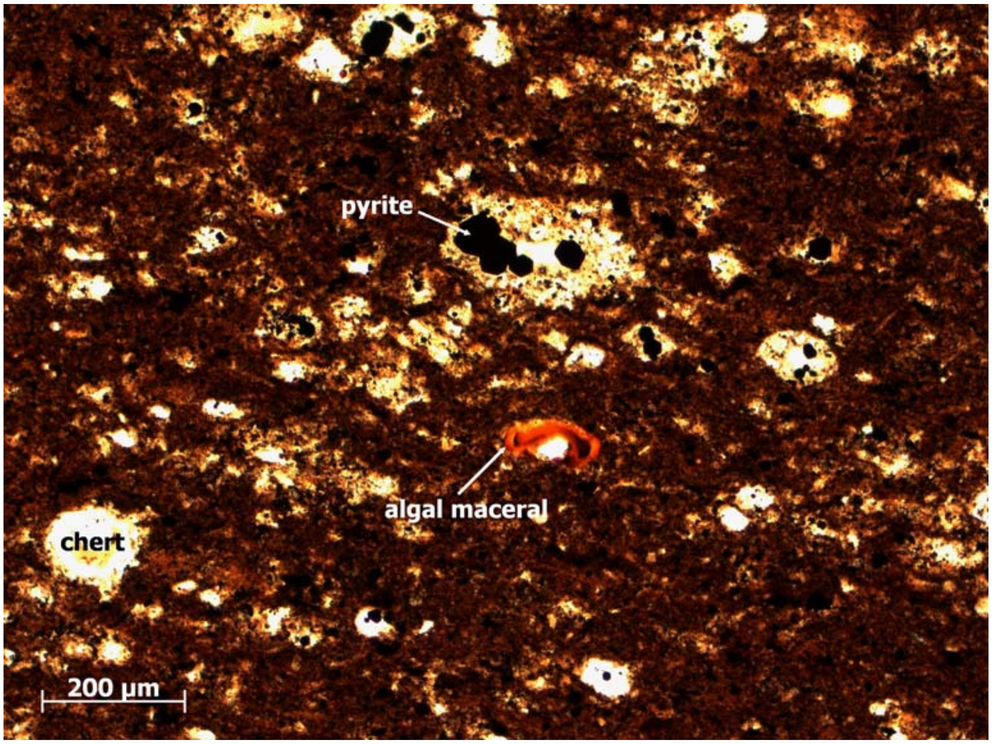

Figure 38. Photomicrograph image of a cherty zone in S2 that contains algal macerals and pyrite. Ingram Exploration, Circle Creek #1, Depth 3651.5 feet.

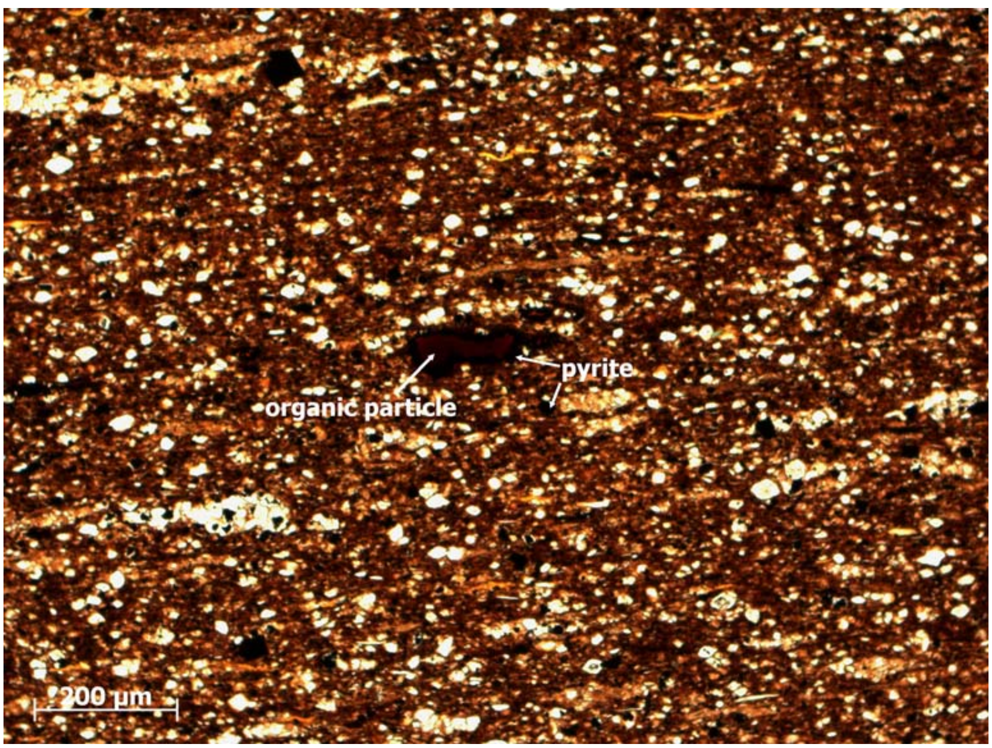

Figure 39. Photomicrograph of an argillaceous mudstone from S2, showing algal macerals, an organic particle with pyrite lining, and abundant pyrite within the matrix. Ingram Exploration, Circle Creek #1. Depth 3,678 feet.

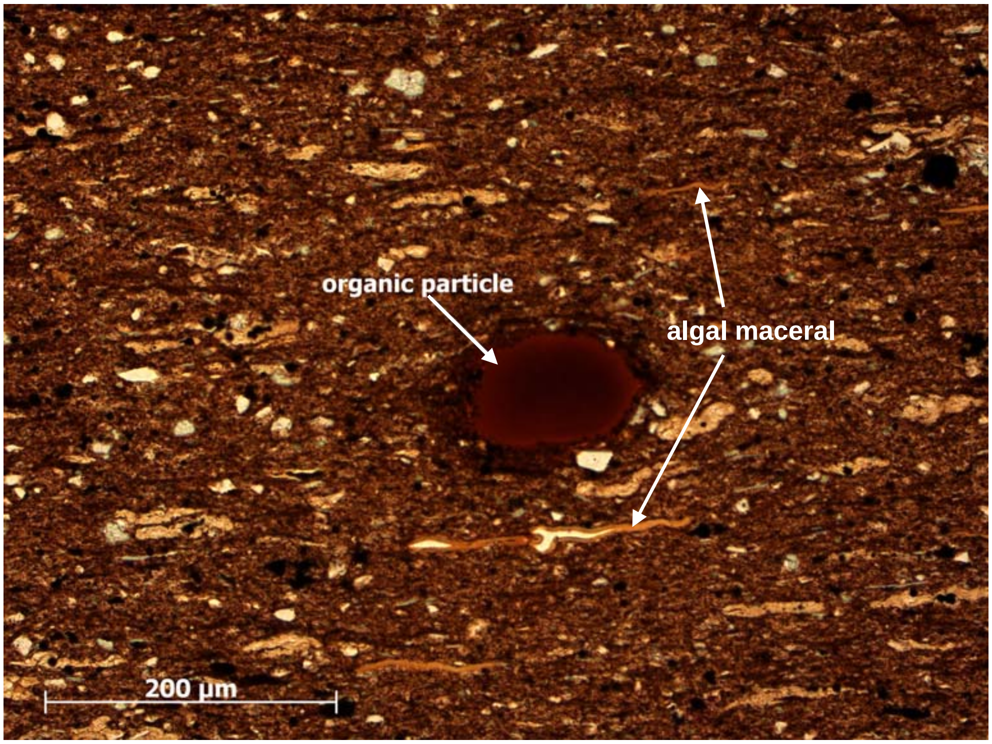

Figure 40. Photomicrograph of S2, showing an unidentified organic particle and algal macerals. Ingram Exploration, Circle Creek #1. Depth 3,715.3 feet.

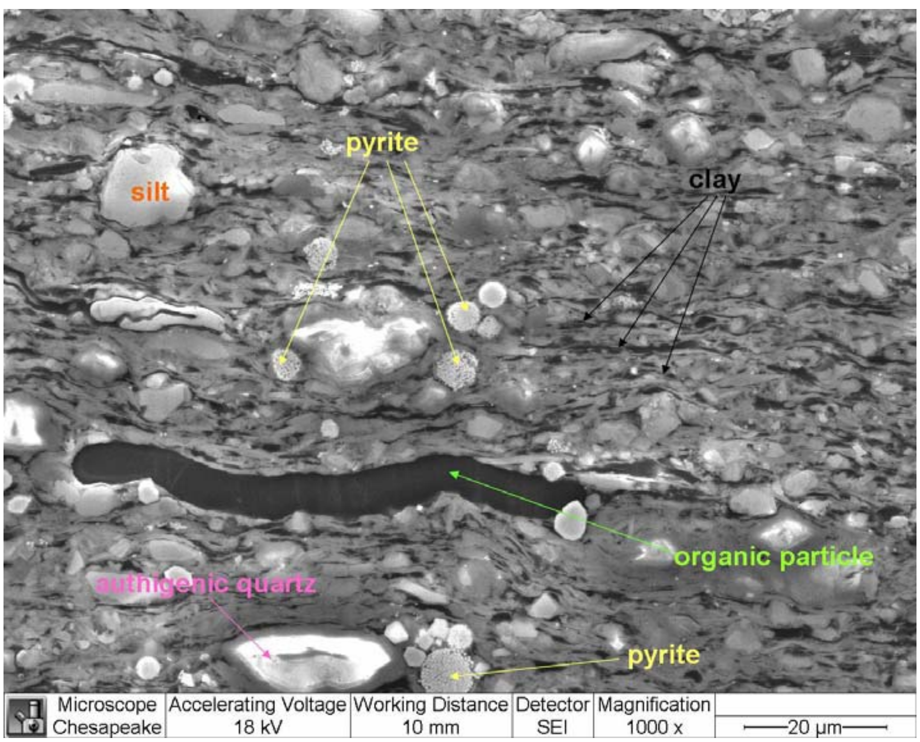

Figure 41. SEM image from S2 showing detrital and authigenic constituents including silt and clay grains, organic particles, quartz cement and pyrite. Ingram, Circle Creek #1. Depth 3,674.3 feet. (Image taken by Rick Urash).

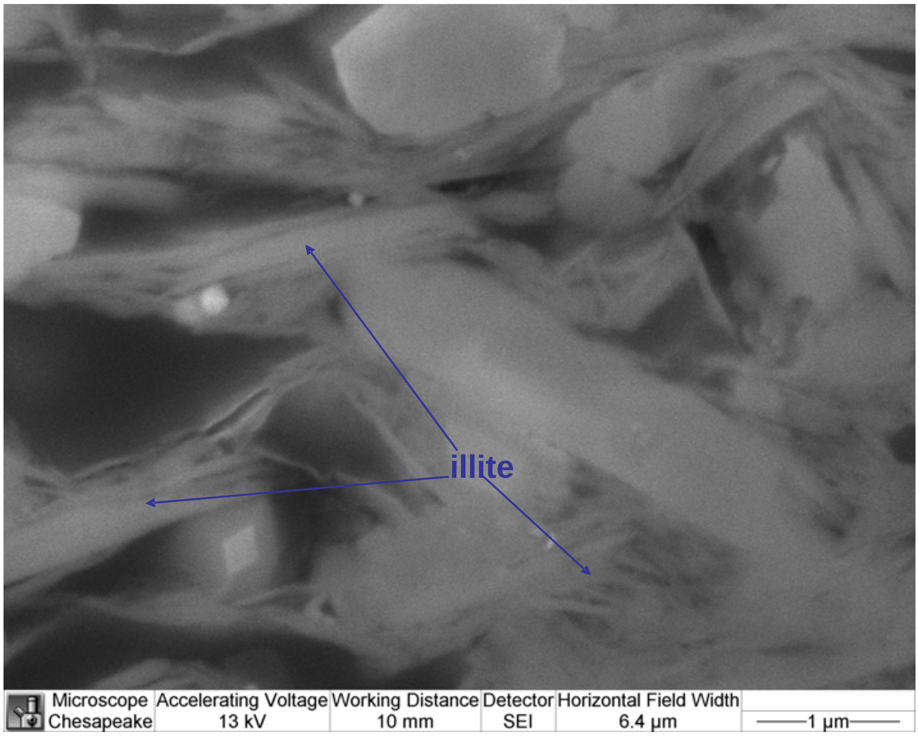

Figure 42. SEM image of authigenic illite in subunit S2 of the Woodford Shale. Ingram Exploration, Circle Creek #1. Depth 3,674.3 feet. (Image taken by Rick Urash).

Subunit 3 (3,730'-3,755' core depth) is a dolomitic, siliceous mudstone, which can be silty or clay-rich. Authigenic minerals include dolomite, quartz, chert, quartz cement, pyrite, and marcasite. The matrix is dominantly illite and dolomite. This interval consists of approximately 25% silt and sand, which is more than the amounts evident in S1 and S2. Accessory grains include mica and glauconite, with no skeletal grains observed. Minor amounts of algal macerals are present. Most of the organic matter appears flattened or compressed. S3 is laminated, which is a result of varying dolomite and organic content.

The argillaceous mudrock near the top of S3, contains small amounts of potassium ferrocyanide stained, gray-blue Fe-rich dolomite as well as pyrite, and silt grains (Figure 43). Figures 44 and 45 show abundant ferroan dolomite as well as compacted organic particles and algal macerals.

In the SEM images of S3 (Figures 46 and 47), the rhombohedral shape of the dolomite is apparent. Fe-rich rinds surrounding the dolomite appear brighter and can be seen with the backscatter electron composition imaging (BEC) due to their high electron density. Framboidal pyrite is also brioght for the same reason. Organic matter and porosity are not easily discriminated as they have similar electron densities; therefore, they both appear as dark/black areas in BEC.

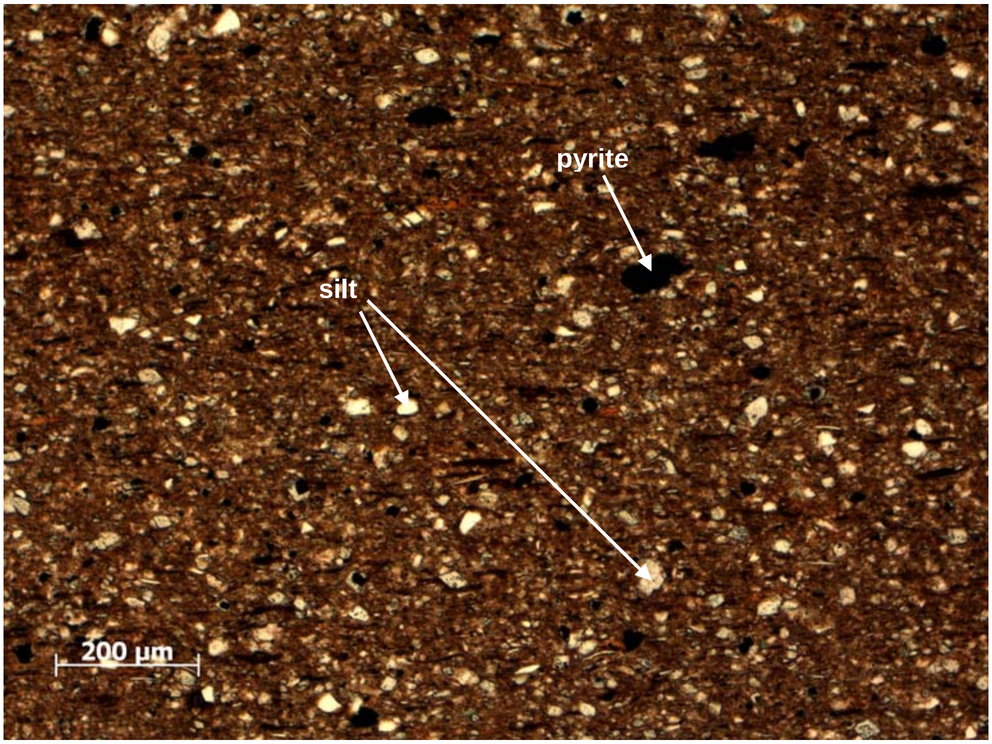

Figure 43. Thin-section photomicrograph of an argillaceous mudstone from S3 of the Woodford Shale. Detrital silt, pyrite, and iron-rich dolomite (Fe-dol) are common. Fe-dol appears as small blue-green rhombs and may be difficult to see in this image. Ingram, Circle Creek #1. Depth 3,734.2’.

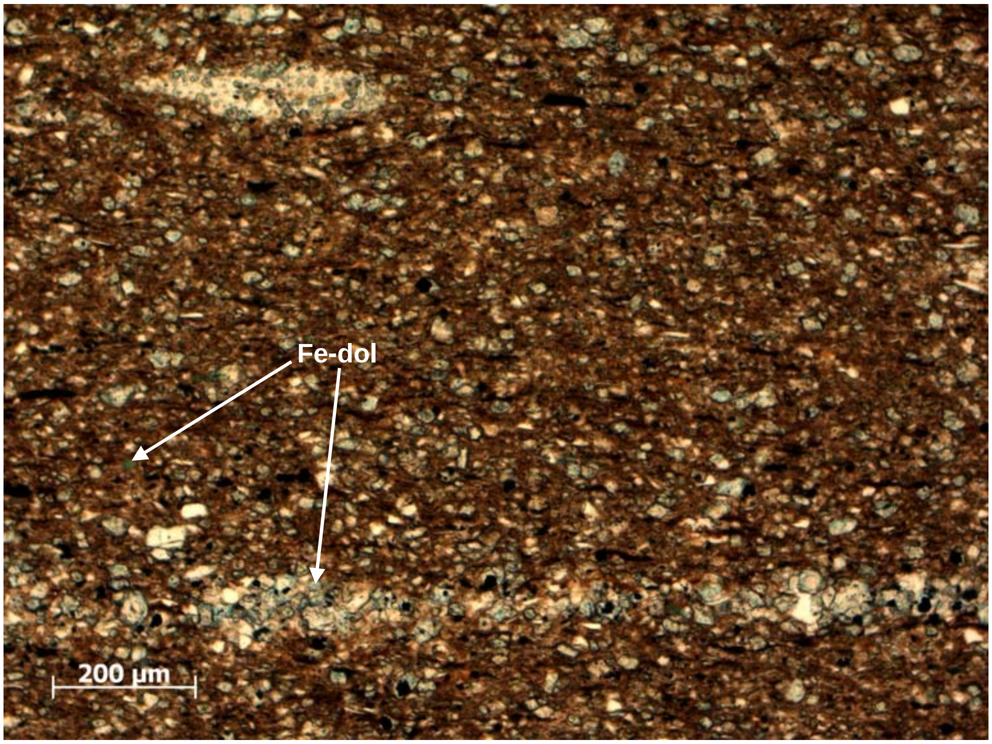

Figure 44. Photomicrograph from 3,746.3' core depth of dolomitic mudstone (dolo-mudstone) from S3. Iron-rich dolomite is the dominant carbonate mineral (gray-green grains). Ingram Exploration, Circle Creek #1.

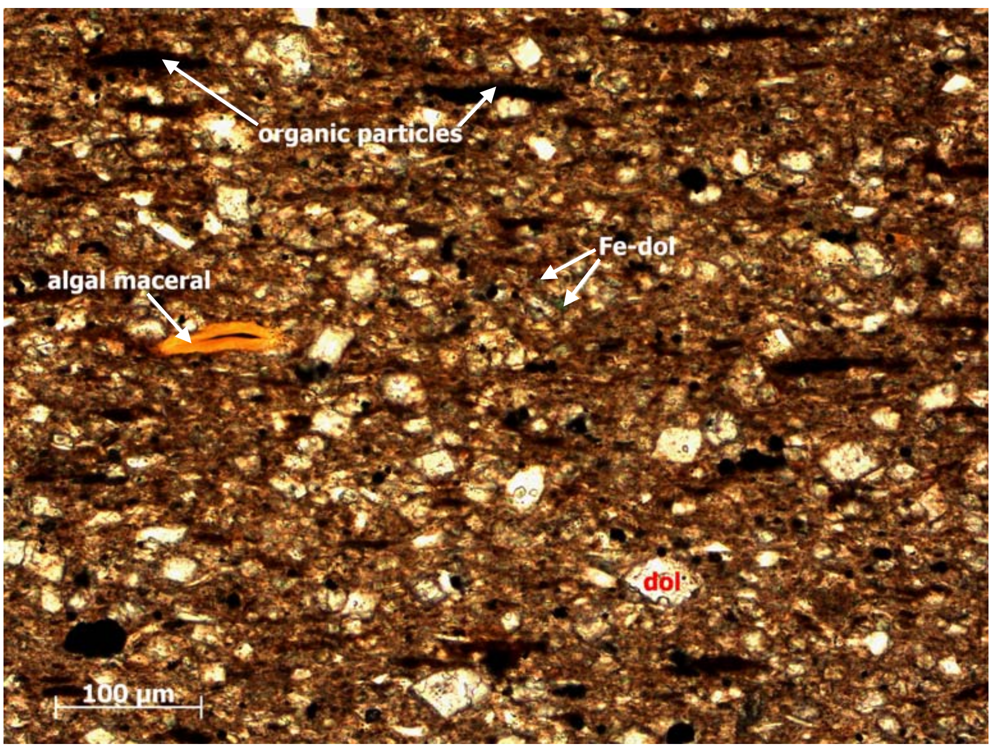

Figure 45. Detailed thin-section photomicrograph of S3 showing algal macerals, organic particles, dolomite, and iron-rich dolomite. Ingram Exploration, Circle Creek #1. Depth 3,746.3 feet.

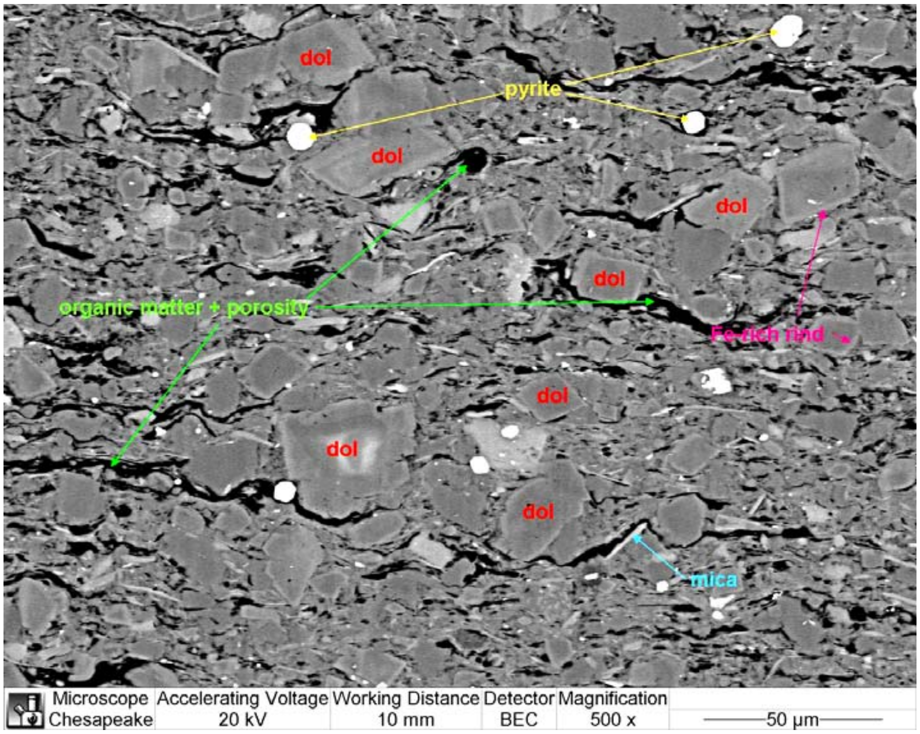

Figure 46. SEM backscatter composition image of dolomitic mudstone (dolo-mudstone) from S3 of the Woodford Shale. Backscatter imaging does not allow differentiation between porosity and organic matter, as both have low electron densities. Ingram Exploration, Circle Creek #1. Depth 3,735.6 feet. (Image taken by Rick Urash).

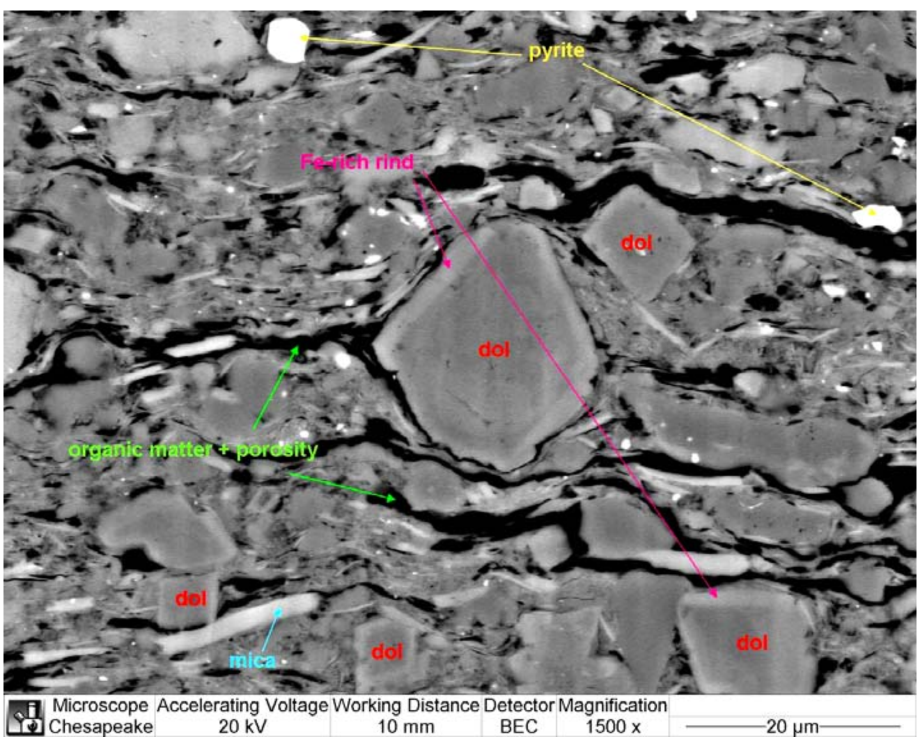

Figure 47. SEM backscatter composition image, a dolomitic mudstone (dolo-mudstone) from S3 showing zonation of dolomitic rhombs (dol), other constituents, and rock fabric. Ingram Exploration, Circle Creek #1. Depth 3,735.6 feet. (Image taken by Rick Urash).

Subunit 4 (3,755’-3,800’ core depth) is an organic-rich siliceous, clay-rich mudrock, with pyrite-rich intervals. Authigenic minerals include silica cement in the matrix, authigenic quartz, chert, dolomite, and pyrite. Matrix composition is dominated by silica and illite. S4 can be laminated or non-laminated. The approximate silt and sand content is 15-20%, which is similar to S1 and S2, and less than S3. Accessory grains include mica and glauconite, and conodont fragments are rare but observed in the lower section of the facies. Algal macerals are abundant and are mostly replaced or infilled with authigenic quartz or chert. Unidentified brown organic particles may be present.

In Figure 48, a thin-section from 3791.9’, an algal maceral is shown with authigenic quartz in-filling. Pyrite, which occurs as black masses, and clays help create the dark chroma of this image. SEM images from S4 reveal the presence of silica cement, organic matter with intergranular and intragranular porosity, and mica (Figure 49).

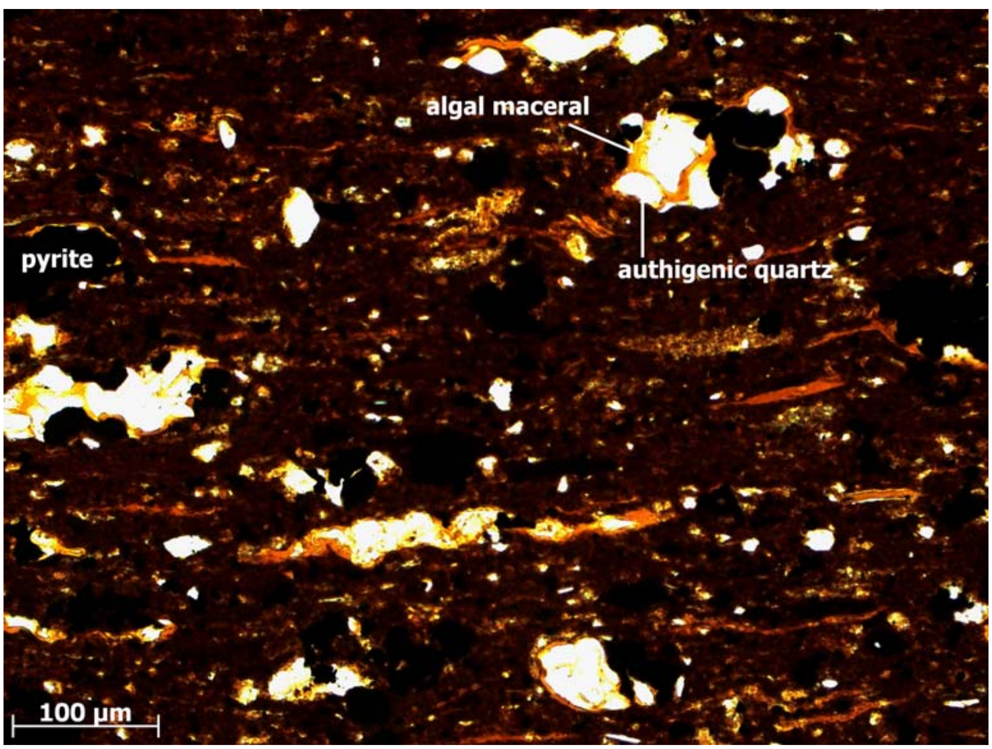

Figure 48. Thin-section photomicrograph of a pyrite-rich siliceous/argillaceous mudrock from S4 of the Woodford Shale showing algal macerals, authigenic quartz, and abundant pyrite. Ingram Exploration, Circle Creek #1. Depth 3,791.9 feet.

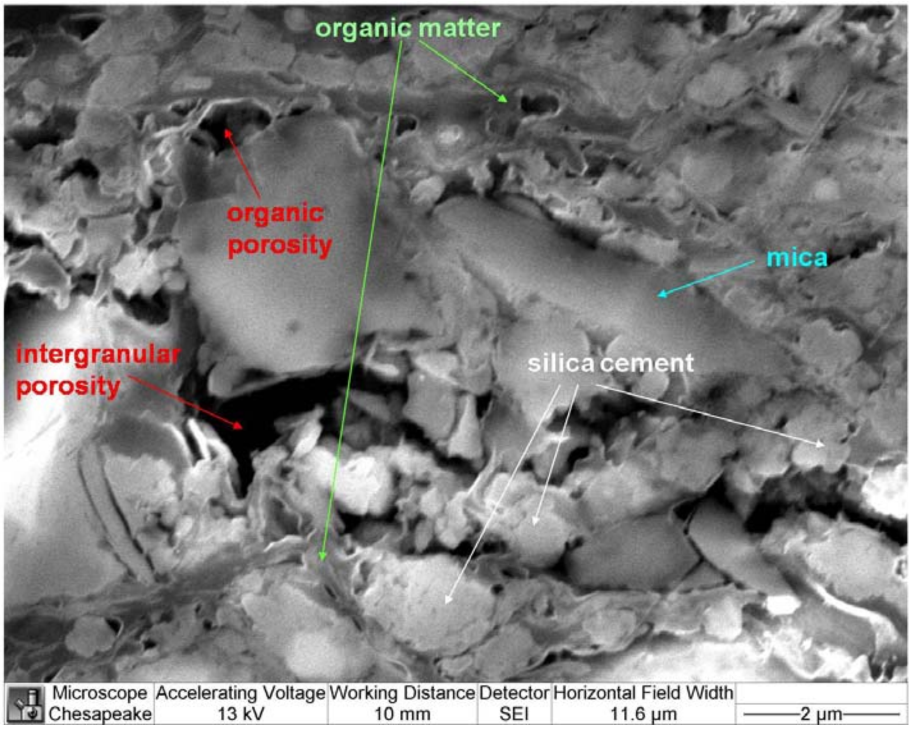

Figure 49. SEM image from 3,791.9' core depth (11,000X magnification), of siliceous/argillaceous mudrock from S4. Ingram Circle Creek #1. Depth 3,791.9 feet. (Image taken by Rick Urash).

The Sylvan Shale (3,800'-3,807' core depth) is a silty, argillaceous mudrock. In hand sample, it is a gray-green shale, which is much lighter in color than the overlying Woodford Shale. The composition of the matrix is dominantly illite and silica in the form of quartz. It is non-laminated and contains very few organic particles, most of which are elongated and orange-brown in color. Authigenic minerals include quartz cement in the matrix, dolomite, pyrite, and marcasite. Carbonate cement also occurs in the matrix. Pyrite-rich laminations and nodules are common, and can be seen in thin-section as black grains. Fe-rich dolomite occurs as small blue-gray grains, 5 to 20 microns in size (Figure 50).

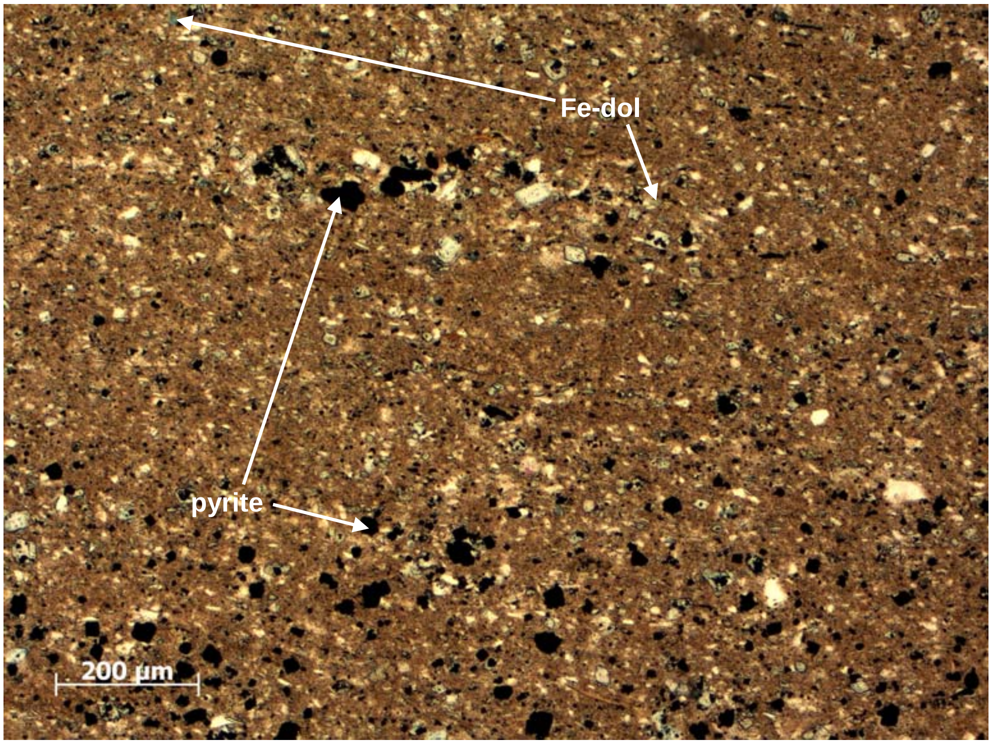

Figure 50. Thin-section of the Sylvan Shale. Constituents include clay, pyrite, silt, and Fe-rich dolomite. Ingram, Circle Creek #1. Depth 3,800.5 feet.

Calibration with Electric Logs

The four Woodford Shale subunits were delineated based on changes in gamma-ray and resistivity logs which were then correlated to petrologic properties. The gamma-ray curve and the average TOC curve from the Circle Creek #1 core are shown in Figures 51 and 52, respectively. A summary of XRD (X-ray diffraction) data for each subunit can be found in Table 3, along with a summary of TRA (tight rock analysis), spectral gamma-ray, and TOC (total organic carbon) data. The data set for these is found in Plates 1, 2, 9 and 10.

XRD results show that S3 contains 15% dolomite on average; it also has the highest clay content. S2 and S4 have the most pyrite at 3.4%. S1 has the highest weight-

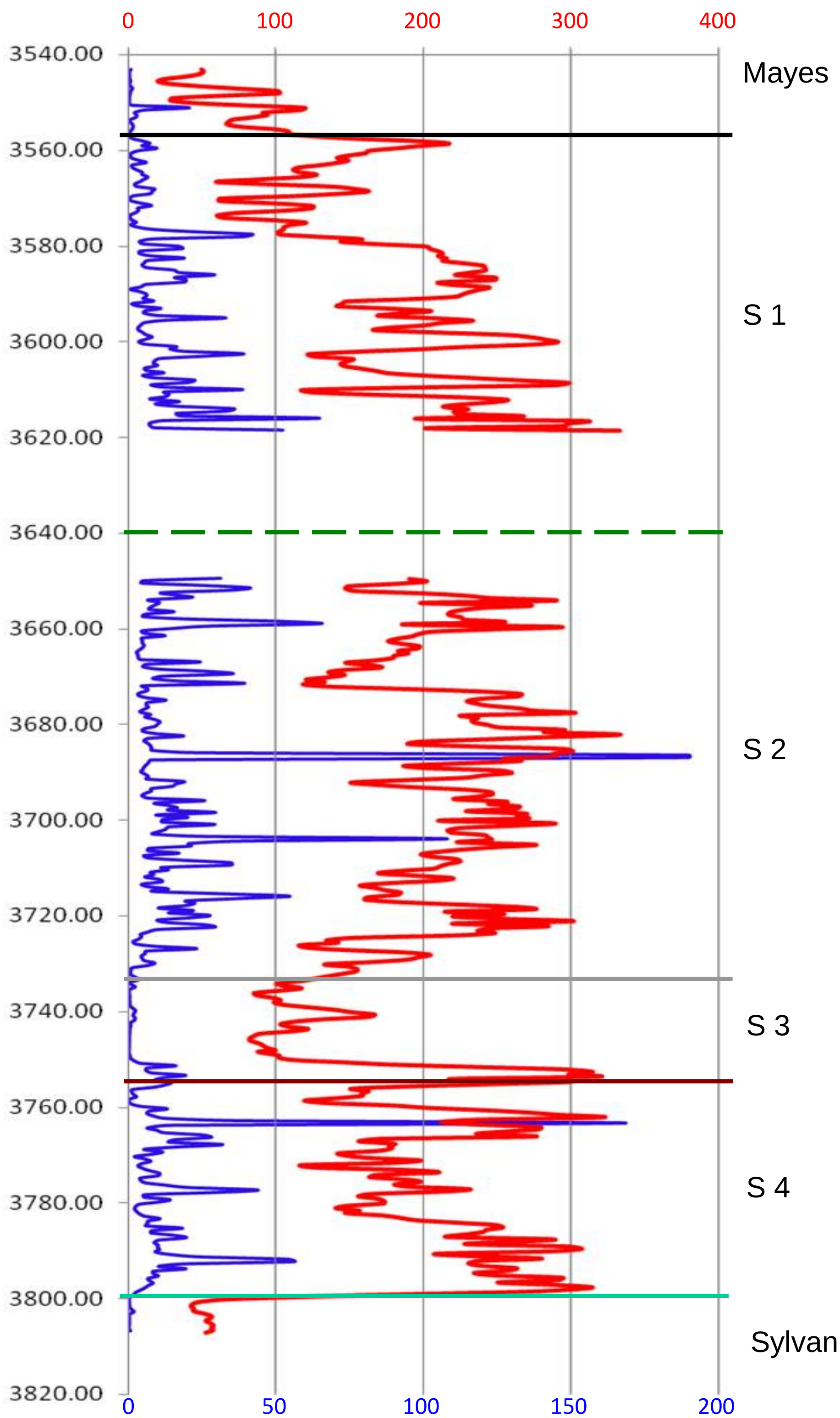

Figure 51. Total Gamma-ray curve (red) and U/Th curve (blue) of the Woodford Shale from the Circle Creek #1 core. S4 and S2 are more organic-rich based on core analyses. Carbonate-rich S3 has the lowest total gamma-ray value and U/Th ratio. There is a missing section of core from 3,618.7' to 3,649'.

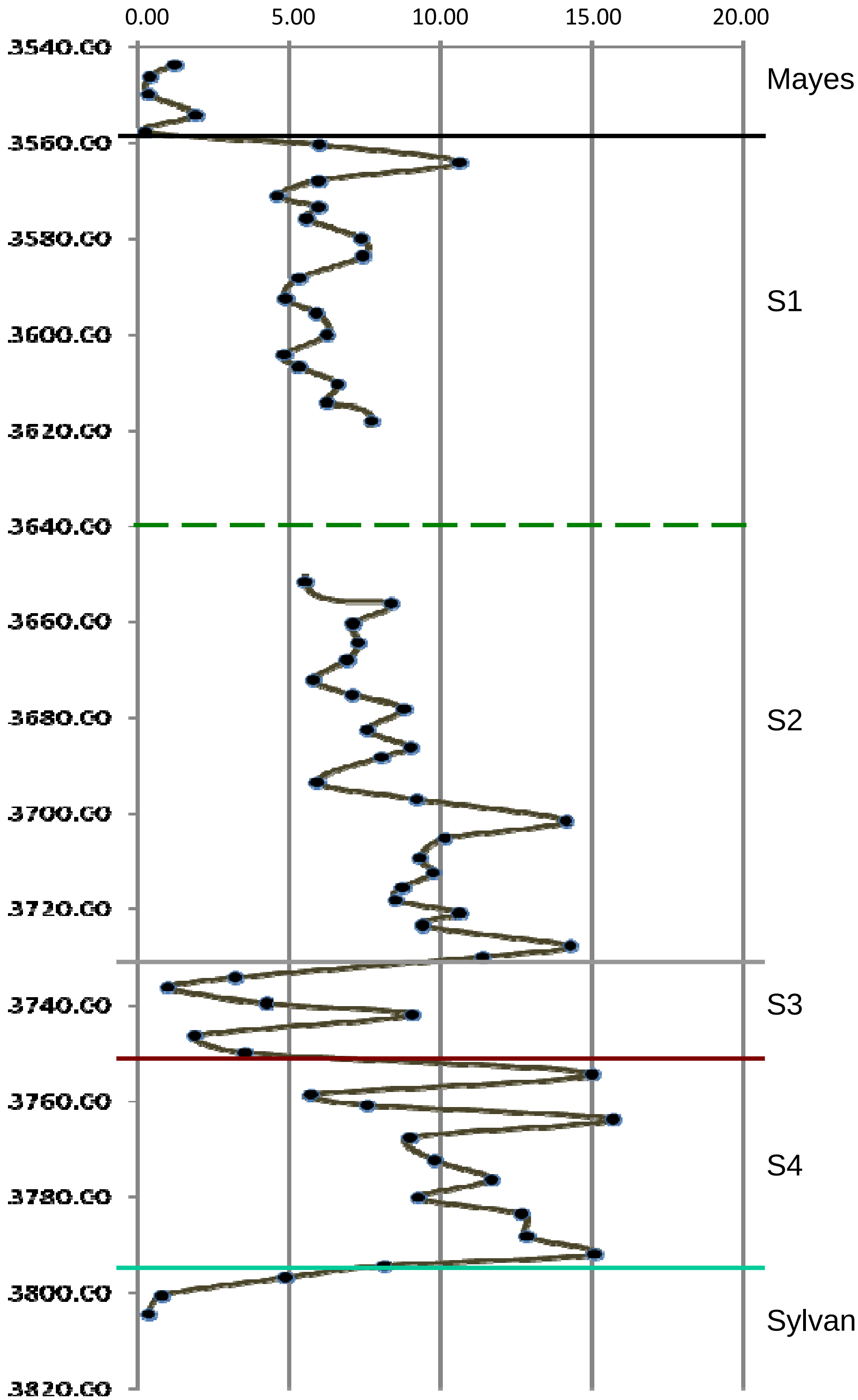

Figure 52. Total Organic Carbon (TOC) curve (in wt.%) from the Circle Creek #1 core

XRD

	S1 wt.%	S2 wt.%	S3 wt.%	S4 wt.%
Clay	34.7	30.3	43.1	31.0
Quartz	49.5	47.6	29.2	45.3
K-spar	0.2	0.6	2.8	1.2
Plagioclase	1.4	2.0	1.8	1.0
Apatite	1.8	0.1	0.2	1.1
Pyrite	2.6	3.4	1.7	3.4
Marcasite	1.1	1.9	0.7	0.9
Calcite	0.0	0.0	0.0	0.0
Dolomite	2.5	5.9	15.0	6.0
Illite/Smectite	3.9	2.2	5.8	4.1
Illite+Mica	30.6	28.0	37.0	26.7
Chlorite	0.1	0.1	0.3	0.2
Kaolinite	0.1	0.0	0.0	0.0

TRA

	S1	S2	S3	S4	
Bulk Density	2.36	2.29	2.41	2.19	g/cc
Porosity (Φ)	9.33	9.64	7.87	11.10	% of bulk vol.
Water Sat.	25.63	15.81	48.13	16.03	% of pore vol.
Gas Sat.	24.95	20.39	23.08	18.88	% of pore vol.
Mobile-Oil Sat.	49.43	63.80	28.89	65.10	% of pore vol.
Gas-filled Φ	2.18	1.83	1.66	1.84	% of bulk vol.
Exp. Clay Water	5.35	6.53	4.4	7.67	% of bulk vol.
Bound HC Sat.	6.33	8.12	5.58	10.22	% of bulk vol.
Bound Clay Water	5.00	4.41	6.29	3.79	% of bulk vol.
Permeability (k)	554	508	889	377	6-12 mesh (nd)

GR

	S1	S2	S3	S4
Total Gamma (API)	241	330	175	309
- Low	59	131	85	75
- High	460	618	465	587
K (fraction)	0.02	0.02	0.03	0.02
U (ppm)	14.07	21.46	6.78	18.86
Th (ppm)	2.29	2.42	4.37	2.60
U/Th (ratio)	6.14	8.87	1.55	7.25

TOC

	S1 wt.%	S2 wt.%	S3 wt.%	S4 wt.%
Average	6.26	8.81	3.81	10.56
Maximum	10.63	14.28	9.07	15.68
Minimum	4.59	5.51	0.97	4.88

Table 3. Detailed chart of average XRD, TRA, GR, and TOC data based on petrographic analysis of the subunits in the Circle Creek #1 core

percent of quartz at 49.5%; however, S2 and S4 have comparable amounts quartz at 47.6 and 45.3 wt-% respectively.

The average permeability (k) over the S1 interval is 554 nd and porosity (Φ) is 9.33%. S2 has an average permeability (k) of 508 nd and porosity (Φ) of 9.64%. The average values over the S3 interval are permeability of 889 nd and Φ of 6.95%. The average permeability of S4 is 377 nd with porosity averaging 11.10%.

The average total gamma-ray of S1 is 241 API units, but ranges from 59 to 460 API units. The average total gamma-ray for S2 is 330 API units but ranges from 131-618 API units. S3 is the dolomitic interval, and as a result has lower gamma counts with an average total gamma-ray of 175 API units, ranging from 85 to 465 API units. S4, similar to S2, has an average total gamma of 309 API units but can range from 75 to 587 API units.

In addition to the total gamma ray curve, a U/Th ratio curve is also shown in Figure 51. Intervals that are rich in uranium, and therefore have high uranium/thorium ratios (>0.5), were deposited in environments that promoted uranium fixation under reducing conditions and were most commonly marine (Adams and Weaver, 1958). Uranium-poor intervals, those with U/Th <0.15, were deposited in an environment which promoted uranium mobilization through weathering or leaching (Adams and Weaver, 1958). This would be an oxidizing, likely terrestrial environment. Averages of spectral gamma-ray data for each electrofacies are also provided in Table 3. The average U/Th ratio is 6.14 for S1, 8.87 for S2, 1.55 for S3, and 7.25 for S4. The ratio can exhibit sharp increases up to 64 in S1, 228 in S2, and 168 in S4. However, the majority of S3 has a U/Th ratio of less than 1.0.

The average TOC of S1 is 6.26 wt.%, with a maximum value of 10.63 wt.%. For S2, the average is higher at 8.81 wt.%, with a maximum of 14.28 wt.%. S3, which is the dolomitic interval, has the lowest TOC on average with 3.81 wt.% and a maximum value of 9.07 wt.%. The TOC of S4 is 10.56 wt.% on average, with a maximum of 15.68 wt.%. S2 and S4 are the most organic-rich intervals and have the highest U/Th on average.

Nancy 1-17H

The Chesapeake Nancy 1-17H is located approximately 25 miles northwest of the Circle Creek #1, in Section 17, T.10N, R.5E (Figure 26). The Nancy 1-17H was cored from the Mississippian Caney Shale and Mayes Limestone (4,531' to 4,565.7' MD), through the Woodford Shale (4,565.7'-4,643.5' MD) and the Hunton Group (4,643.5'-4,676.5' MD), and into the top of the Sylvan Shale (4,676.5'-4,710' MD).

Only about 78' of Woodford is present in the Nancy 1-17H. Subunits 3 and 4 are not encountered in this well, which is most likely the result of the presence of paleo-highs on the Hunton surface. Apart from consisting of a thinner, younger portion of the Woodford Shale, the Nancy 1-17H core is also differs from the Circle Creek #1 core in other ways.

The Nancy 1-17H consists primarily of dark brown to dark gray shale with a few thin cherty (silica-rich) laminae and a few small phosphate nodules. Thin-sections were not availablefor the Nancy 1-17H, but SEM and XRD analyses show that in the Nancy 1-17H, the Woodford Shale is more silty than in the Circle Creek #1 and contains less chert.

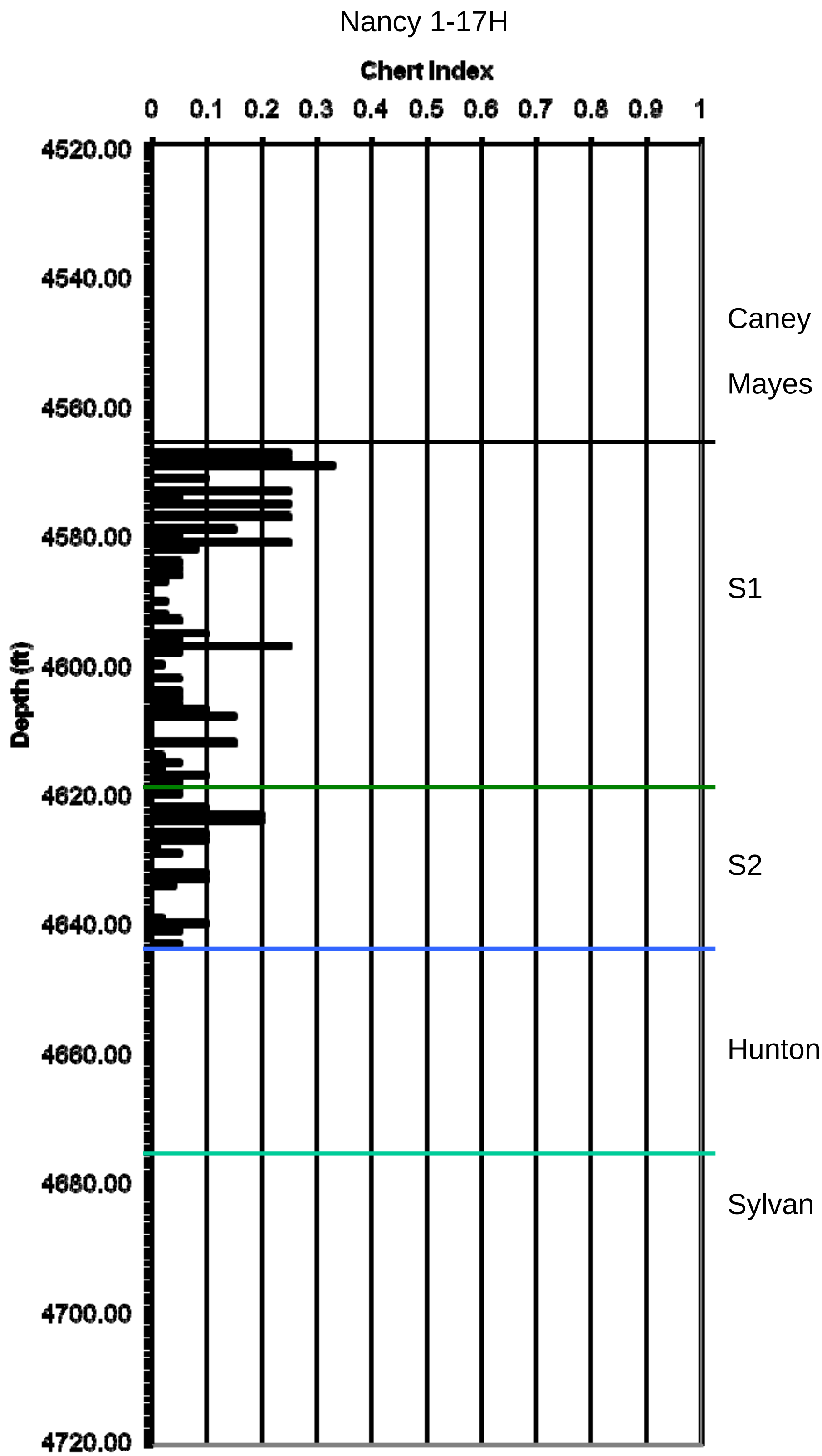

Figure 53. Chert Index Graph of the Woodford Shale from the Nancy 1-17H core, shown as a decimal fraction of chert per foot, with subunits labeled

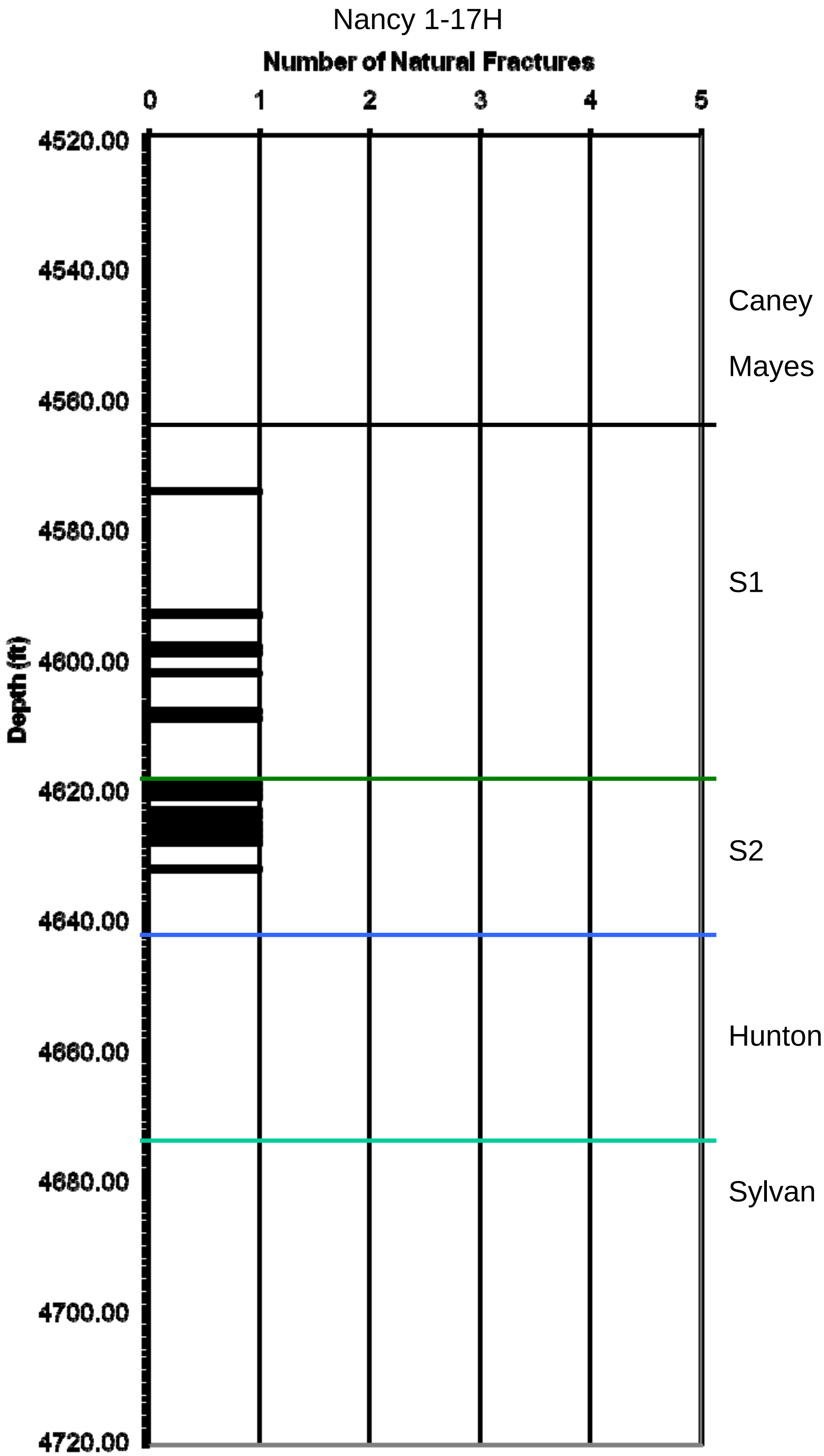

Figure 54. Fracture Intensity Graph of the Woodford Shale from the Nancy 1-17H core, shown as number of natural fractures per foot, with subunits labeled

As was done for the Circle Creek #1 core, chert and fractures were counted for the Woodford portion of the Nancy 1-17H in order to create Chert Index (Figure 53) and Natural Fracture Intensity (Figure 54) graphs. The most cherty interval is found at 4569.5’ and has a chert index of 0.33, in contrast to a high of 0.5 in the Circle Creek #1 core. Other chert-rich intervals are found in the upper thirty feet of the Woodford Shale (S1) and have average chert index values of 0.2-0.25. Portions of S2 also contain chert laminae with values typically less than 0.1 on the chert index scale. However, the uppermost portion of S2 (4,623’-4,625’) does have chert index values of 0.2. This chert-rich interval at the top of S2 also contains more natural fractures per foot than lower portions of S2.

The top of the Woodford Shale is located at 4,565.7’ core depth. The uppermost subunit, S1, was cored from 4,565.7’ to 4,621’. Thin sections, and therefore lithologies, are not yet available for the Nancy 1-17H core; however, SEM images are available and are detailed here.

Based on core analysis, it was determined that S1 contains minor phosphate nodules in the upper portion. SEM images reveal similarities between the Nancy 1-17H and the Circle Creek #1. Porosity within organic matter (Figures 55 through 57 and 59 through 62), silica cement (Figures 55, 58, and 61 through 63), framboidal pyrite (Figures 56 and 60), illite (Figures 55 and 56), and mica (Figures 56 and 61) are found in both cores. The Nancy 1-17H appears to be more silty as indicated by the presence of silt-sized quartz grains at various depths throughout the core (Figures 55 and 58).

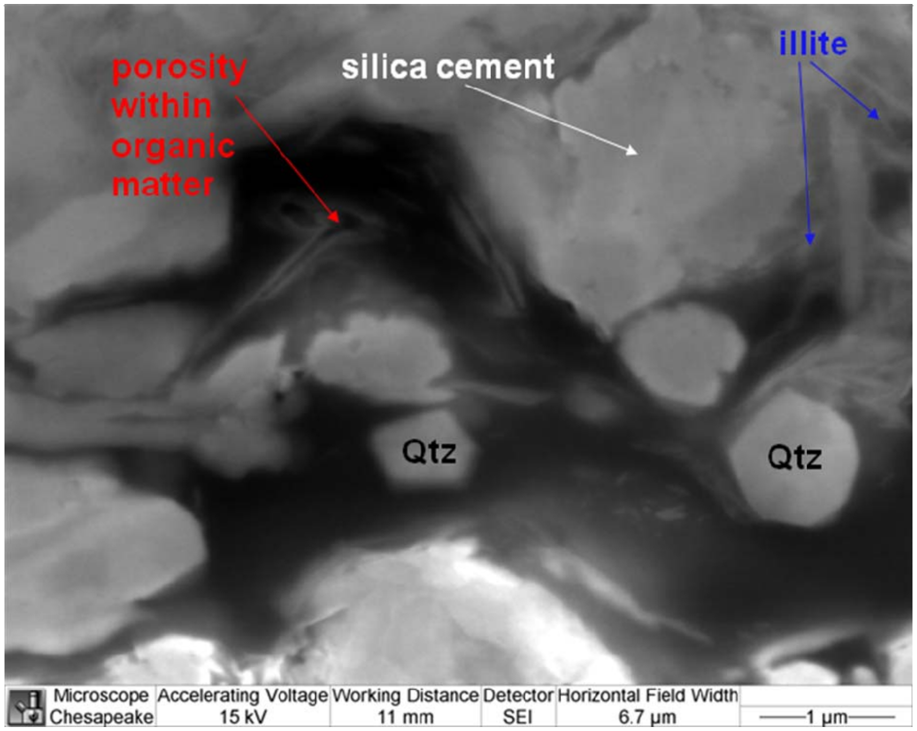

Figure 55. Scanning Electron Microscope image from 4,572.16' core depth showing porosity contained within organic matter, quartz grains, silica cement, and illite. From S1 of the Chesapeake, Nancy 1-17H. (Image taken by Leonardo Alcantar-Lopez).

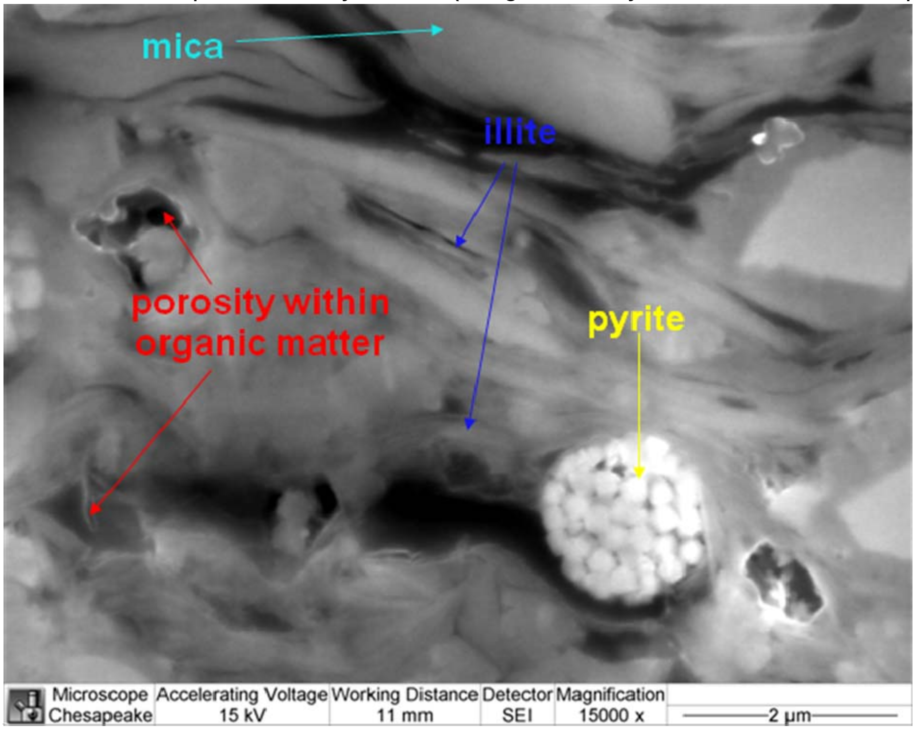

Figure 56. SEM image from 4,572.16' core depth (15,000X magnification) from S1 of showing framboidal pyrite, mica, illite, and porosity contained within organic matter. From the Chesapeake, Nancy 1-17H. (Image taken by Leonardo Alcantar-Lopez).

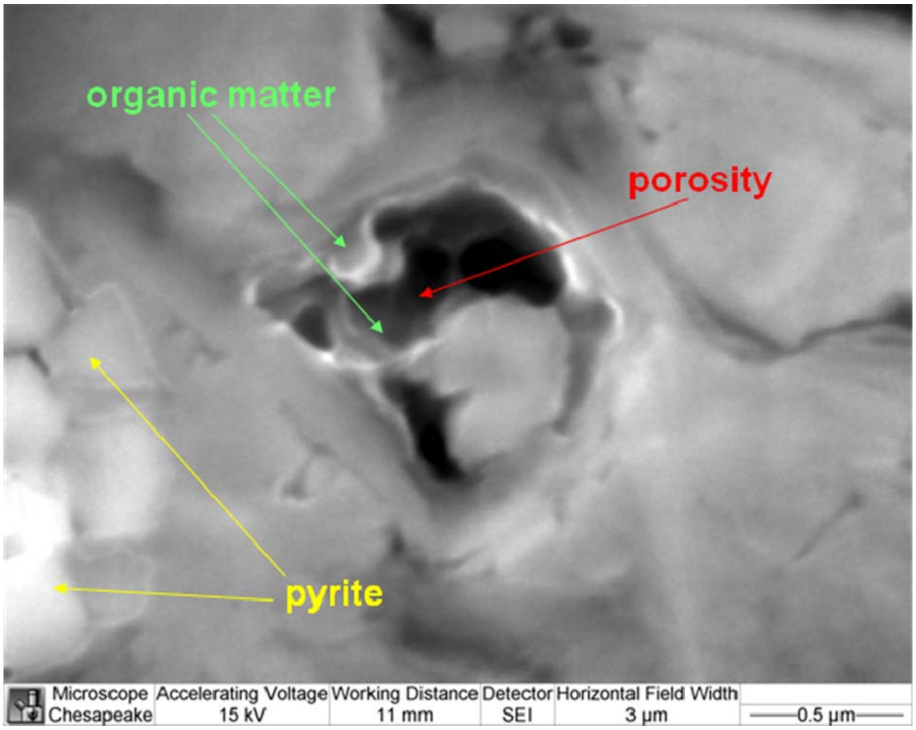

Figure 57. SEM image from S1 showing framboidal pyrite and porosity contained within organic matter. Chesapeake, Nancy 1-17H. Depth 4,572.16 feet. (Image taken by Leonardo Alcantar-Lopez).

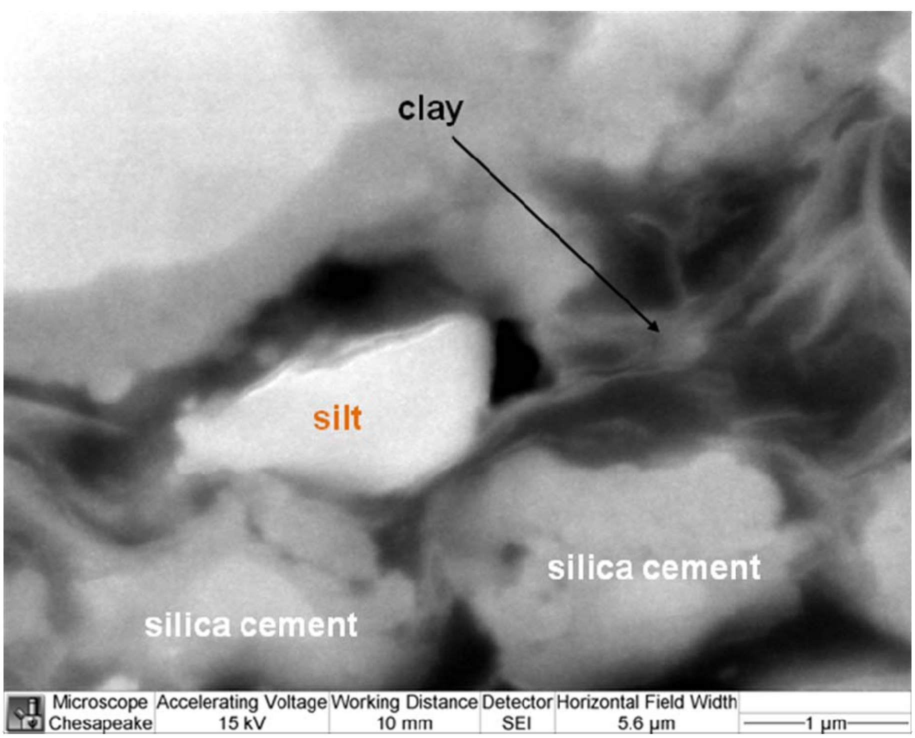

Figure 58. SEM image from S1 showing silt, clay, and silica cement. Chesapeake, Nancy 1-17H. Depth 4,595.9 feet. (Image taken by Leonardo Alcantar-Lopez).

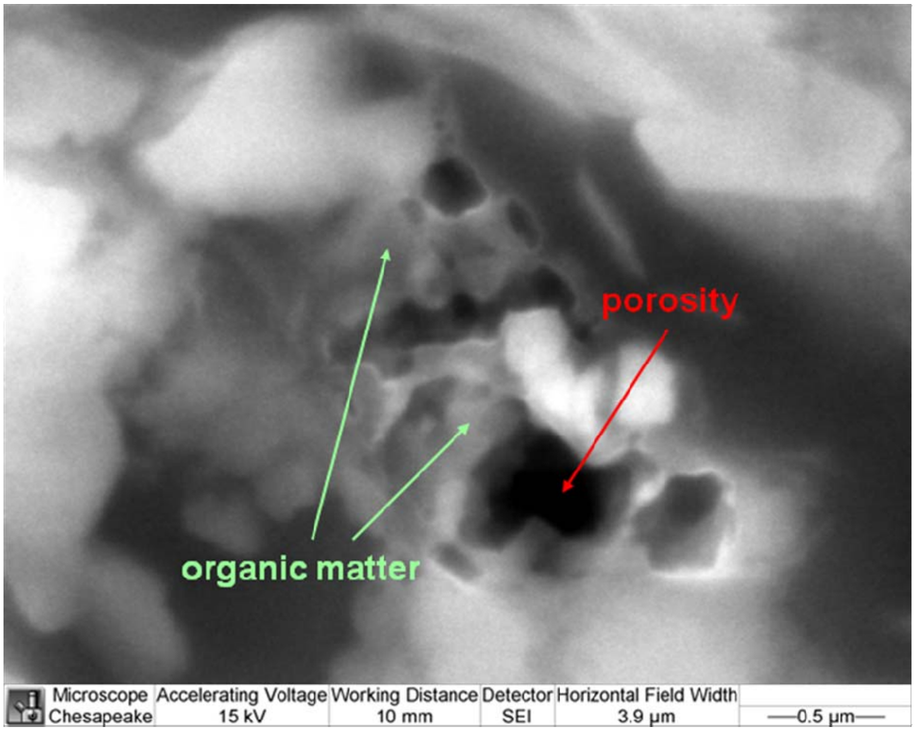

Figure 59. SEM image from S1 showing porosity contained within organic matter. Chesapeake, Nancy 1-17H. Depth 4,595.9 feet. (Image taken by Leonardo Alcantar-Lopez).

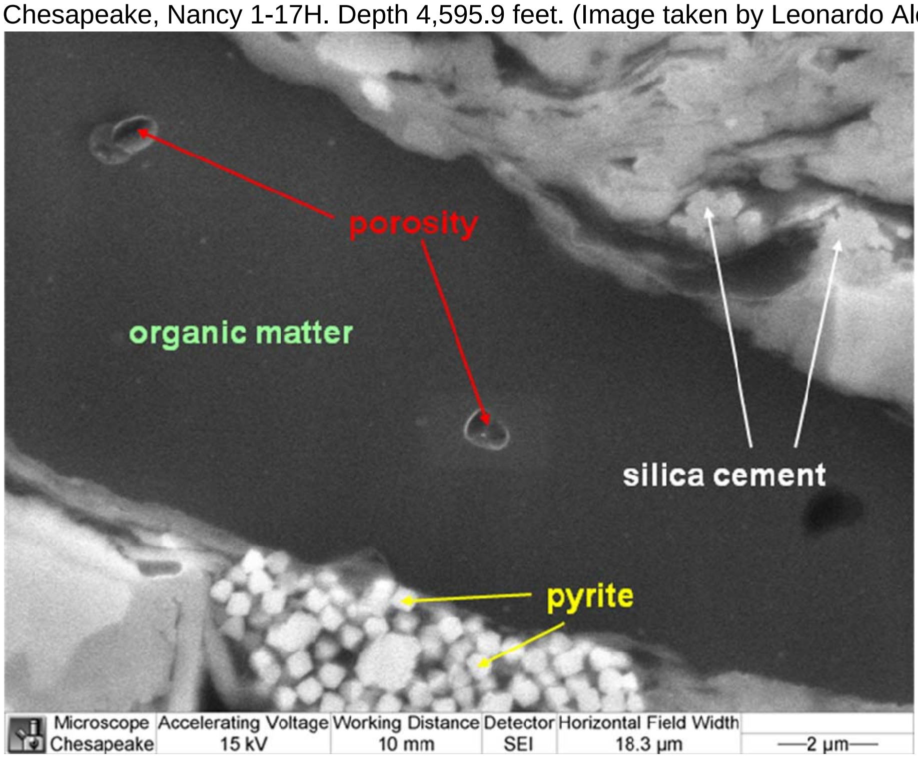

Figure 60. SEM image from 4,595.9' core depth from S1 showing framboidal pyrite, silica cement, and porosity contained within organic matter. Chesapeake, Nancy 1-17H. (Image taken by Leonardo Alcantar-Lopez).

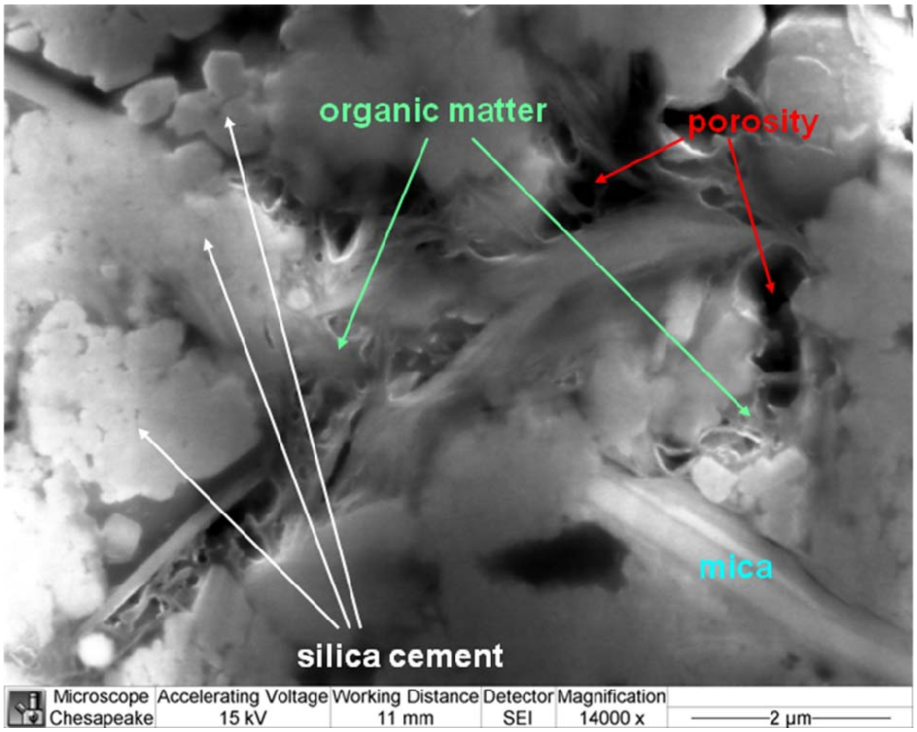

Figure 61. SEM image from 4,627.94' core depth (14,000X magnification) from S2 of the Woodford Shale showing mica, silica cement, and porosity contained within organic matter. (Image taken by Leonardo Alcantar-Lopez).

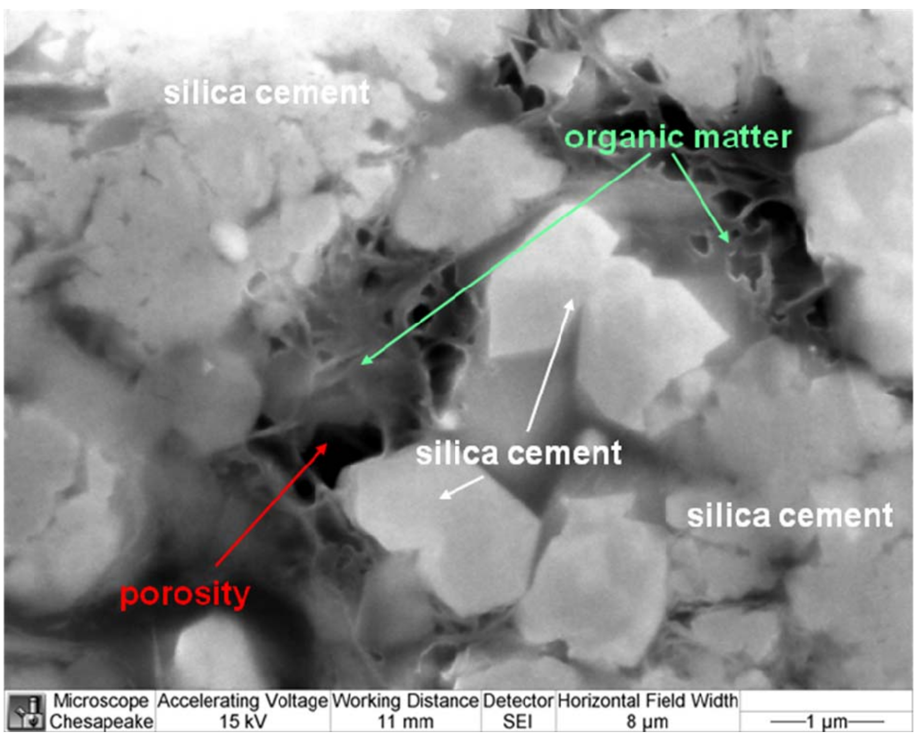

Figure 62. SEM image from 4,627.94' core depth from S2 of the Woodford Shale showing silica cement and porosity contained within organic matter. (Image taken by Leonardo Alcantar-Lopez).

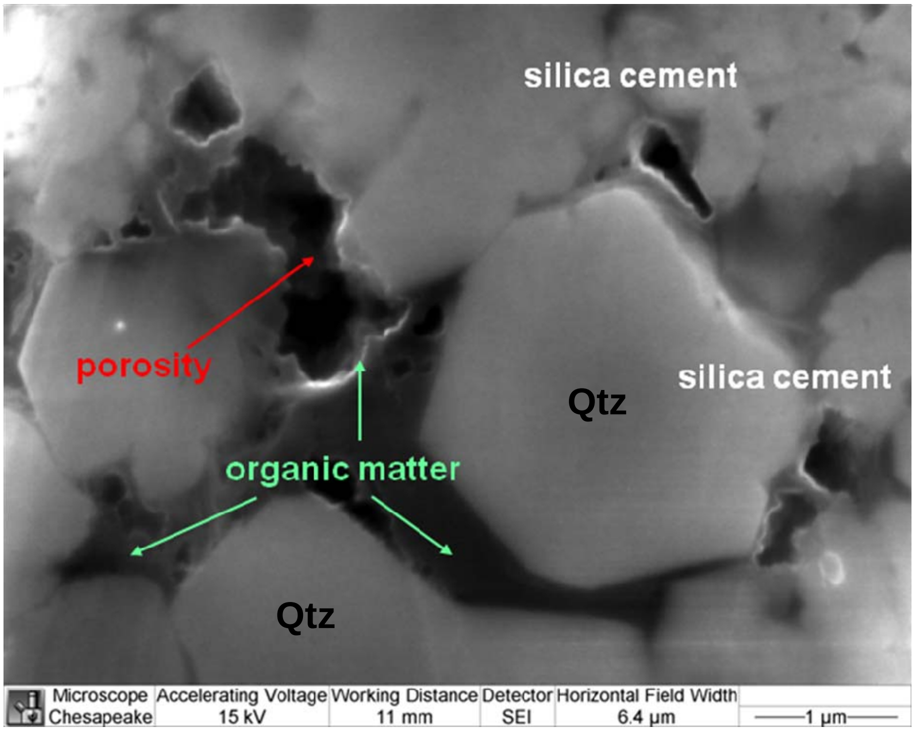

Figure 63. SEM image from 4,627.94' core depth from S2 of the Woodford Shale showing silica cement and porosity contained within organic matter. (Image taken by Leonardo Alcantar-Lopez).

Subunit 2 is similar to subunit 1 in the Nancy 1-17H. This interval was cored from 4,621' to 4,643'. As in the Circle Creek #1, SEM images reveal the "popcorn" appearance of silica cement and spongy nature of organic matter (Figures 62 and 63). The images also reveal the euhedral nature of quartz grains (Figure 63).

The gamma-ray curve from the Nancy 1-17H core is shown in Figure 64. The TOC curve is shown in Figure 65. A summary of XRD (X-ray diffraction) data for each subunit can be found in Table 4, along with a summary of TRA (tight rock analysis), spectral gamma-ray, and TOC (total organic carbon) data. The data set for these is found in Plates 3, 4, 9 and 10.

The XRD reveals that S1 and S2 are quite similar with quartz content of 42.9 and 44.6 wt.% respectively. However, S2 has more pyrite with 5.0 wt.-% compared to 3.3

wt.% in S1; and S1 has more clay with 41.5 wt.% versus 35.9 wt.-% for S2. The TRA reveals the average porosity (Φ) of S1 is ~10.7%. S2 has an average porosity (Φ) of ~9.8%.

The average total gamma-ray of S1 is 311 API units, but ranges from 103 to 484 API units. The average total gamma-ray for S2 is 295 API units but ranges from 140-633 API units. In addition to total gamma ray data, averages of spectral gamma-ray data are provided in this chart. The average U/Th ratios for S1 and S2 are 7.25 and 7.56, respectively.

The average TOC of S1 is 7.32 wt.%, with a maximum value of 9.45 wt.%. For S2, the average is slightly higher at 7.44 wt.% with a maximum of 10.74 wt.%.

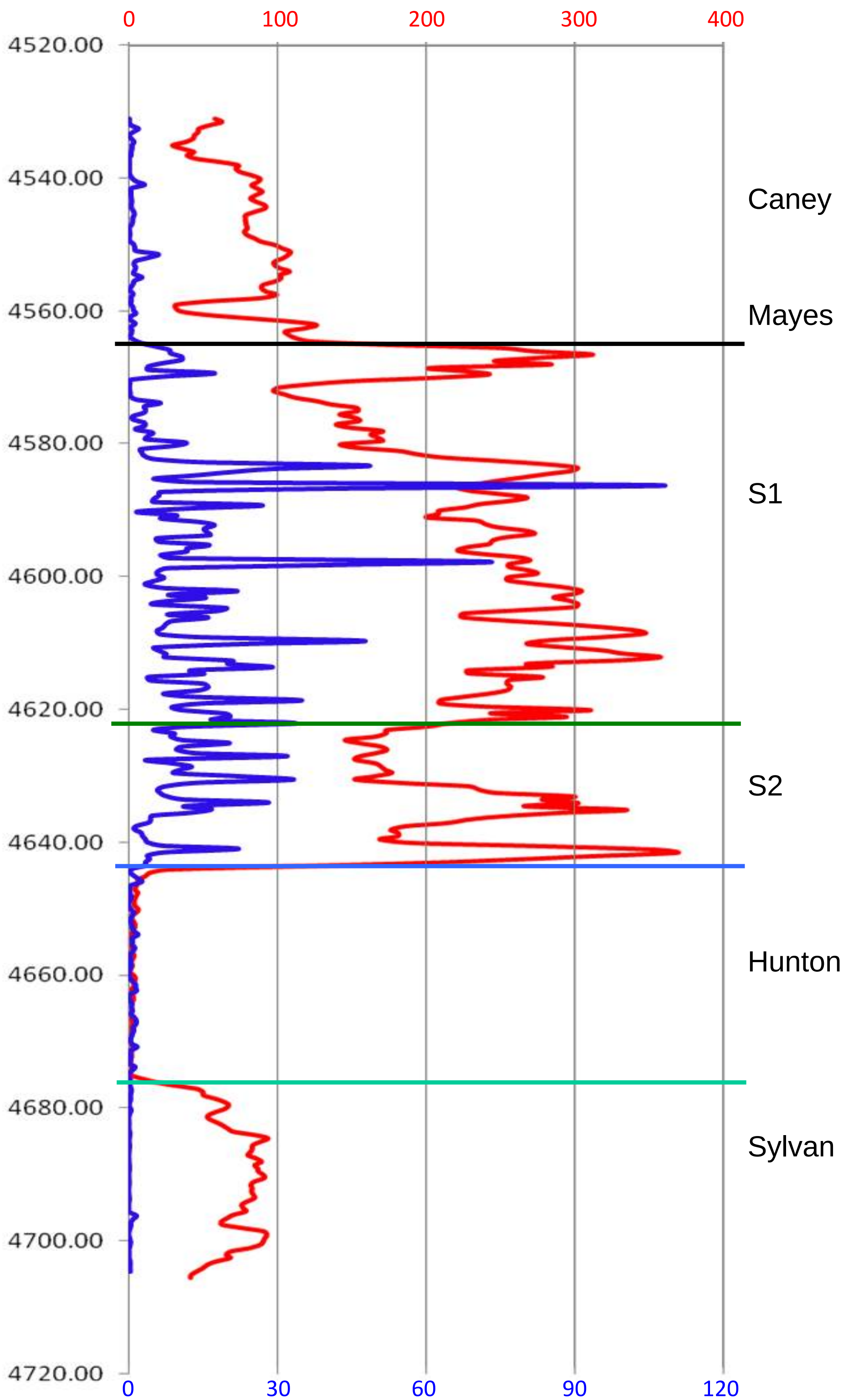

Figure 64. Total gamma-ray curve (red) and U/Th curve (blue) of the Woodford Shale from the Nancy 1-17H core

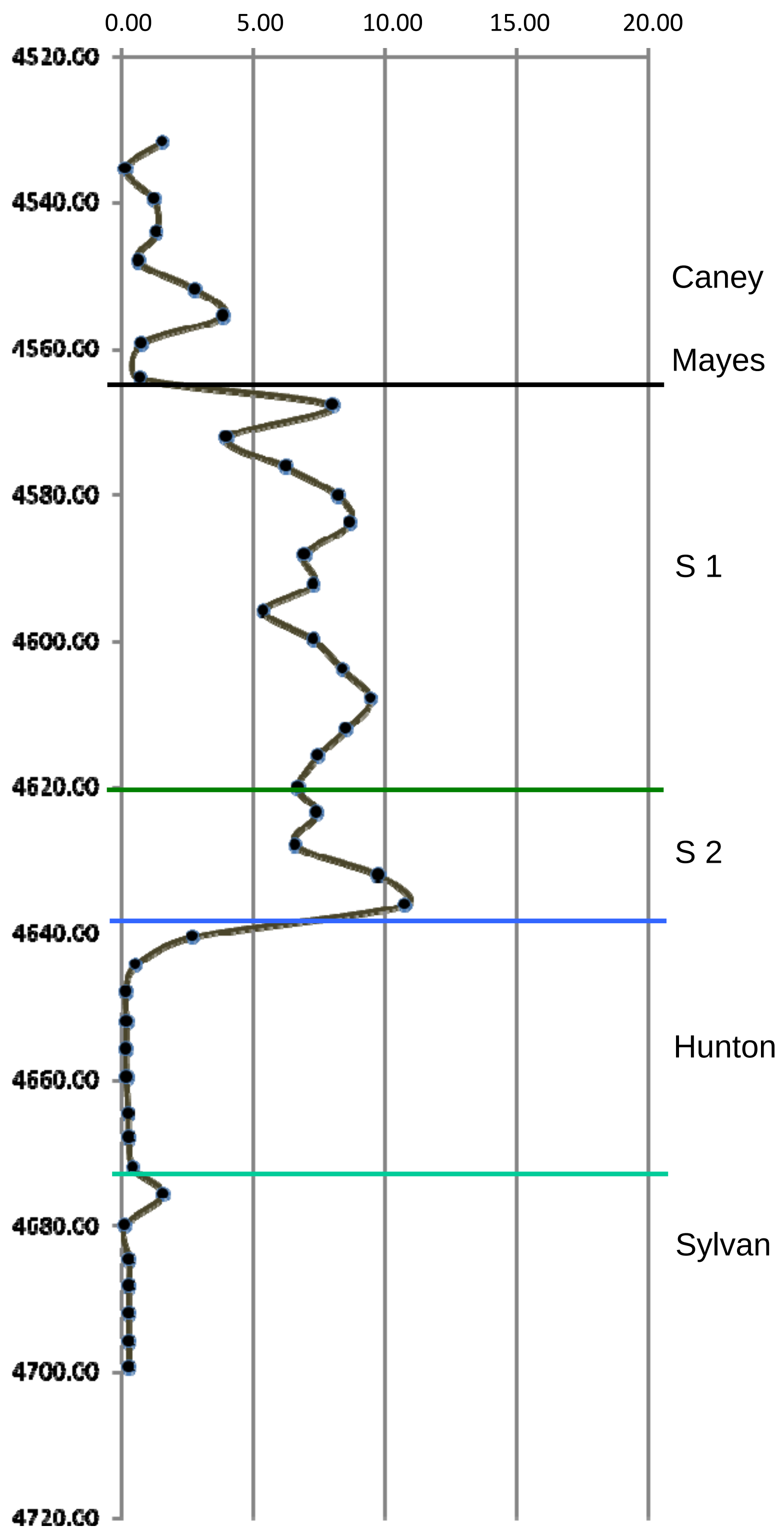

Figure 65. Total Organic Carbon (TOC) curve (in wt.%) from Nancy 1-17H core

XRD

	S1 wt.%	S2 wt.%
Clay	41.5	35.9
Quartz	42.9	44.6
K-spar	0.8	0.7
Plagioclase	1.5	1.7
Apatite	0.2	0.2
Pyrite	3.3	5.0
Marcasite	1.1	1.7
Calcite	0.0	0.0
Dolomite	1.3	2.8
Illite/Smectite	5.1	4.1
Illite+Mica	36.1	31.4
Chlorite	0.2	0.3

TRA

	S1	S2	
Bulk Density	2.34	2.37	g/cc
Porosity (Φ)	10.68	9.79	% of bulk vol.
Water Sat.	30.50	21.69	% of pore vol.
Gas Sat.	14.89	15.76	% of pore vol.
Mobile-Oil Sat.	54.61	62.55	% of pore vol.
Gas-filled Φ	1.58	1.50	% of bulk vol.
Exp. Clay Water	6.49	6.43	% of bulk vol.
Bound HC Sat.	6.05	6.07	% of bulk vol.
Bound Clay Water	4.45	4.25	% of bulk vol.

GR

	S1	S2
Total Gamma (API)	311	295
- Low	103	140
- High	484	633
K (fraction)	0.02	0.02
U (ppm)	17.26	16.94
Th (ppm)	2.38	2.24
U/Th (ratio)	7.25	7.56

TOC

	S1 wt.%	S2 wt.%
Average	7.32	7.44
Maximum	9.48	10.74
Minimum	3.98	2.71

Table 4. Detailed chart of average XRD, TRA, GR, and TOC data based on petrographic analysis of the subunits in the Nancy 1-17H core

CHAPTER VI

COMPOSITION AND DEPOSITIONAL MODEL

Woodford sediments were deposited from south to north as marine transgression extending from the Oklahoma Basin, which formed over the Southern Oklahoma Aulacogen (SOA) depocenter. Sediments (i.e. silt) entering the Oklahoma Basin were derived from areas of high topographic relief to the north and east.

The water depth at the time of Woodford deposition is estimated to have been between 50 and 400 meters (Over and Barrick, 1990). The sea was shallower in northern Oklahoma and deepened towards southern and western Oklahoma, nearer the SOA depocenter.

Watney et al. (2008) describe a core from Pontotoc County, Oklahoma, which contains dark and light gray shale, silt-rich beds that are burrowed and non-skeletal phosphate without prominently bedded cherts.

Puckette et al. (2008) describe the bedded cherts and non-skeletal phosphate-rich Woodford Shale of southern Oklahoma outcrops and dark, non-cherty, silty Noel (Chattanooga) Shale in the Ozark uplift that lacks non-skeletal phosphate. Puckette et al. (2008) interpret the Ozark black shale as inner shelf deposition, the southern Oklahoma outcrops as distal shelf/slope deposits, and the Pontotoc County core as mid-shelf deposits. Locations of these studies are shown in Figure 66.

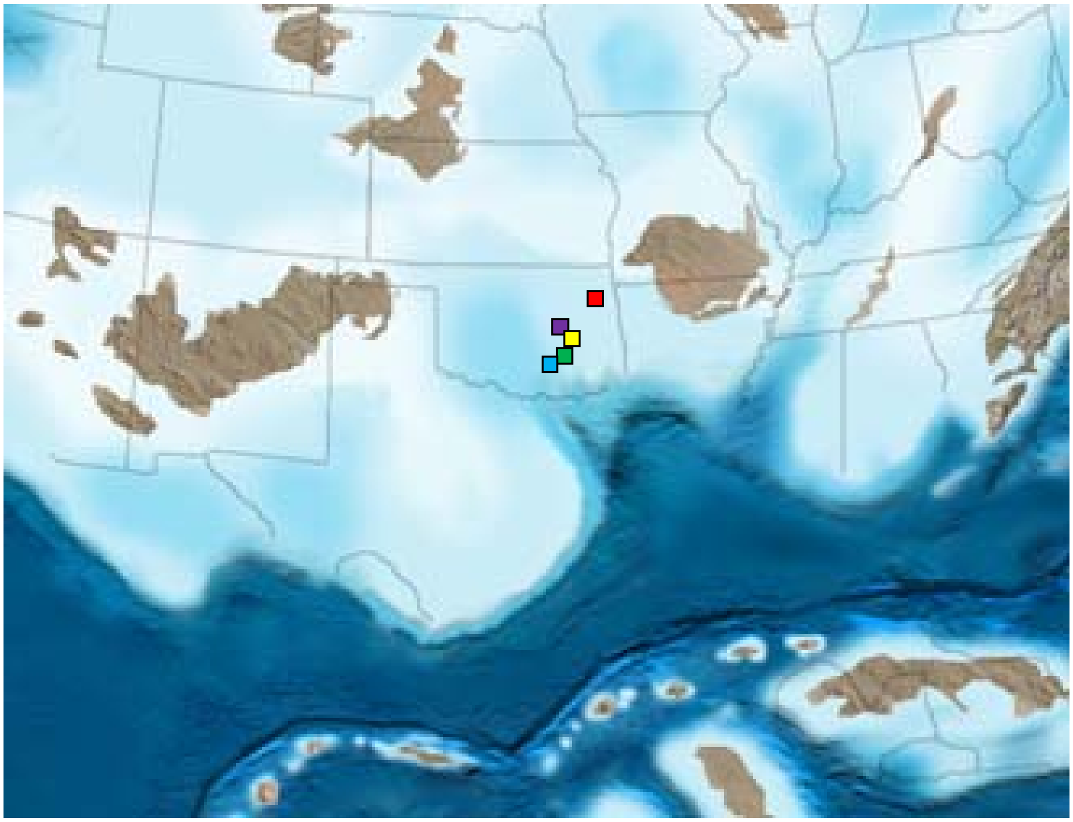

Figure 66. Map of Late Devonian Paleogeography (after Blakey: http://www2.nau.edu/, accessed: February 8, 2008), approximate locations marked: Northeastern Oklahoma Noel Shale outcrop ■, Pottawatomie County Nancy 1-17H ■, Seminole County Circle Creek #1 ■ , Pontotoc County KGS-OGS Current #1 ■ , and Criner Hills and Arbuckle Uplifts outcrops ■ .

Circle Creek #1

Core analysis of the Ingram Exploration, Circle Creek #1 (Section 13, T.6N., R.6E.) in southern Seminole County, including XRD and thin-section petrography, determined that the bulk of the Woodford Shale contains 15-20% silt. The average amounts of silt for the subunits as determined by rock analysis were: S1 ~17.5%, S2 ~ 15%, S3 ~25%, and S4 ~17.5%. A comparison of TOC, chert, and the average values of silt per unit, reveals relationships between those three parameters.

In the Circle Creek #1, the Woodford Shale is 241.5 feet thick and contains minor phosphate nodules. These are small, sparse and present in the upper 20 feet of the S1 interval. S1 (3,558.5'-3,618' core depth) contains cherty bands, with an average chert index of 0.15, higher than the other three subunits present in the well. The presence of phosphate nodules and the relative abundance of chert in this interval suggests it is near an upwelling zone (Over, 1992), deeper than the inner shelf than but not as deep as the margin of the slope. The average TOC of S1 is 6.26 wt.%. The average U/Th ratio for S1 is 6.14 indicating a dominant marine influence.

S2 (3,650'-3,730' core depth) also contains chert, with an average chert index of 0.04. The average U/Th ratio of 8.87 indicates a strong marine influence and minor terrestrial influence. The average TOC is 8.81 wt.%. The high TOC and U value suggest slow deposition in quiescent, anoxic waters.

S3 (3,730'-3,755' core depth) has a greater percent silt than the other three subunits at ~25%. Chert and TOC are lower in S3 at 0.01 and 0.97 wt.%, respectively. Carbonate (dolomite) increases to 15 wt.% in this interval, which suggests possible shallowing. The average U/Th ratio in S3 is 1.55, indicating a stronger terrestrial influence.

S4 (3,755'-3,800' core depth) has an average chert index of 0.07. This subunit contains the highest average TOC at 10.56 wt.%. The average U/Th ratio is 7.25 indicating a dominant marine influence.

Figure 67 is a new synthesis figure, similar to Figure 27 from the Petrographic Analysis chapter. The TOC curve has been added so that inferences can be made about relative sea-level. Lower TOC readings are interpreted as corresponding to lower sea-level and lower chert index. Higher TOC values correspond to a higher chert index and are interpreted as representing a deeper, more distal depositional setting. The generalized

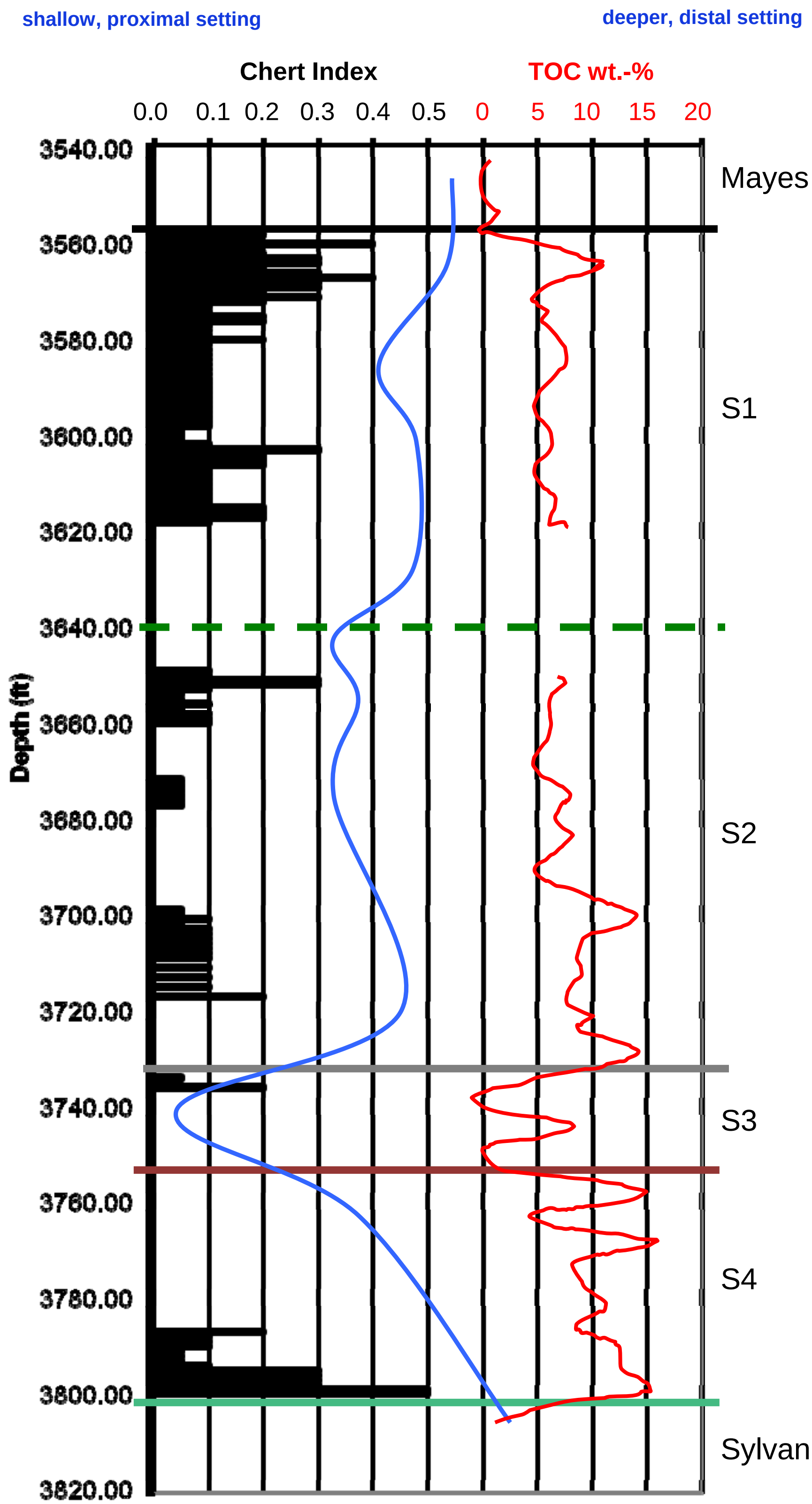

Figure 67. Chert Index Graph of the Woodford Shale (except for a missing section from 3,618.7' to 3,649') from the Circle Creek #1 core, amount of chert per foot expressed as a decimal fraction, relative sea level shown in blue, TOC curve shown in red

sea-level curve was created based on the assumption that chert, higher TOC, and higher uranium concentrations indicate deeper water.

S1, S2, and S4 are believed to represent deposition in deeper water than S3 and therefore have higher TOC and chert indices. S3 has the lowest TOC value, least amount of chert, and was likely deposited in shallow water. The dolomitic nature of the interval supports this interpretation as shallow water settings provide favorable environments for dolomite formation (Lumsden, 1985).

Nancy 1-17H

Core analysis of the Nancy 1-17H (Section 17, T.10N., R.5E.) in eastern Pottawatomie County, included TOC, XRD, SEM, and spectral GR. The Nancy 1-17H contains 77.8 feet of compacted Woodford Shale consisting entirely of S1 and S2.

As in the Circle Creek #1, the Nancy 1-17H contains minor phosphate nodules in the upper portion of the S1 subunit. S1 contains chert with an average chert index of 0.07. As in the Circle Creek #1, the phosphate nodules and chert index are interpreted to indicate a depositional setting near an upwelling zone. The average TOC of S1 is 7.32 wt.%, and the average U/Th ratio is 7.25, indicating a dominant marine influence.

S2 has an average chert index of 0.06. The average TOC of the subunit is 7.44 wt.%. The average U/Th ratio is 7.56, indicating a dominant marine influence.

Figure 68 is a new synthesis figure, similar to Figure 53 from the Petrographic Analysis chapter. The TOC curve, as well as a relative sea-level curve, have been added. In the vicinity of the Nancy 1-17H, S1 and S2 have similar TOC values. S1 appears to have more chert and was likely deposited in slightly deeper water than S2. S2 has less chert, particularly at the base of the subunit, which may indicate shallowing.

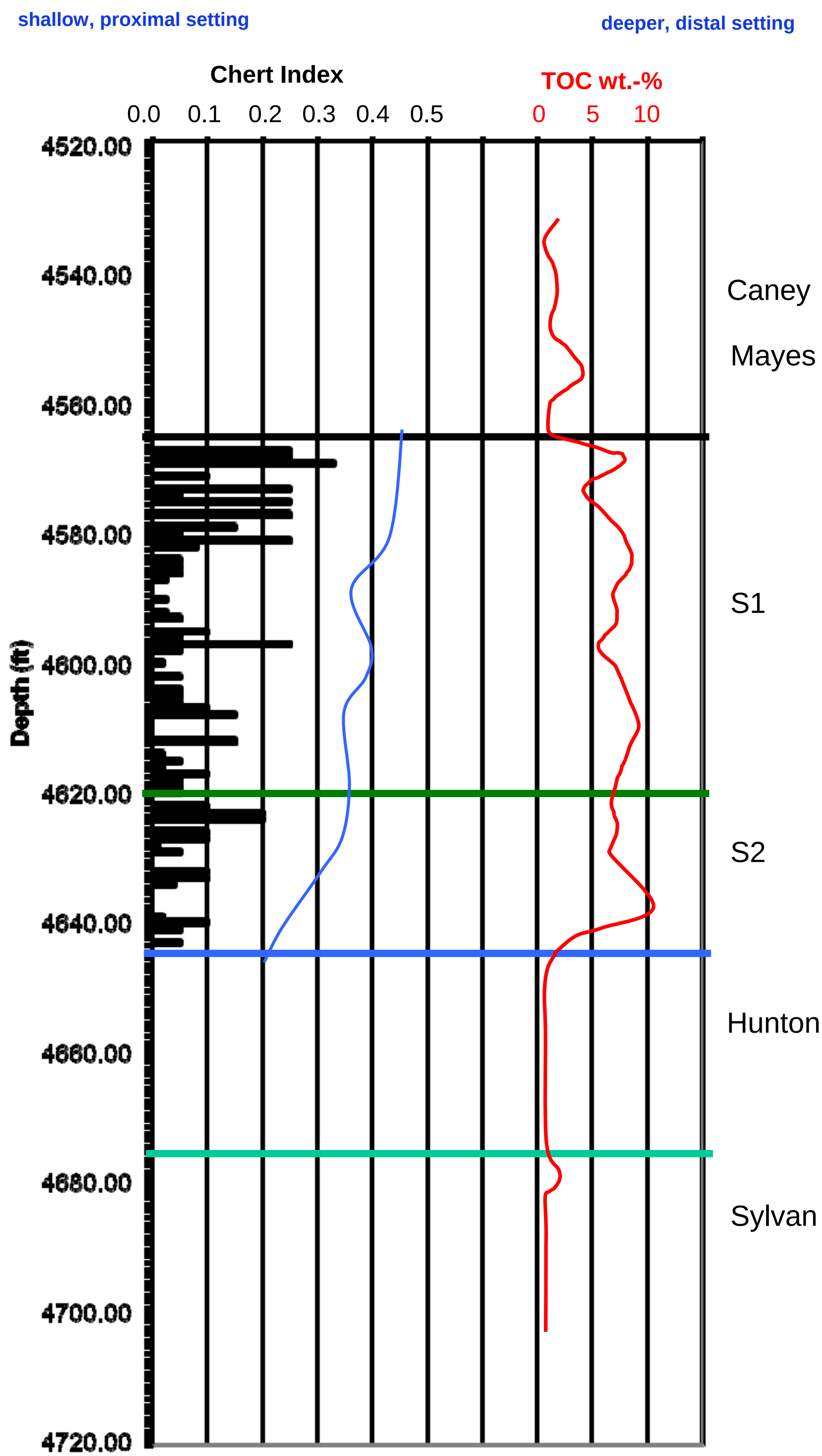

Figure 68. Chert Index Graph of the Woodford Shale from the Nancy 1-17H core, amount of chert per foot expressed as a decimal fraction, relative sea level shown in blue, TOC curve shown in red

Based on wire-line log correlation, it is suggested that the Woodford sediments onlapped to the north. Subunits 3 and 4 are present in the Circle Creek #1, but are apparently missing in the Nancy 1-17H . Subunits 1 and 2 thin to the north. The similarities in the resistivity curves suggest like sections are in the Nancy 1-17H and Circle Creek and that post Woodford erosion is not the cause of the thinning (Figure 69).

Since the Woodford Shale was deposited as a marine transgression from south to north, one would expect to see a northern limit of subunits 3 and 4, a boundary north of which only S1 and perhaps S2 would be present. S3 and S4, if present, could be represented by the Misener Sandstone, a fluvial to shallow marine deposit of Upper Devonian age (Busanus, 1988).

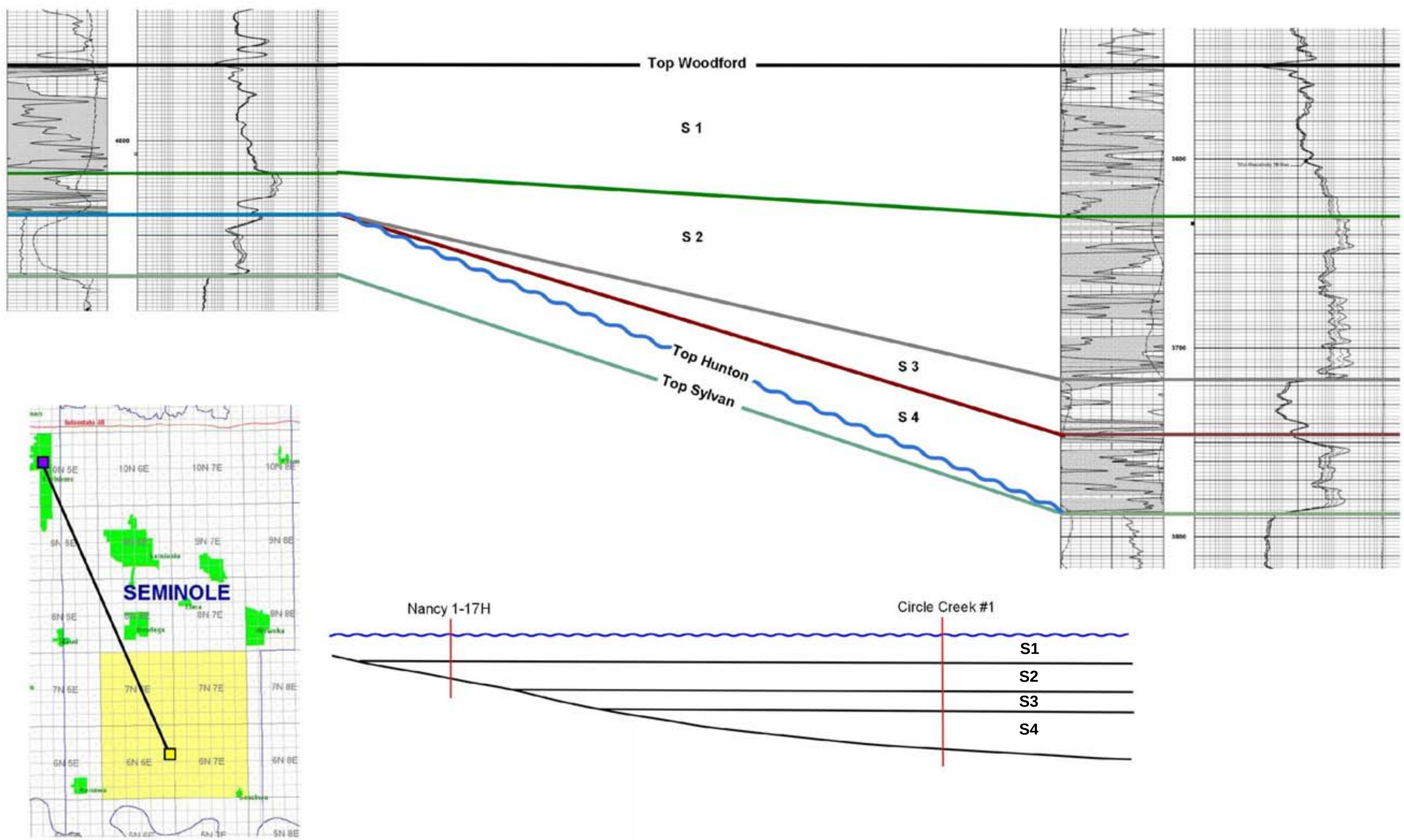

Figure 69. Cross-section illustrating change in Woodford Shale between the Circle Creek #1, located within study area, and the Nancy 1-17H, located ~25 miles to the northwest. Gamma-ray and resistivity signatures support the premise that S1 and S2 are present in both wells and that S3 and S4 were not deposited to the north in the vicinity of the Nancy 1-17H.

Composition

Puckette et al. (2008) as well as Watney et al. (2008) discuss other outcrop and core locations in Oklahoma, which are indicated in Figure 66.

In northeastern Oklahoma, the Late Devonian (Famennian) is represented by the Noel Shale, a Woodford Shale equivalent. The Noel Shale was analyzed by Hurst (2008) and Puckette et al. (2008), who reported that the Noel is a black, fissile shale (Figure 70). It is silty and sandy, lacks radiolarians, and has no evident chert or non-skeletal phosphate. This location is interpreted as an inner shelf. The uranium/thorium (U/Th) ratio ranges from 0-1.0, indicating a major terrestrial influence (Adams and Weaver, 1958).

Figure 70. Photo showing outcrop of the Noel Shale in northeastern Oklahoma (after Puckette et al., 2008)

In southern Oklahoma, on the Lawrence Uplift in Pontotoc County, the Woodford Shale was recently cored in the Kansas Geological Survey (KGS)-Oklahoma Geological Survey (OGS) Current #1 (Section 26, T.3N., R.6E.) (Figure 71). The Current #1 core consists of 284 feet of Woodford Shale that contains bedded silt, burrowing, and phosphate nodules but lacks cherty beds (Watney et al., 2008). The Woodford Shale in this location is a black-gray fissile shale and is interpreted to be a mid-shelf environment. The U/Th ratio ranges from <0.1 to >10, indicating fluctuating source of sediment between marine and terrestrial domination.

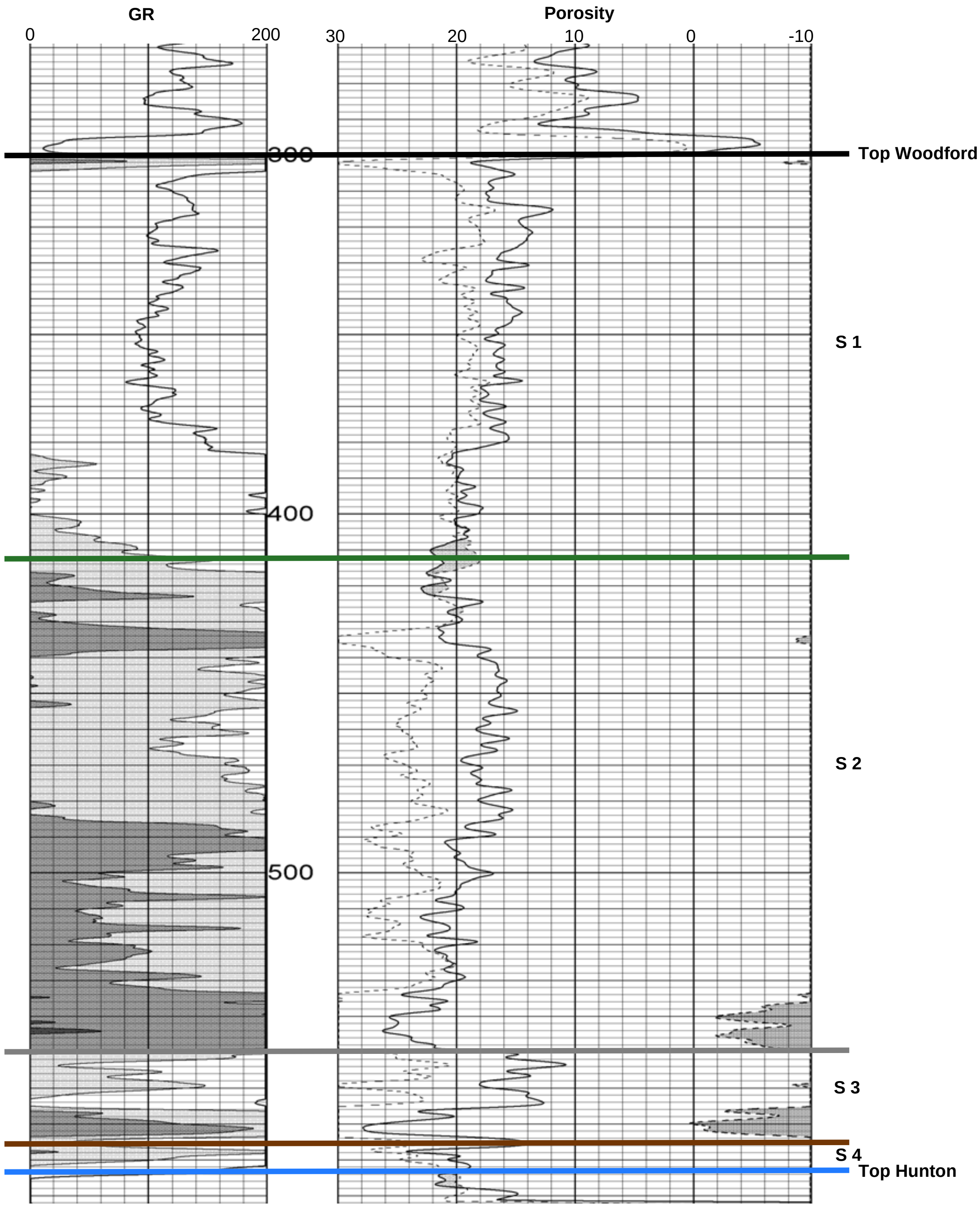

Figure 71. Portion of KGS-OGS, Current #1 well-log (Puckette et al., 2008), with formation tops and subunits labeled

In contrast, the Woodford Shale outcropping on the Arbuckle Mountain (Figure 72) and Criner Hills (Figure 73) uplifts consists of interbedded siliceous cherts and dark fissile laminated shale, and contains abundant radiolarians and common phosphate nodules. These locations are interpreted as a distal shelf/slope with minor terrestrial influence. U/Th ratio ranges from 3 to 22, which shows a strong marine signature for deposition across the entire interval.

Figure 72. Photo showing outcrop location in Arbuckle Mountin Uplift, showing siliceous “cherty” beds with clay rich laminated beds (after Puckette et al., 2008)

Figure 73. Phosphate nodules in a cherty zone toward the top of the Woodford Shale, Criner Hills Uplift (after Puckette et al., 2008)

It is presumed that intervals containing a higher percentage of silt were deposited in shallower water, closer to the sediment source, whereas intervals which are more chert-rich were deposited in deeper water. Chert beds are rich in radiolarian tests that are replaced by chalcedony, microfibrous quartz. Algal debris is also common and believed to have settled out with other organic matter and pelagic forms. Algae and radiolarians likely “bloomed” in phosphate-rich waters associated with the upwelling zone. Radiolarians accumulated in deeper water as siliceous oozes.

Based on the information from northeastern Oklahoma, the Current #1 core, and the Criner Hills and Arbuckle uplifts, it can be concluded that a near shore environment existed in the northeastern part of the state, while a deeper, more distal, environment existed in southern Oklahoma. The Current #1 core in Pontotoc County, may represent a setting proximal to the upwelling zone, as indicated by the presence of phosphate (Over, 1992). However, the Current #1 lacks bedded chert that occurs to the south on the present Arbuckle and Criner Hills uplifts. Based on this observation, it can be inferred that the Woodford Shale in Seminole County is located somewhere between the near shore and distal shelf/slope (Figure 74) and should contain silt, dark shale, possible biotic activity in more oxygenated intervals, and scarce to absent chert and phosphate nodules.

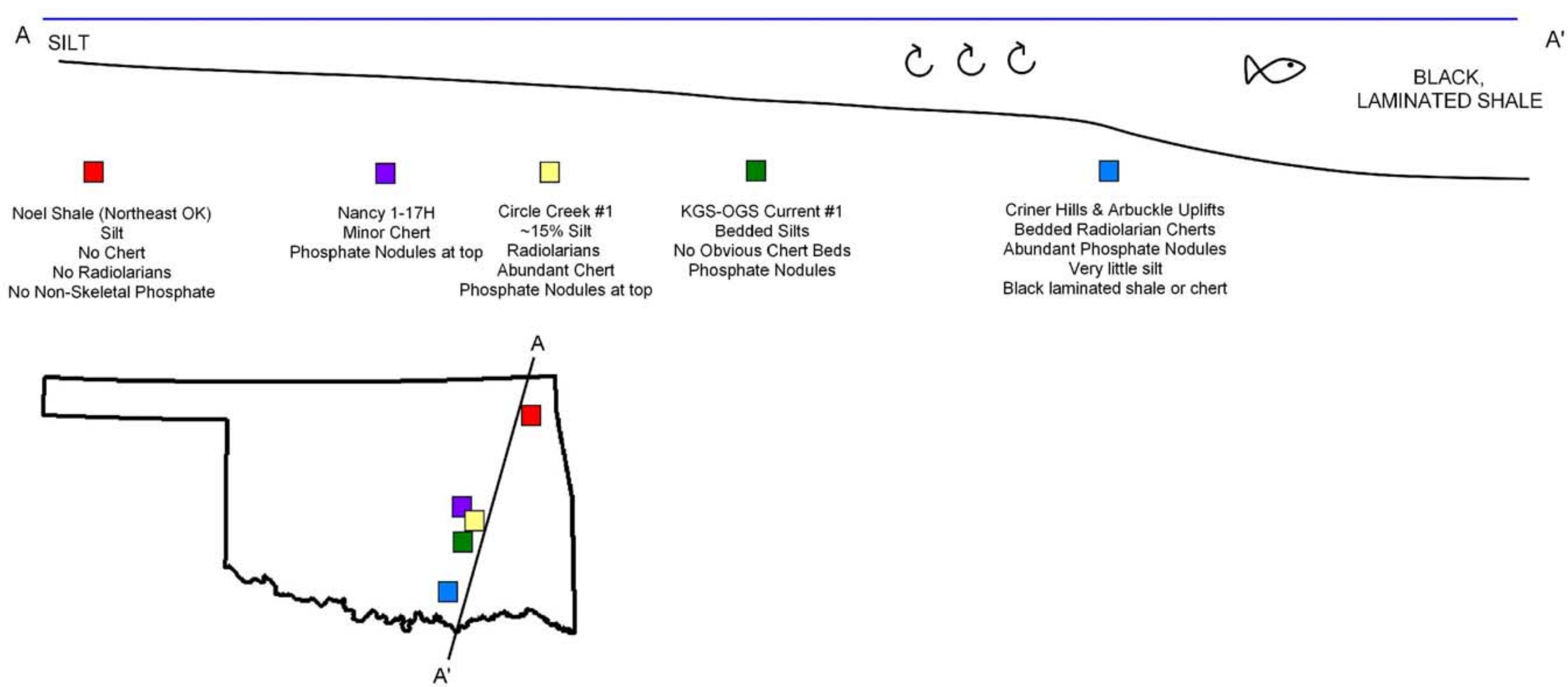

Figure 74. Cross-section A-A' illustrating depositional model for Woodford Shale in Oklahoma (Upper Devonian)

Depositional Model

A comparison of lithology for the Noel Shale in the Ozarks, the Woodford Shale in outcrop in southern Oklahoma, and the cored Woodford Shale in Pottawatomie, Pontotoc, and Seminole Counties reveals the following compositional relationships.

The Noel Shale represents deposition in stratified water, more proximal to the source of sand and silt. According to Hurst (2008) as well as Puckette et al. (2008), the water was occasionally oxygenated as indicated by burrowing and absence of chert or nodular phosphate.

The Woodford Shale in the Arbuckle Mountain and Criner Hills outcrops represent distal, deeper water deposition. The Famennian section is dominated by fissile, dark shale and radiolarian-rich cherts. Large phosphate nodules are abundant near the Famennian-Tournaisian boundary, indicating proximity to the upwelling zone.

The Current #1 core in Pontotoc County contains laminae, bedded and some nodular phosphate, but also contains a silty interval with sparse burrowing. Bedded cherts are absent. The Woodford Shale in the Current #1 core is interpreted as representing a mid-shelf position that was influenced by terrestrial sediments in part during sea-level lowstands, but was close enough to the upwelling zone and deeper water to develop occasional conditions suitable for nodular phosphate precipitation.

The Woodford Shale in the Circle Creek #1 is interpreted to occupy a position similar to that of the Current #1. Phosphate is present as small nodules, but is sparse. Chert is present as thin bands (centimeter scale), but continuous, thicker beds like those that occur in outcrop are not developed. The Nancy 1-17H core represents a mid-shelf setting, but one where paleotopography influenced mud accumulation. The Nancy 1-17H contains sparse phosphate nodules near the top and a few chert laminae.

Figure 74 is a schematic that shows a preliminary interpretation of the depositional setting for the Famennian Woodford Shale. This interpretation is considered preliminary because biostratigraphic constrained boundaries are not established. With this caveat, the following interpretation is proposed:

The Arbuckle Mountain and Criner Hills outcrops contain Woodford Shale as chert in a slope to basinal setting with greater than 300 feet of the formation. The Woodford Shale in the Current #1 core is 284 feet thick, but lacks the thick, bedded cherts and large phosphate nodules of the slope setting. The Woodford Shale in the vicinity of the Current #1 core is interpreted as a mid-slope setting.

The Nancy1-17H (~78 feet of Woodford Shale) and the Circle Creek #1 (~240 feet of Woodford Shale) cores have characteristics similar to the Current #1 core and are also interpreted to be in a mid-shelf setting. The thin Woodford Shale in the Nancy 1-17H appears to be a function of paleotopography.

The Noel Shale is interpreted as representing deposition relatively high on the shelf as it lacks chert and nodular phosphate and is only ~ 30 feet thick.

CHAPTER VI

SUMMARY AND CONCLUSIONS

The purpose of this study was to examine the origin and nature of compositional heterogeneities within the Devonian (Famennian) section of the Woodford Shale, to compare with black shales across the southern Midcontinent region, and to determine any compositional differences. To establish compositional differences, it was necessary to construct an internal stratigraphic framework and subdivide the Woodford Shale into mappable units.

Two basic questions were considered: 1) What does the informal internal electro-stratigraphy utilized by the petroleum industry represent? and 2) What was the depositional setting of the Woodford Shale in southern Seminole County? In an attempt to answer these questions, two hypotheses were developed: 1) distinct wire-line log signatures of the Woodford Shale are the result of compositional heterogeneity, and 2) the Woodford Shale lithofacies in Seminole County are the result of deposition in a mid-shelf setting. This setting is located between the proposed inner shelf setting in the Ozarks (Noel Shale) and the distal shelf/slope of the Arbuckle Region (Puckette et al., 2008).

As a result of the examination of core, wire-line electrical logs, rock data, and the results of previous studies, the following conclusions are reached:

1. The Woodford Shale in southern Seminole County has lithologies and petrophysical characteristics that allow it to be divided into subunits S1, S2, S3, and S4 in descending order.
2. All subunits, and as a result the total Woodford Shale, thin in a northward direction and also in localized areas over thick Hunton Group sections in the southwest corner of the study area.
3. S3 and S4 thin to the north and are absent to the north of the study area.
4. The Woodford Shale in the Circle Creek #1 core is compositionally heterogeneous. The highest percentages of total organic carbon (TOC) occur in S2 and S4. Carbonate is highest in S3.
5. Gamma-ray and U/Th ratios respond to the total organic carbon and non-clay components (silt, chert/chalcedony, and carbonate), and the higher gamma-ray and uranium readings occur in S2 and S4. Lower gamma-ray readings occur in S3.
6. If variability in TOC, uranium and chert are indicators of changes in sea level, a generalized sea-level curve can be constructed for the Woodford Shale interval. Maximum sea level corresponds to the higher uranium and total gamma-ray curves, especially if they accompany cherts and phosphate. Lowering of sea level corresponds to silty, especially burrowed beds and carbonate-rich intervals such as S3.
7. In the context of other outcrops and cores, Southern Seminole County appears to occupy a mid-shelf position between the outer shelf Arbuckle Mountain and Criner Hills outcrops and the inner shelf Noel Shale outcrop in the Ozarks.

Future Work

A biostratigraphic framework would be immensely useful in analyzing compositional differences within chronostratigraphic units of the Woodford Shale. In addition, a comparison of oil and gas production, if established, to subunits could enhance exploration strategies.

REFERENCES

Adams, J.A.S., and C.E. Weaver, 1958, Thorium to uranium ratios as indicators of sedimentary processes: Example of concept of geochemical facies: AAPG Bulletin, v. 42, p. 387-430.

Altenbaumer, P., 1972, The Viola and Sylvan Formations: Paleozoic geology of the Arbuckle Mountains, Oklahoma, p. 17-20.

Amorosi, A., 1995, Glaucony and sequence stratigraphy: a conceptual framework of distribution in siliciclastic sequences: Journal of Sedimentary Research, v. B65, no. 4, p. 419-425.

Amsden, T.W., 1975, Hunton Group (Late Ordovician, Silurian, and early Devonian) in the Anadarko Basin of Oklahoma: Oklahoma Geological Survey Bulletin 121.

Amsden, T.W., 1989, Depositional and post-depositional history of middle Paleozoic (Late Ordovician through Early Devonian) strata in the ancestral Anadarko Basin, *in* Kenneth S. Johnson (ed.), Anadarko Basin Symposium: Oklahoma Geological Survey, Norman, Circular 90, p. 143-146.

Aufill, M.G., 2007, Outcop-based correlation of Magnetic Susceptibility with Spectral Gamma-Ray Spectrometry in the Woodford Shale of South-Central Oklahoma: Oklahoma State University, unpublished M.S. thesis, pp. 210.

Blackford, M.A., 2007, Mapping the Woodford Shale and Assessment of the Woodford Gas-Shale Play in the Arkoma Basin of Southeast Oklahoma: Oklahoma State University, unpublished M.S. thesis, pp. 54.

Blakey, R.C., 2008, Global Paleogeographic Views of Earth History - Late Precambrian to Recent, http://www2.nau.edu/rcb7/namD360.jpg, (accessed February 8, 2008).

Bloxam, T.W., 1964, Uranium, thorium, potassium and carbon in some black shales from the South Wales coalfield: Geochimica et Cosmochimica Acta, v. 28, p.1177-1185.

Bohacs, K.M., and O.R. Lazar, 2008, The role of sequence stratigraphy in unraveling and applying the complex controls from mudstone reservoir properties: AAPG Annual Convention, San Antonio, Texas, April 20-23, 2008.

Bramlett, R.R., 1981, The relationship of hydrocarbon production to fracturing in the Woodford Formation of Southern Oklahoma: Oklahoma State University, unpublished M.S. thesis, pp. 106.

Bunker, B., Witzke, B., Watney, W., and Ludvigson, G., 1988, Phanerozoic history of the midcontinent United States, in L. Sloss, ed., Sedimentary cover—North American craton: the geology of North America, v. D-2: Geological Society of America, p. 243-260.

Busanus, J.W., 1988, The Misener strike-valley sandstone reservoir, Grant and Garfield Counties, Oklahoma: TGS Special Publ. no. 3, pp. 74.

Bustin, A.M., Cui, X., and Bustin R.M., 2008, The influence of matrix diffusion on production rates of gas shales: results from experimental and numerical analyses: AAPG Annual Convention, San Antonio, Texas, April 20-23, 2008.

Cameron, M., Bereskin, S.R., Kieschnick, J., and Suarez-Rivera, R., 2005, Facies architecture and lithologic heterogeneity: a precursor to productivity in the Barnett Shale-Newark East Field, North Central Texas: AAPG Annual Meeting, Calgary, Alberta, June 19-22, 2005.

Cardott, B.J., 2007, Overview of Woodford gas-shale play in Oklahoma: OGS, Woodford Gas Shale Conference, May 23, 2007, PowerPoint presentation, http://www.ogs.ou.edu/pdf/WoodfordOverview.pdf.

Cardott, B.J., 2001, Thermal maturation of the Woodford shale in Eastern Oklahoma: OGS Circular, 106, p.193.

Cardott, B.J., and M.W. Lambert, 1985, Thermal maturation by vitrinite reflectance of Woodford Shale, Anadarko Basin, Oklahoma: AAPG Bulletin, v. 69, no. 11, p. 1982-1998.

Chesapeake Study, 2007: Proprietary.

Comer, J.B., and H.H. Hinch, 1987, Recognizing and quantifying expulsion of oil from the Woodford Formation and age-equivalent rocks in Oklahoma and Arkansas: AAPG Bulletin, v. 71, no. 7, p. 844-858.

Comer, J.B., 2008, Reservoir characteristics and production potential of the Woodford Shale: World Oil Magazine, v. 229, no. 8.

Cruse, A.M., Paxton, S.T., and Aufill, M.G., 2006, Uranium diffusion into the proto-Woodford Shale: Geological Society of America, Annual Meeting, October 22-25, 2006.

Dennis, N.L.F., 2004, The Woodford Shale in portions of Logan County, Oklahoma: feasibility of defining an algorithm for mapping and exploration: Oklahoma State University, unpublished M.S. thesis, pp. 73.

Dow, W.G., 1974, Application of oil-correlation and source rock data to exploration in Williston basin: AAPG Bulletin, v. 58, p. 1253-1262.

Eissa, M.A., and J.P. Castagna, 2003, Case study: AVO analysis in a high-impedance Atoka Sandstone (Pennsylvanian), North Arkoma Basin, McIntosh County, Oklahoma: The Leading Edge, October 2003, p. 988-997.

Feinstein, S., 1981, Subsidence and thermal history of Southern Oklahoma Aulacogen: implications for petroleum exploration: AAPG Bulletin, v. 65, no. 12, p. 2521-2533.

Fertl, W.H., and G.V. Chilingarian, 1989, Hydrocarbon resource evaluation in the Woodford shale using well logs: Journal of Petroleum Science and Engineering (4), p. 347-357.

Flannery, J., and J. Kraus, 2006, Integrated analysis of the Bakken petroleum system, U.S. Williston Basin: Poster presentation, at AAPG Annual Convention, Houston, Texas, April 10-12, 2006.

Franseen, E.K., Byrnes, A.P., Cansler, J.R., Steinhauff, D.M., and Carr T.R., 2004, The Geology of Kansas, Arbuckle Group: Current Research in Earth Sciences, Bulletin 250, part 2, pp. 43.

Goldstein, J., Newbury, D.E., Echlin, P., Lyman, C.E., Joy, D.C., Lifshin, E., Sawyer, L.C., and Michael J.R., 2003, Scanning Electron Microscopy and X-ray Microanalysis, 3rd ed., New York, Kluwer Academic/Plenum Publishers, 689 p.

Hass, W.H., and J.W. Huddle, 1965, Late Devonian and Early Mississippian age of the Woodford Shale in Oklahoma, as determined from conodonts: U.S. Geological Survey professional paper, p. 125-132.

Heckel, P.H., and B.J. Witzke, 1979, Devonian world paleogeography determined from distribution of carbonates and related lithic palaeoclimatic indicators, *in* M.R. House, C.T. Scrutton, and M.G. Bassett eds., The Devonian system: a Palaeontological Association International Symposium, Special Papers in Palaeontology, no. 23, p. 99-123.

Hein, J.R., and J.T. Parrish, 1987, Distribution of siliceous deposits in space and time, *in* Hein, J.R., ed., Siliceous sedimentary rock-hosted ores and petroleum: New York, Van Nostrand Reinhold, p. 10-57.

Hester, T.C., and J.W. Schmoker, 1987, Formation resistivity as an indicator of oil generation in black shales: AAPG Bulletin, v. 71, no. 8, p. 1007.

Hester, T., Sahl, H., and Schmoker, J., 1988, Cross sections based on gamma-ray, density, and resistivity logs showing stratigraphic units of the Woodford Shale, Anadarko basin, Oklahoma: United States Geological Survey Miscellaneous Field Studies Map 2054, 2 plates.

Hoffman, P., 1974, Aulacogens and their genetic relation to geosynclines, with a proterozoic example from Great Slave Lake, Canada: SEPM Special Publication 19, p. 38-55.

Hurst, D., 2008, Lithology and spectrometry of selected outcrops of the Chattanooga Shale in the Appalachian and Ozark regions of North America: Unpublished M.S. thesis, Oklahoma State University, 160 p.

Johnson, K. S., 1989, Geologic evolution of the Anadarko Basin, *in* Kenneth S. Johnson (ed.), Anadarko Basin Symposium: Oklahoma Geological Survey, Norman, Circular 90, p. 3-12.

Jolly, G.D., 1988, Correlation of the Woodford Formation in South-Central Oklahoma using gamma-ray scintillation measurements of the natural background radiation: Stephen F. Austin State University, unpublished M.S. thesis, pp. 154.

Joshi, S.D., 1991, Horizontal well technology: Tulsa, Oklahoma, Penn Well Publishing Company, 535 p.

King, R.F., 1993, Drilling sideways—a review of horizontal well technology and its domestic application: U.S. Department of Energy, Energy Information Administration report, pp. 30.

Krystyniak, A.M., 2005, Outcrop-based gamma ray characterization of the Woodford Shale of south-central Oklahoma: Oklahoma State University, unpublished M.S. thesis, pp. 149.

Kuykendall, M.D., and R.D. Fritz, 2001, Misener Sandstone of Oklahoma: Search and Discovery Article #10018, pp. 74.

LaFever, J., and L. Helms, 2006, Bakken Formation Reserve Estimates: North Dakota Industrial Commission Press Release, http://www.nd.gov/ndic/ic-press/bakken-form-06.pdf, (accessed February 27, 2008).

Lambert, M.W., 1993, Internal stratigraphy and organic facies of the Devonian-Mississippian Chattanooga (Woodford) Shale in Oklahoma and Kansas, in B.J. Katz and L.M. Pratt, eds., Source rocks in a sequence stratigraphic framework: AAPG Studies in Geology 37, p. 163-176.

Lumsden, D.N., 1985, Secular variation in dolomite abundance in deep marine sediments: Geology, v. 13, no. 11, p. 766-769.

Maughan, T.J., and D. Deming, 2006, Gas occurrence in the Caney Shale, part 1: OCGS Shale Shaker, v. 57, pp. 77-89.

_____, 2006, Gas occurrence in the Caney Shale, part 2, conclusion: OCGS Shale Shaker, v. 57, p. 119-135.

Meissner, F.F., 1978, Petroleum geology of the Bakken Formation, Williston Basin, North Dakota and Montana: Williston Basin Symposium, The Montana Geological Society, 24th Annual Conference, Billings, Montana, p. 159-179.

North Dakota Department of Mineral Resources website, https://www.dmr.nd.gov/, (accessed February 28, 2008).

Over, D.J., and J.E. Barrick, 1990, The Devonian/Carboniferous Boundary in the Woodford Shale, Lawrence Uplift, South-Central Oklahoma: Oklahoma Geological Survey Guidebook, v. 27, p. 63-73.

Over, D.J, 1992, Conodonts and the Devonian-Carboniferous boundary in the upper Woodford Shale, Arbuckle Mountains, South-Central Oklahoma: Journal of Paleontology, v. 66, no. 2, p. 293-311.

_____, 2002, The Frasnian/Famennian boundary in central and eastern United States: Palaeogeography, Palaeoclimatology, Palaeoecology, v. 181, p. 153-169.

Parrish, J.T., 1982, Upwelling and petroleum source beds, with reference to Paleozoic: AAPG Bulletin, v. 66, no. 6, p. 750-774.

PI Dwights PLUS on CD. IHS production data, December 2007.

Puckette, J., Boardman, D.R., and Cemen, I., 2008, Shelf to basin transect of Middle Paleozoic organic-rich shales of North America Mid-continent (Chattanooga, Woodford, Arkansas Novaculite): Oklahoma Geological Survey, Oklahoma Gas Shales Conference, October 22, 2008.

Rechlin, K.J., 2003, Reservoir quality of the Frisco Formation, Hunton Group, Seminole County, Oklahoma: Oklahoma State University, unpublished M.S. thesis, pp. 81.

Roberts, C.T., and R.M. Mitterer, 1992, Laminated black shale-bedded chert cyclicity in the Woodford Formation, Southern Oklahoma: Oklahoma Geological Survey Circular 93, p. 330-336.

Schieber, J. 2001. A Role for Organic Petrology in Integrated Studies of Mudrocks: Examples from Devonian Black Shales of the Eastern US. International Journal of Coal Geology, v. 47, issues 3-4, pp. 171 – 187.

Schieber, J., and G. Baird, 2001, On the origin and significance of pyrite spheres in Devonian black shales of North America: Journal of Sedimentary Research, v. 71, no. 1, p. 155-166.

Schmoker, J.W., and T.C. Hester, 1983, Organic carbon in the Bakken Formation, United States portion of Williston basin: AAPG Bulletin, v. 67, no. 12, p. 2165-2174.

Siy, S.E., 1988, Geochemical and petrographic study of phosphate nodules of the Woodford Shale (Upper Devonian-Lower Mississippian) of Southern Oklahoma. Unpublished Masters Thesis, Texas Tech University, pp. 170.

Siy, S.E., 1993, The Woodford Shale (Upper Devonian-Lower Mississippian) and associated phosphate nodules, South-Central and Southeastern Oklahoma, in D.R. Keller and C.L. Reed, eds., Paleokarst, karst-related diagenesis, reservoir development, and exploration concepts; examples from the Paleozoic section of the southern mid-continent:PBS-SEPM Field Trip Guidebook 93-34, p. 85-98.

Tarr, R.S., 1955, Paleogeologic map at base of Woodford, and Hutnon isopachous map of Oklahoma: AAPG Bulletin, v. 39, no. 9, p. 1851-1858.

United States Geological Survey website, http://www.usgs.gov, (accessed March 2, 2008).

Watney, W.L., Boardman, D., Suneson, N., Puckette, J., Thompson, T., Doveton, J., Franseen, E., Victorine, J., Stadler, K, and Walton, R., 2008, Preliminary high-resolution stratigraphic analysis of the Caney and Woodford Shales in a continuous shallow corehole (KGS-OGS Current #1) from the Lawrence Uplift in Pontotoc County, Oklahoma: Oklahoma Geological Survey, Oklahoma Gas Shales Conference October 22, 2008.

Webster, R.L., 1984, Petroleum source rocks and stratigraphy of the Bakken Formation in North Dakota: Hydrocarbon source rocks of the Greater Rocky Mountain region, Rocky Mountain Association of Geologists, p. 57-81.

Williams, J.A., 1974, Characterization of oil types in Williston basin: AAPG Bulletin, v. 58, p. 1243-1252.

APPENDIX I

INGRAM EXPLORATION, CIRCLE CREEK #1

CORE PHOTOGRAPHS

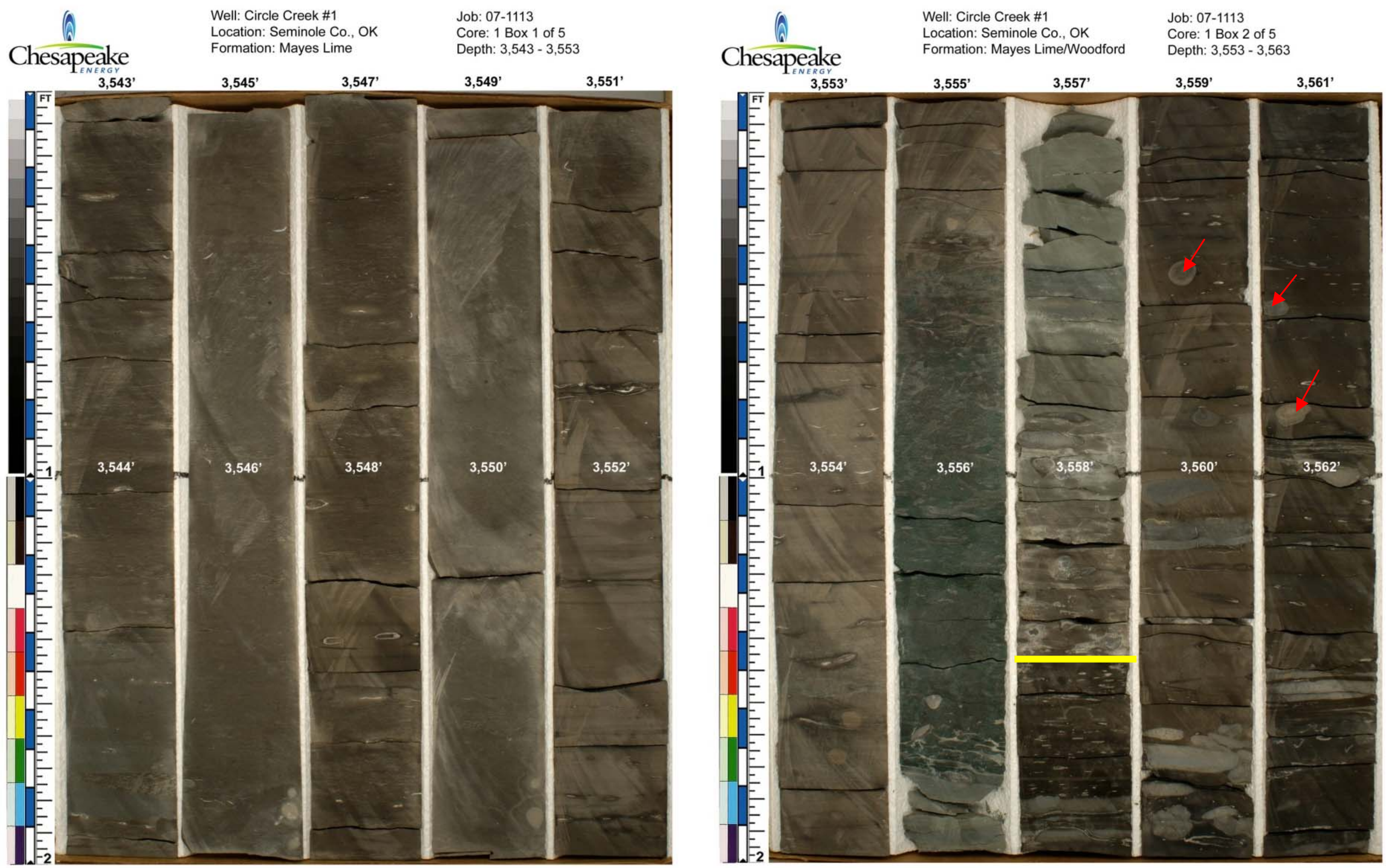

Appendix I. Circle Creek #1 core images: 3,543' – 3,563'
Contact between Woodford Shale and overlying Mayes Formation indicated by yellow line, phosphate nodules indicated by red arrows

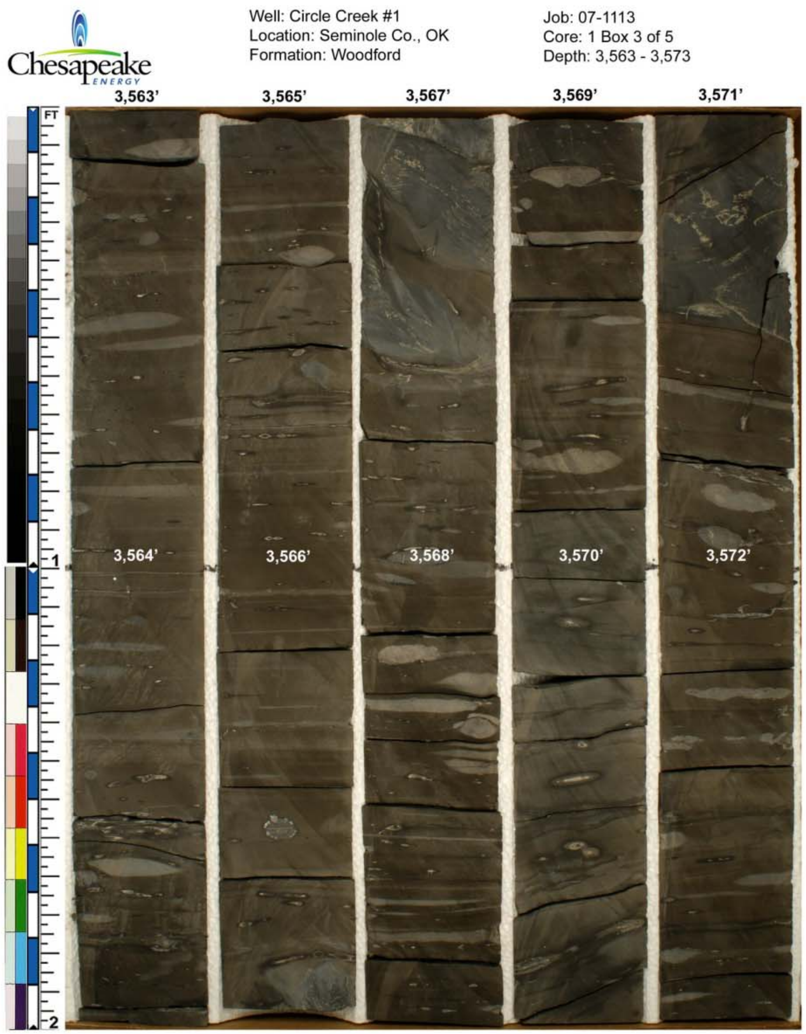

Appendix I. Circle Creek #1 core images: 3,563' – 3,583' (Woodford Shale S1)

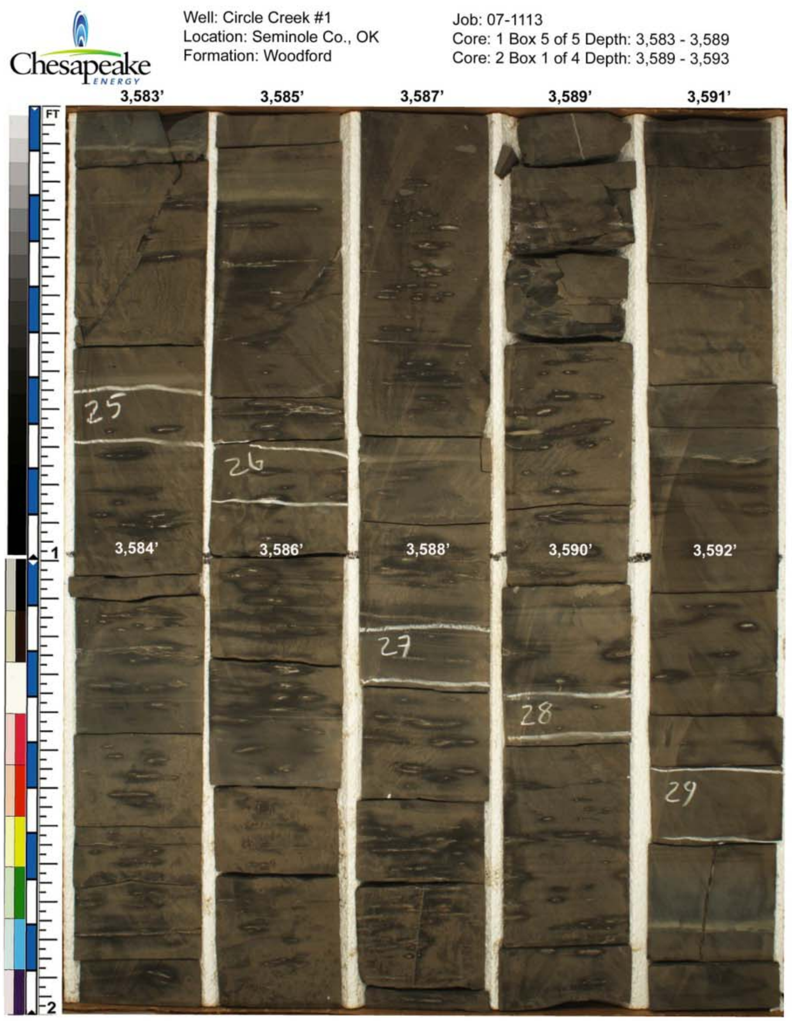

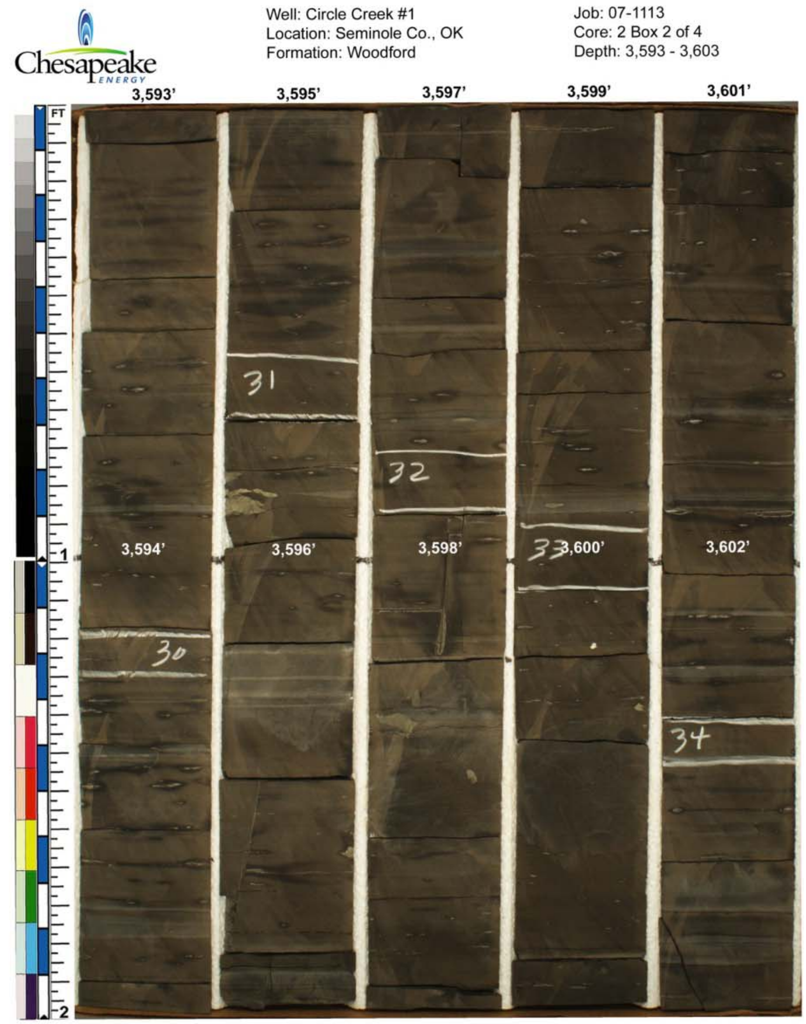

Appendix I. Circle Creek #1 core images: 3,583' – 3,603' (Woodford Shale S1)

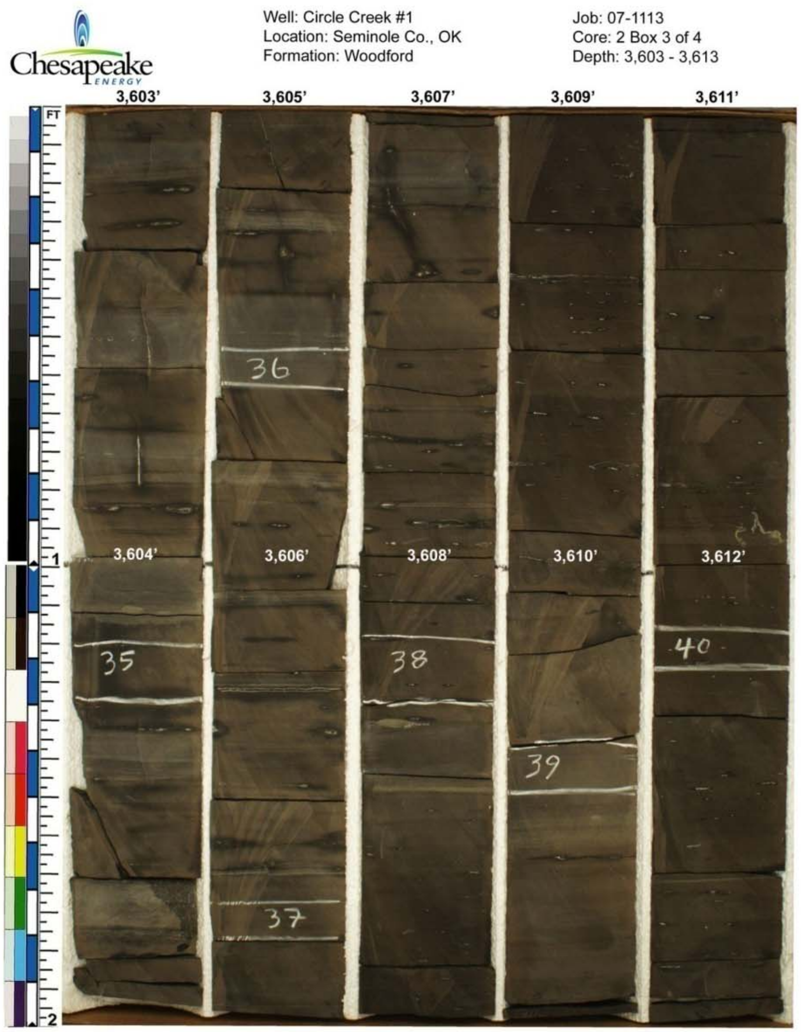

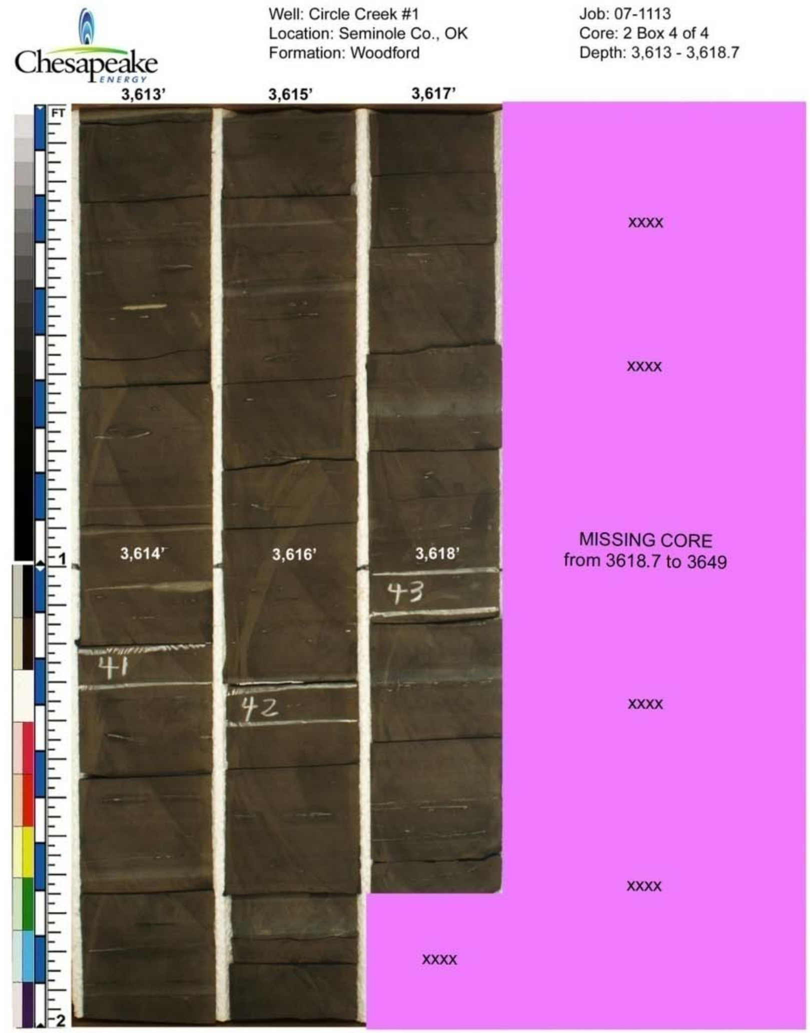

Appendix I. Circle Creek #1 core images: 3,603' – 3,618.7' (Woodford Shale missing core section contains base of S1, top of S2)

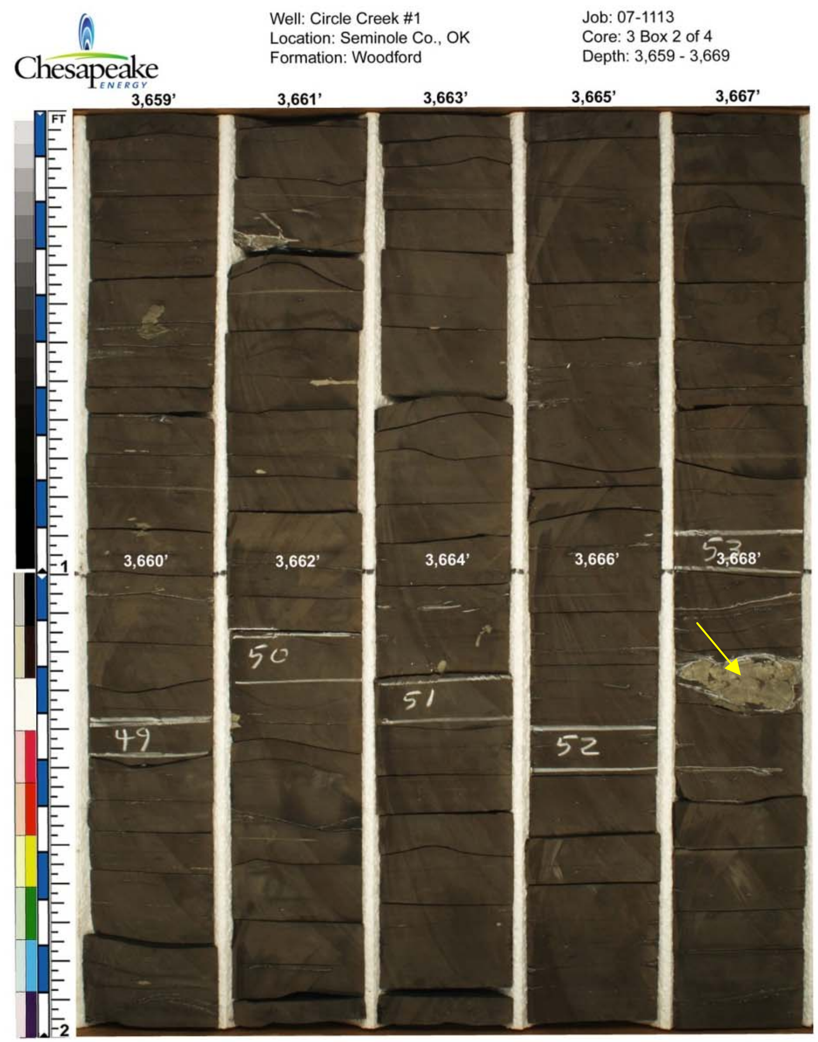

Appendix I. Circle Creek #1 core images: 3,649' – 3,669' (Woodford Shale S2), pyrite indicated by yellow arrow

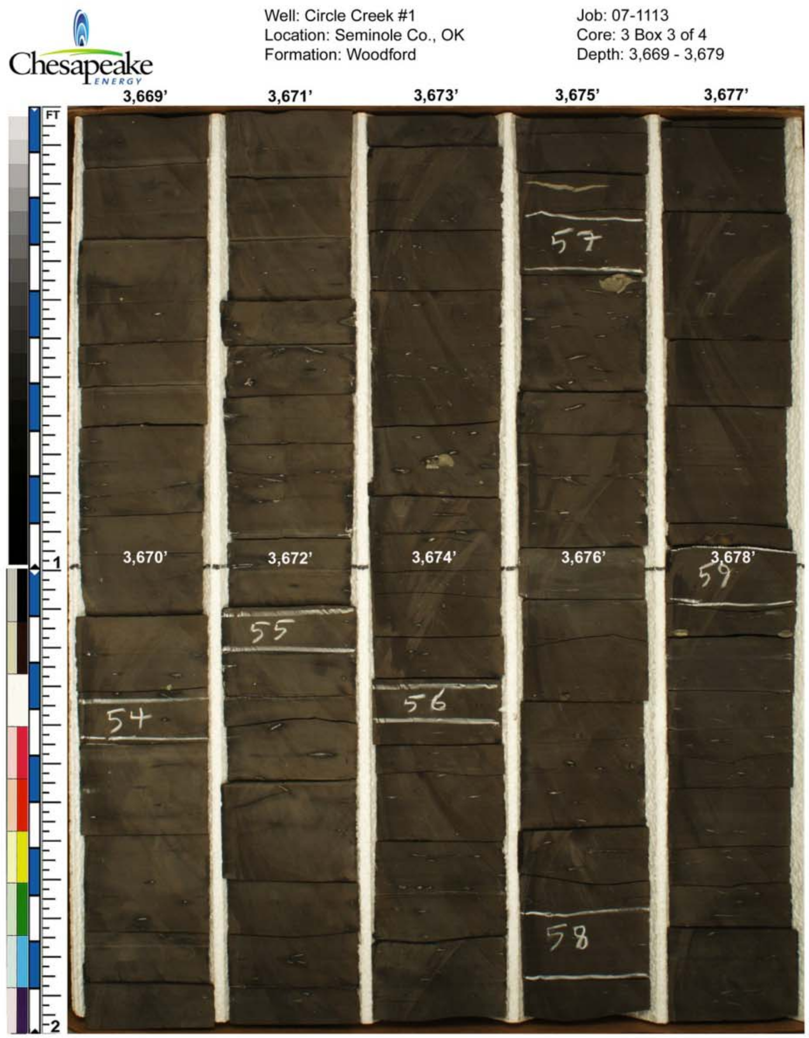

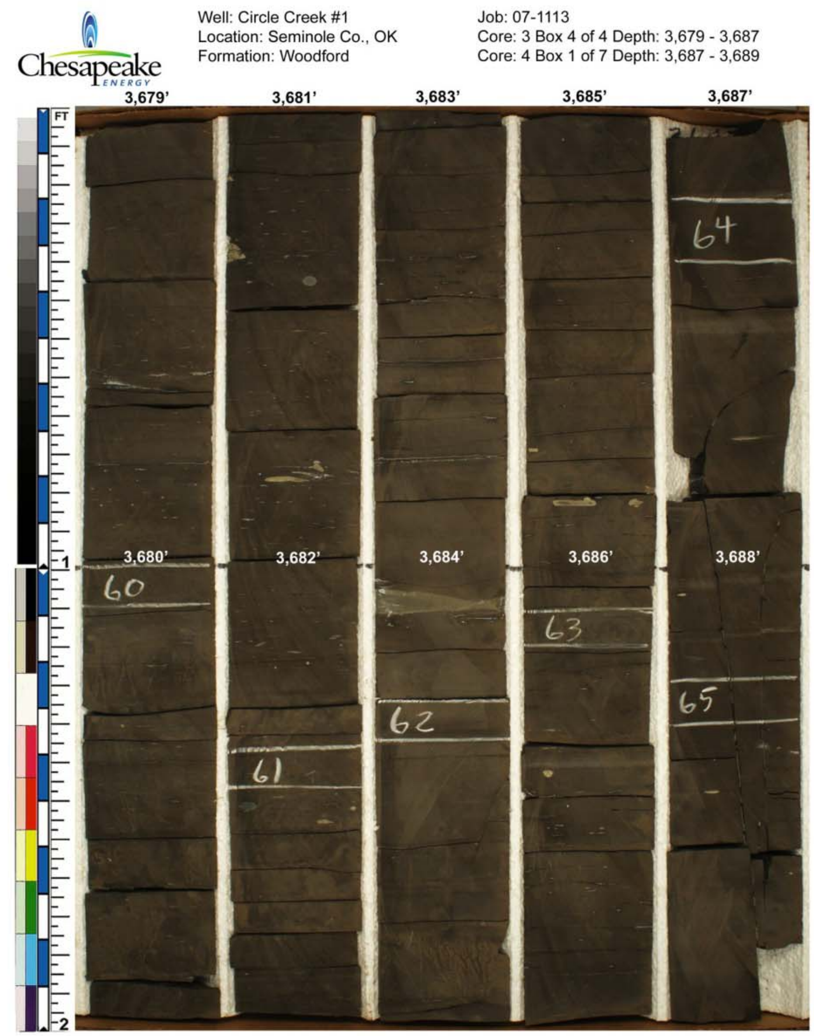

Appendix I. Circle Creek #1 core images: 3,669' – 3,689' (Woodford Shale S2)

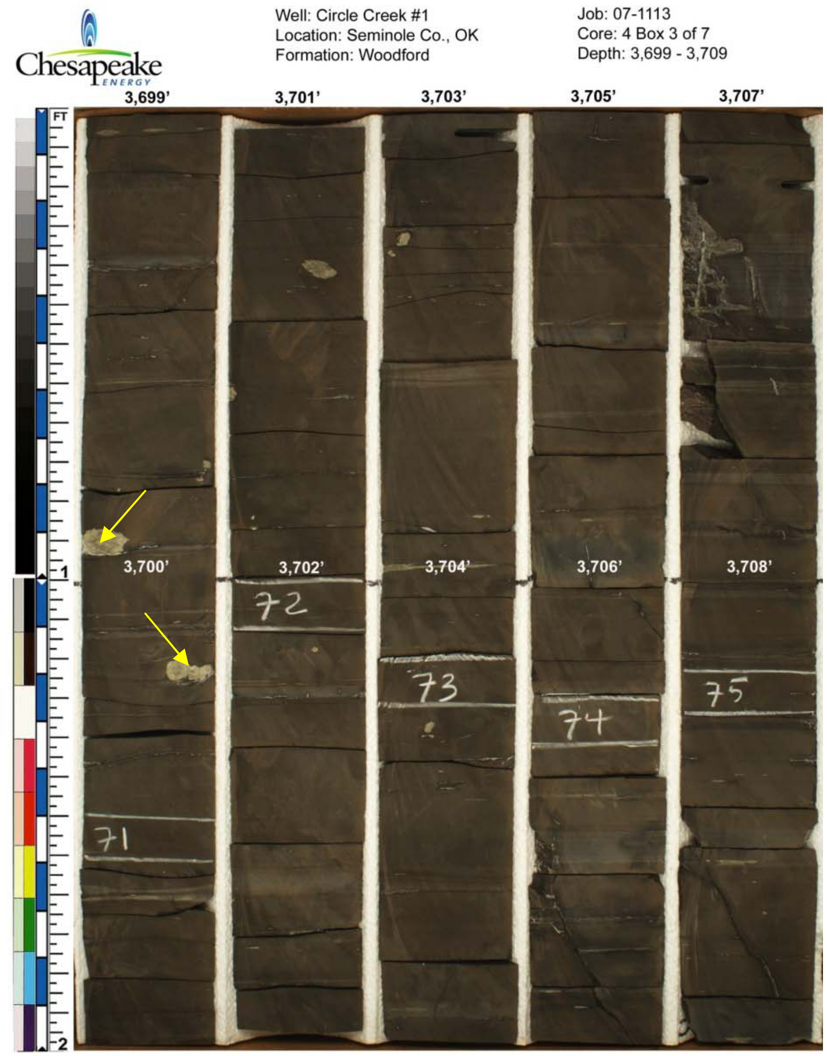

Appendix I. Circle Creek #1 core images: 3,689' – 3,709' (Woodford Shale S2), pyrite nodules indicated by yellow arrows

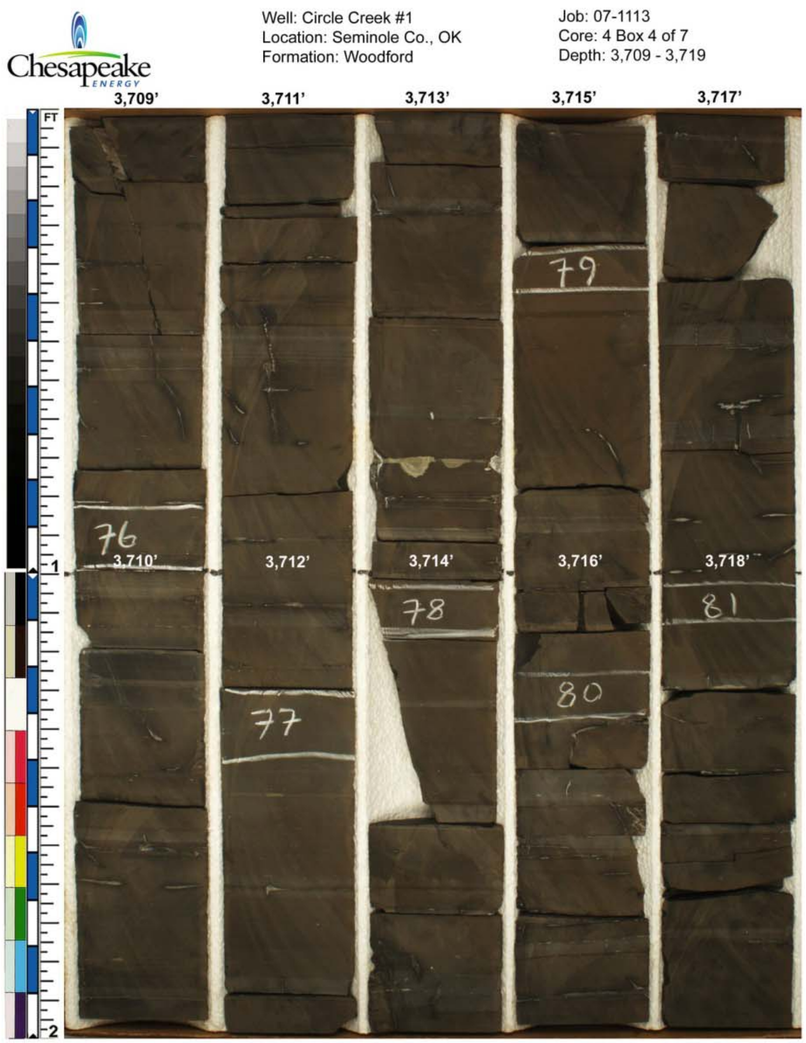

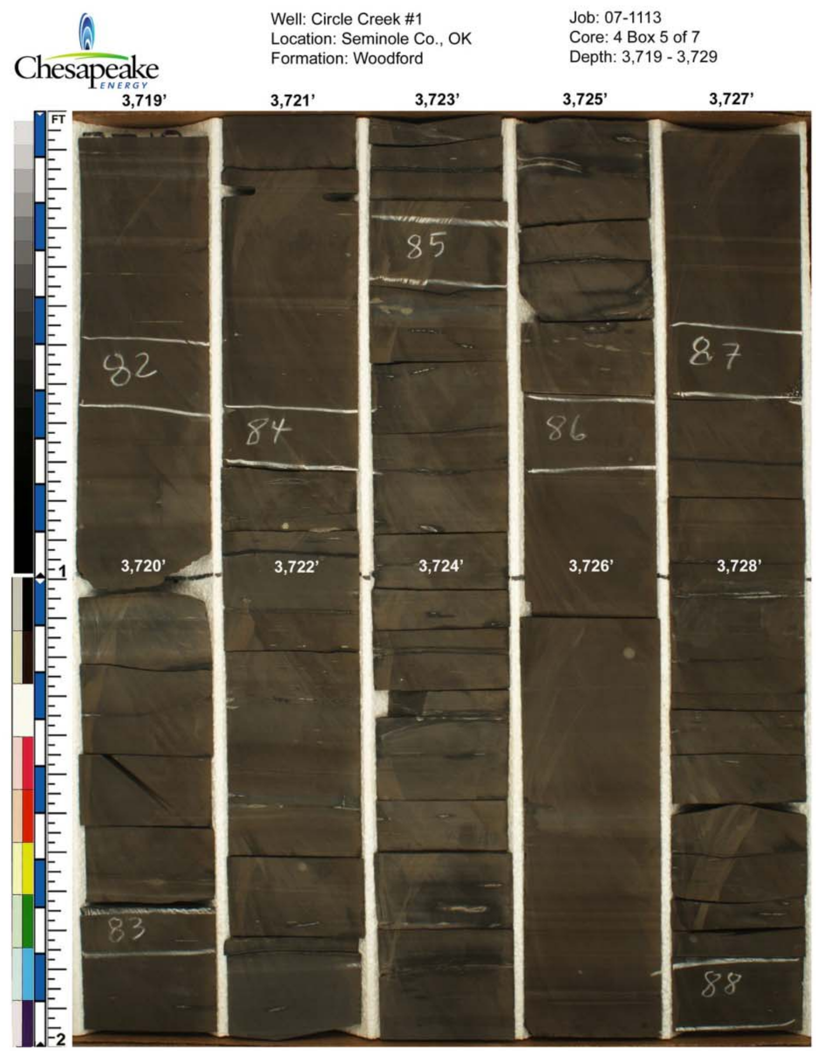

Appendix I. Circle Creek #1 core images: 3,709' – 3,729' (Woodford Shale S2)

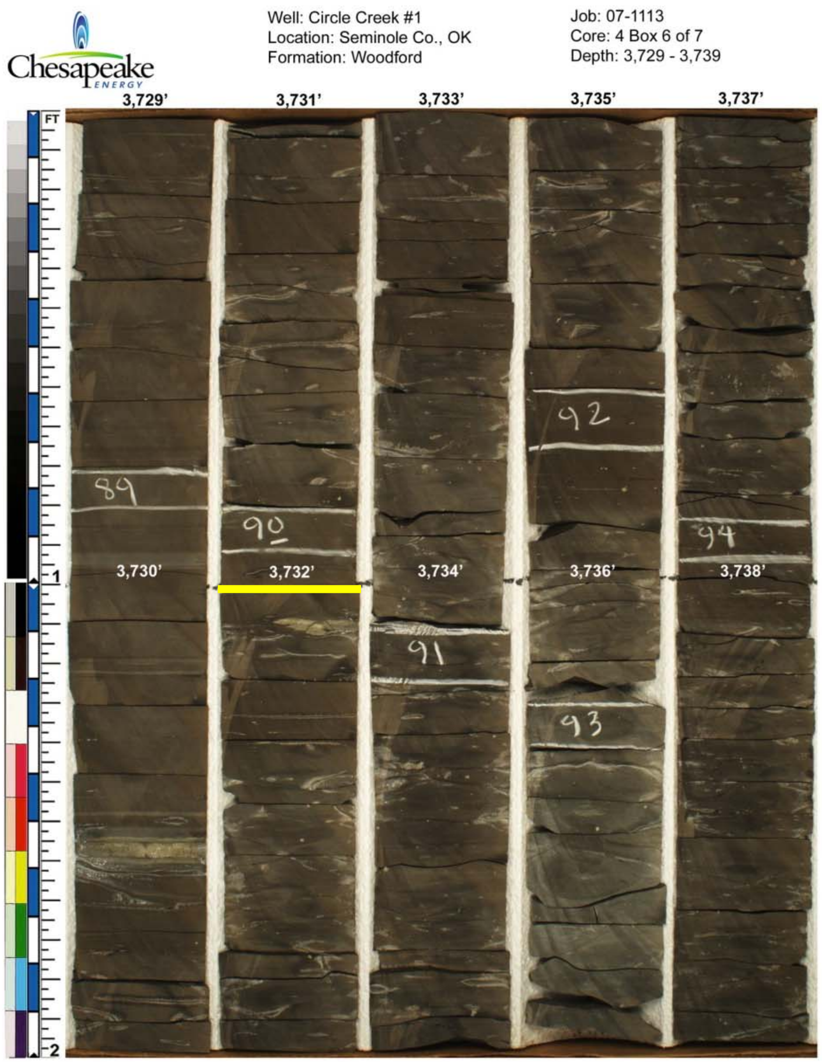

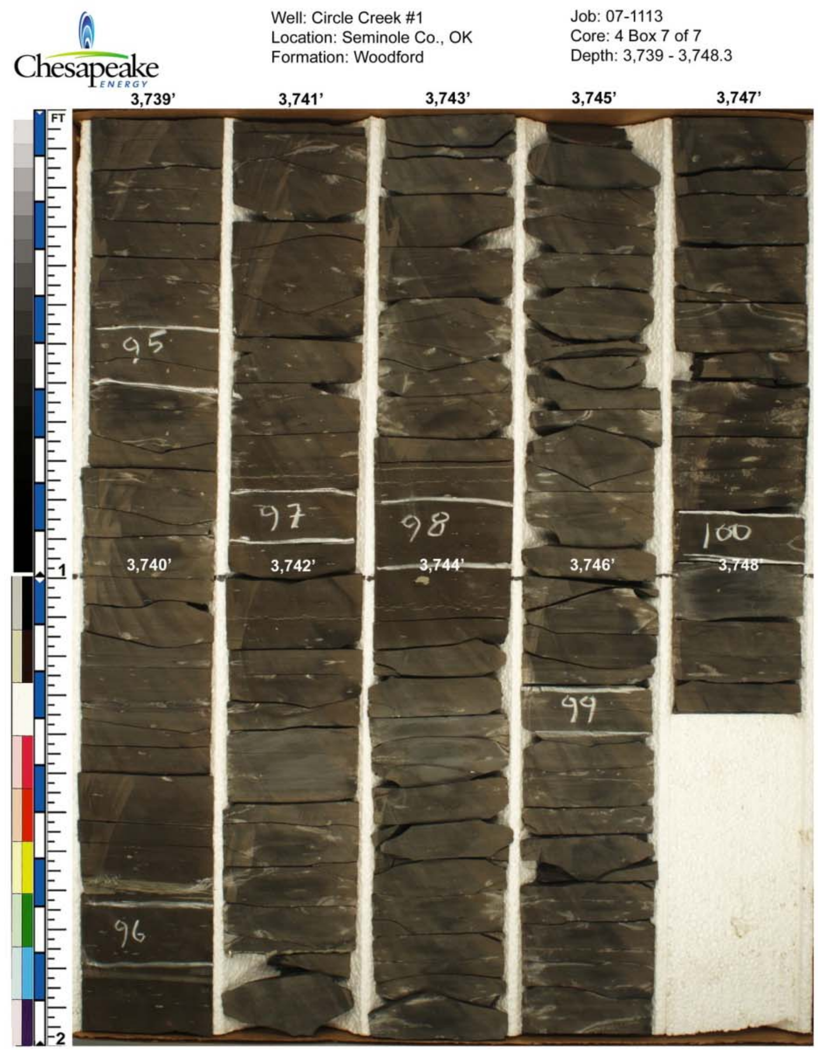

Appendix I. Circle Creek #1 core images: 3,729' – 3,748.3' (contact between Woodford Shale S2 and S3 indicated by yellow line)

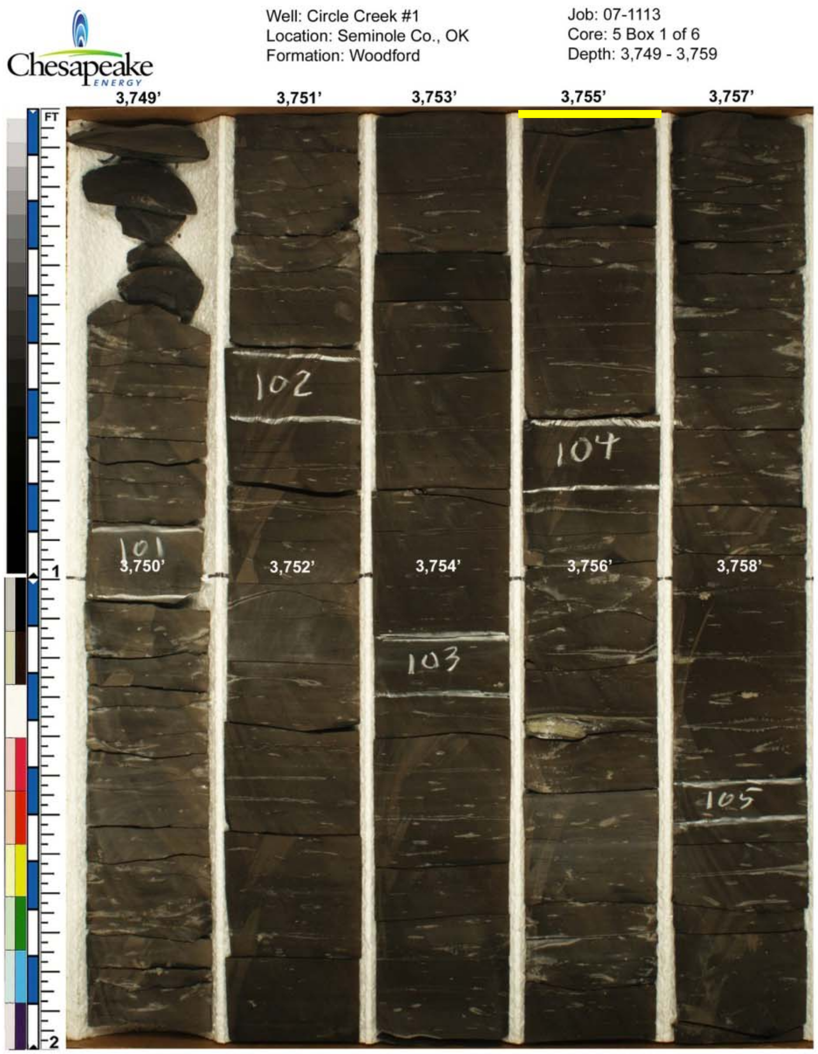

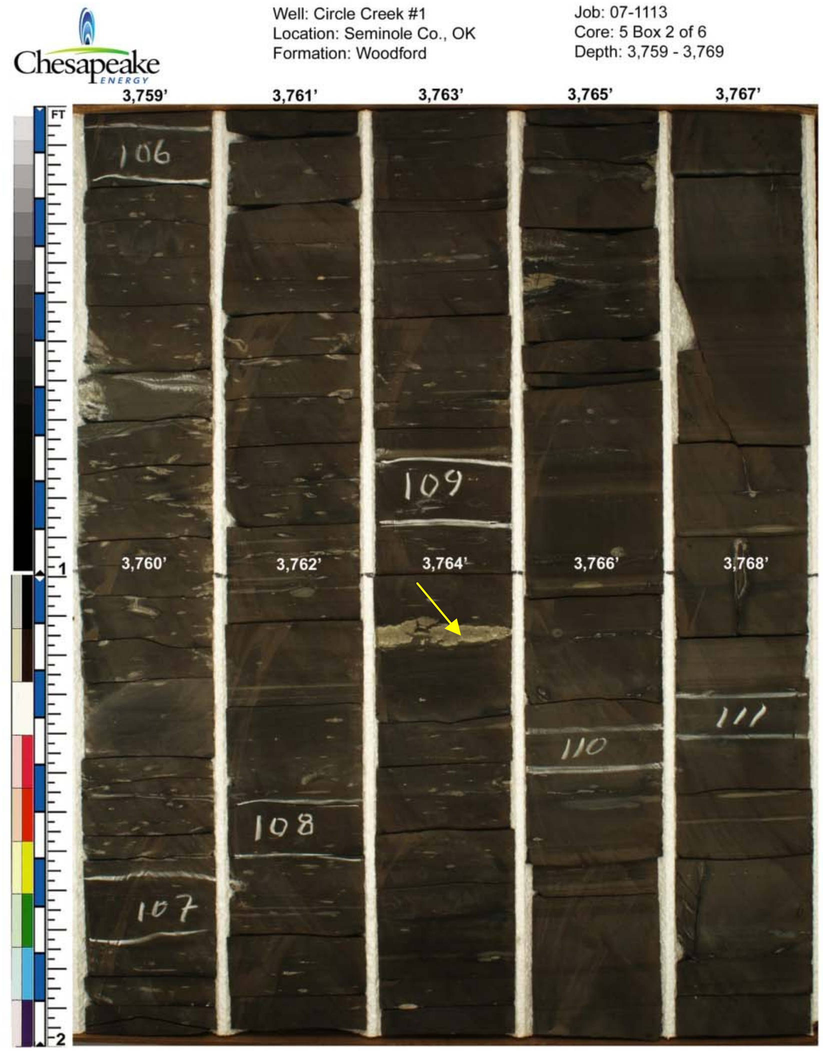

Appendix I. Circle Creek #1 core images: 3,749' – 3,769' (contact between Woodford Shale S3 and S4 indicated by yellow line), pyrite indicated by yellow arrow

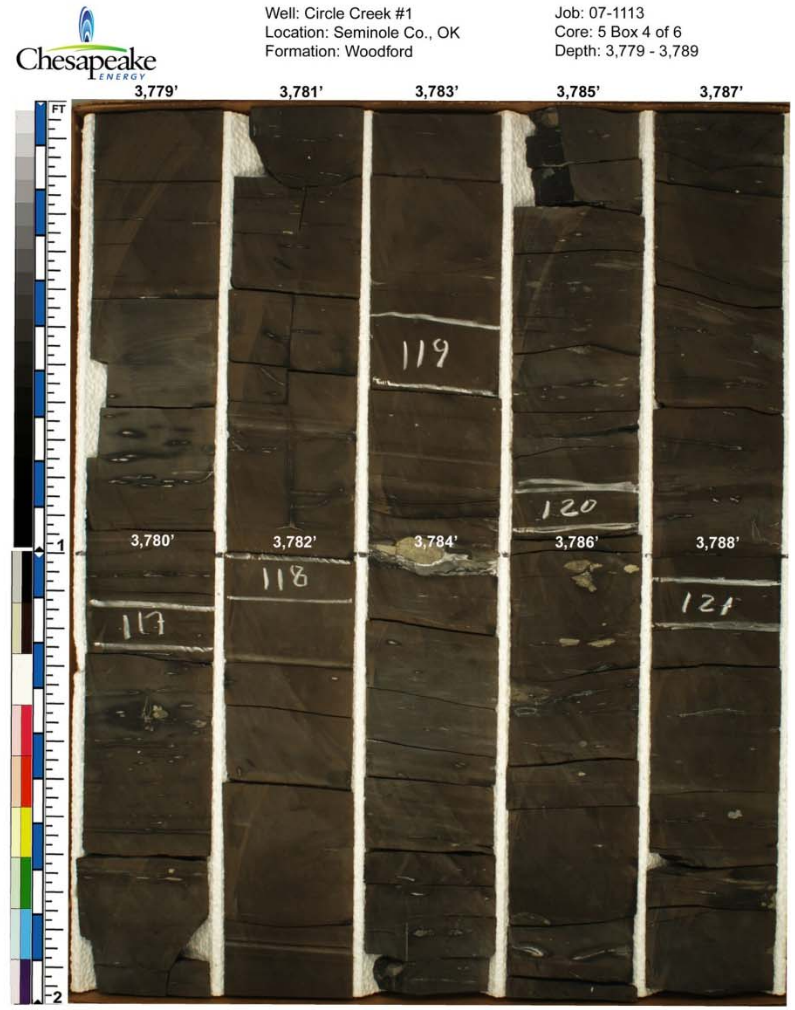

Appendix I. Circle Creek #1 core images: 3,769' – 3,789' (Woodford Shale S4)

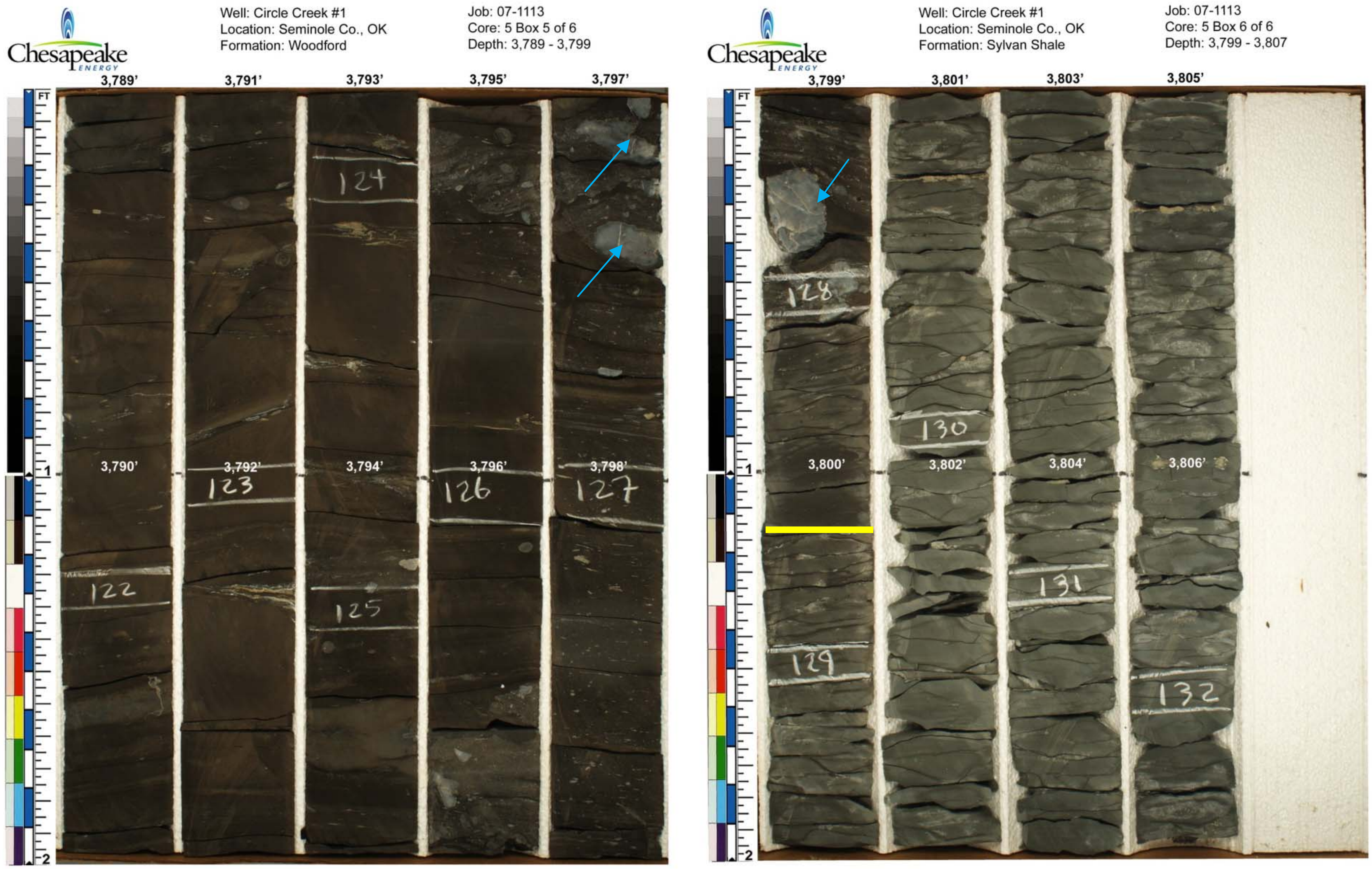

Appendix I. Circle Creek #1 core images: 3,789' – 3,807' (contact between Woodford Shale S4 and underlying Sylvan Shale indicated by yellow line), chert nodules indicated by blue arrows

APPENDIX II

CHESAPEAKE ENERGY, NANCY 1-17H

CORE PHOTOGRAPHS

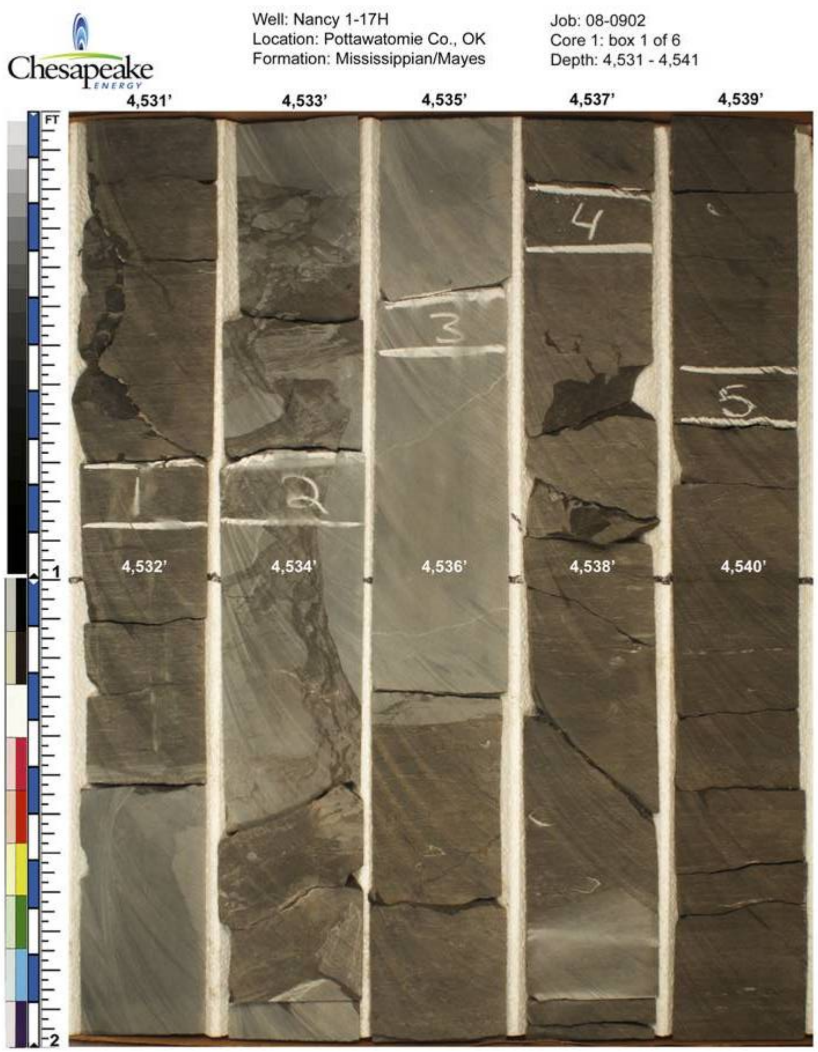

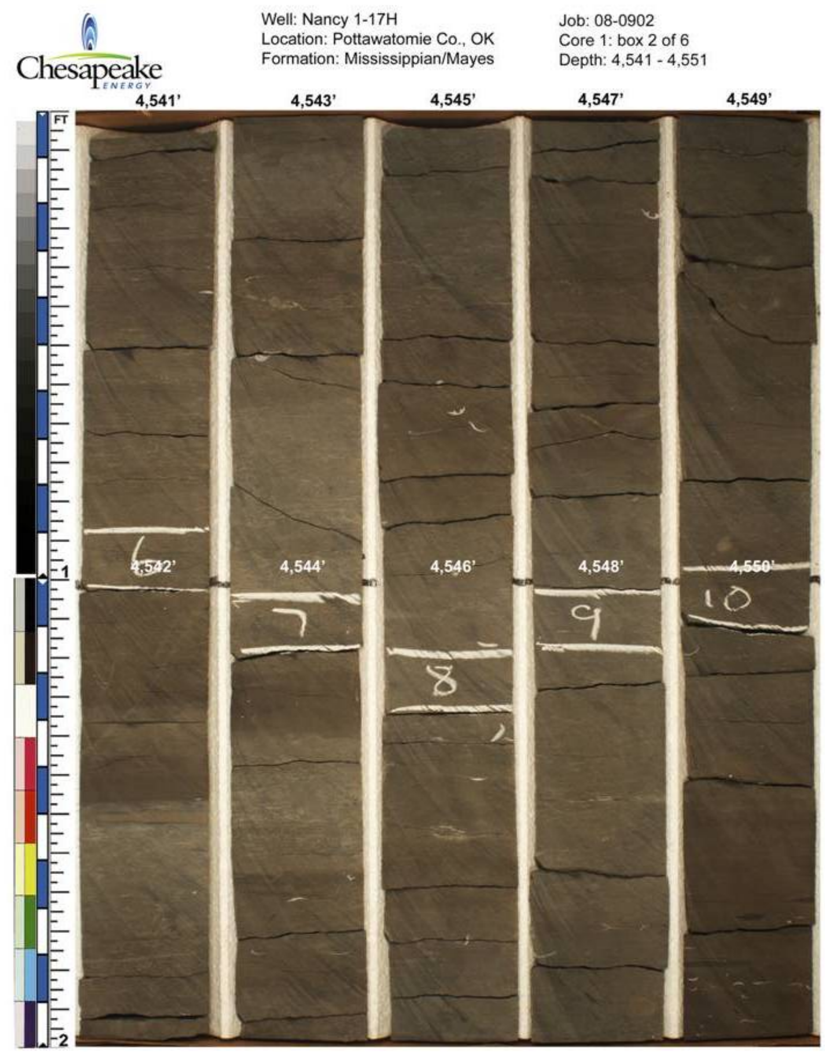

Appendix II. Nancy 1-17 H core images: 4,531' – 4,551' (Mississippian Caney Shale)

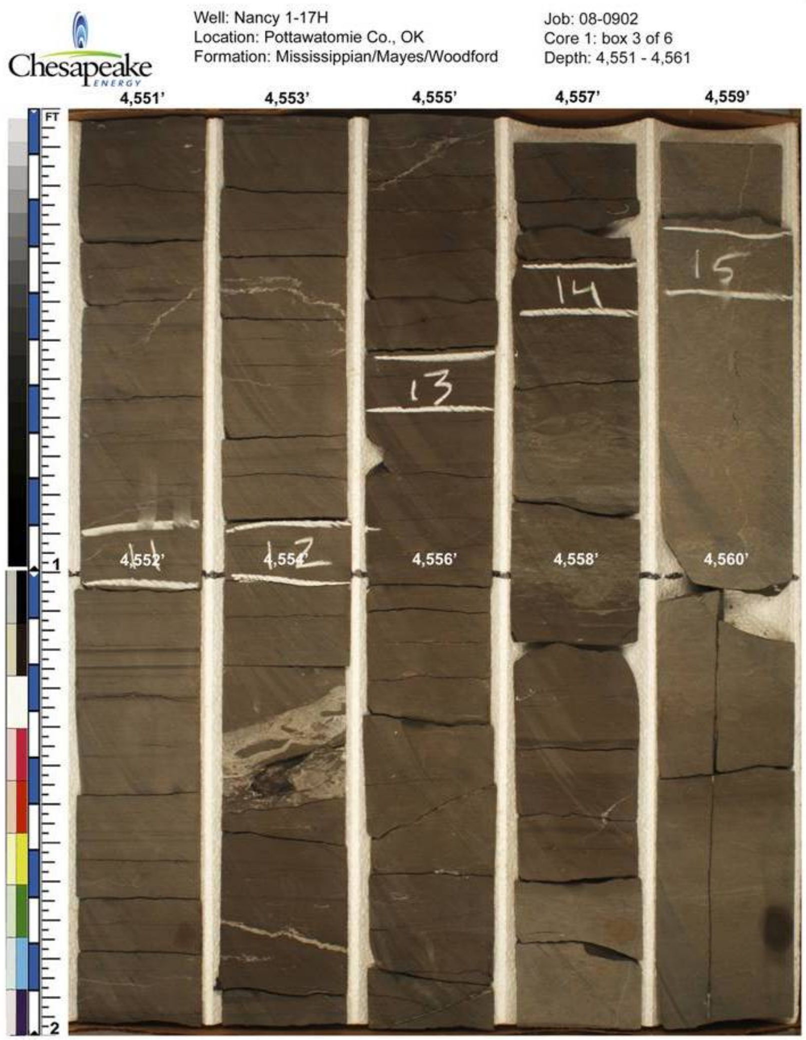

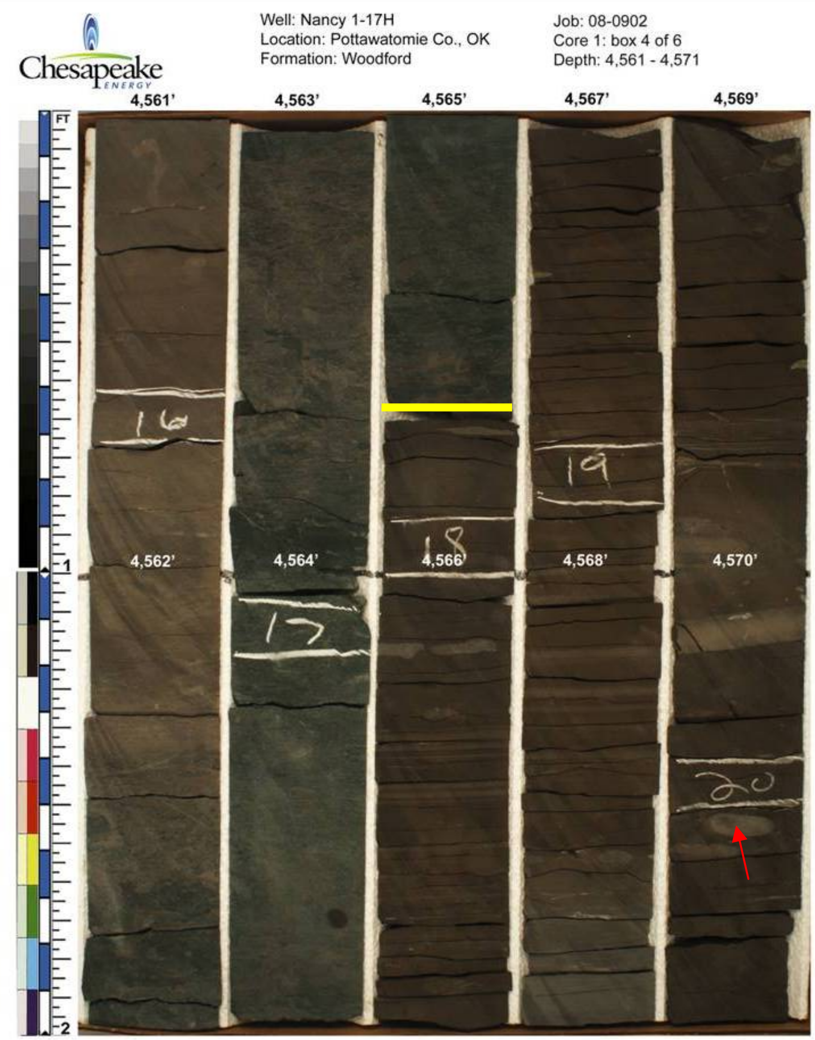

Appendix II. Nancy 1-17 H core images: 4,551' – 4,571' (Caney, Mayes, and Woodford S1)
Contact between Woodford Shale S1 and overlying Mississippian Mayes Limestone indicated by yellow line, phosphate nodule indicated by red arrow

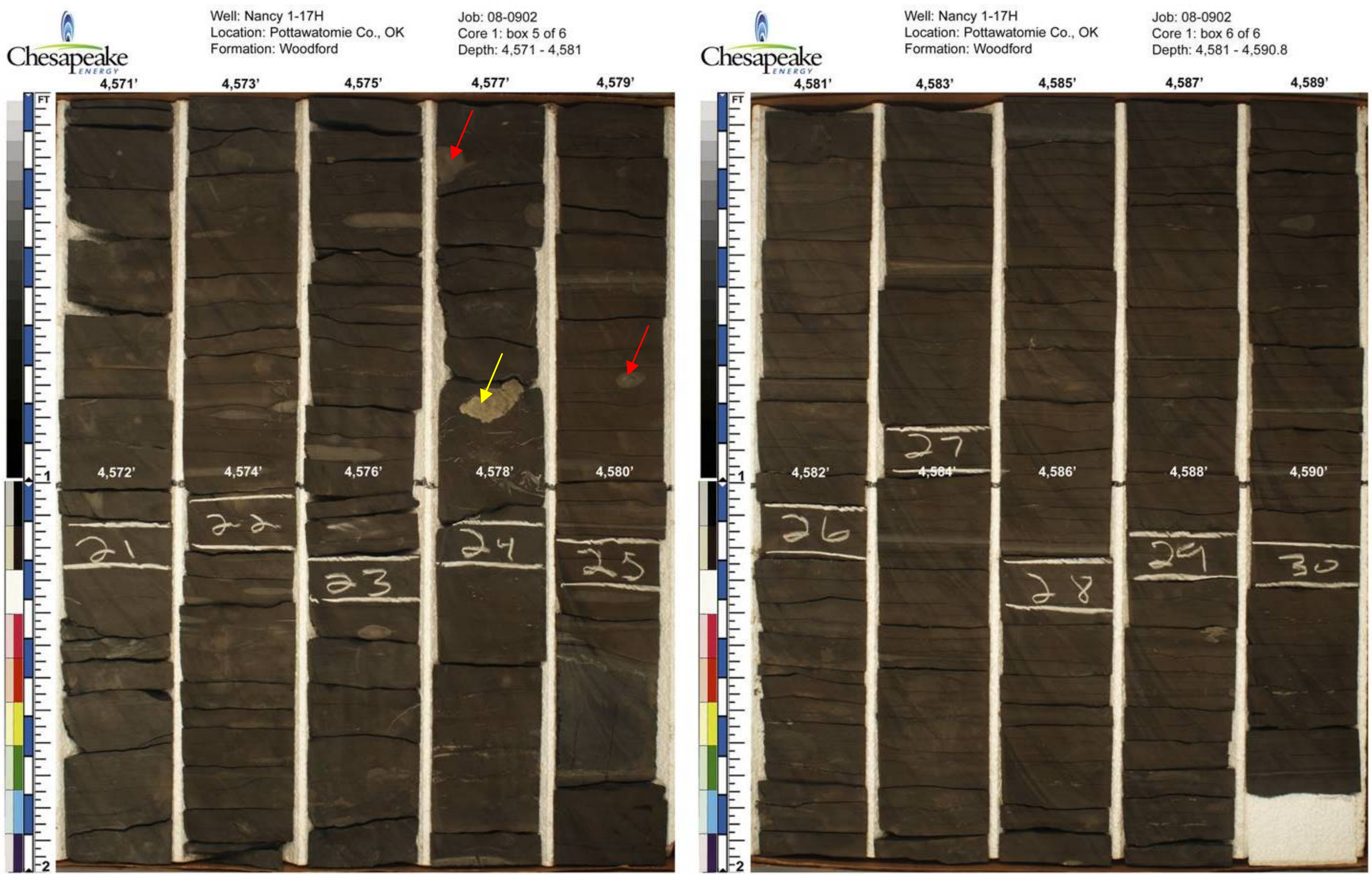

Appendix II. Nancy 1-17 H core images: 4,571' – 4,590.8' (Woodford Shale S1), phosphate nodules indicated by red arrows, pyrite nodules indicated by yellow arrows

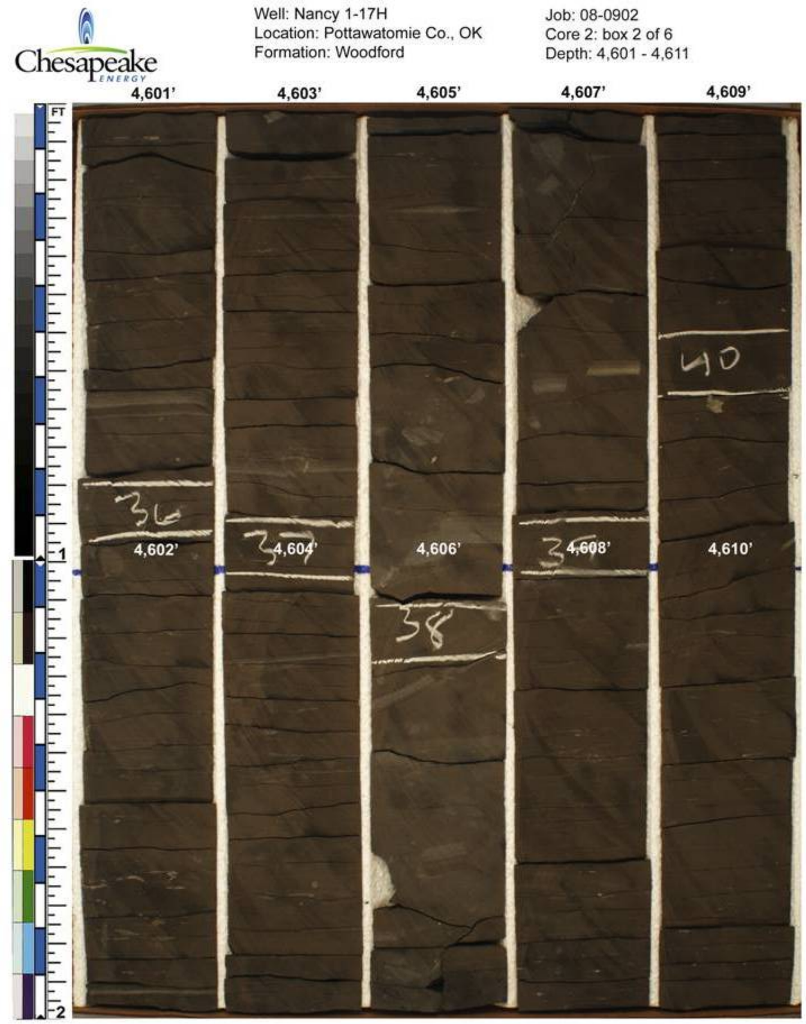

Appendix II. Nancy 1-17 H core images: 4,591' – 4,611' (Woodford Shale S1)

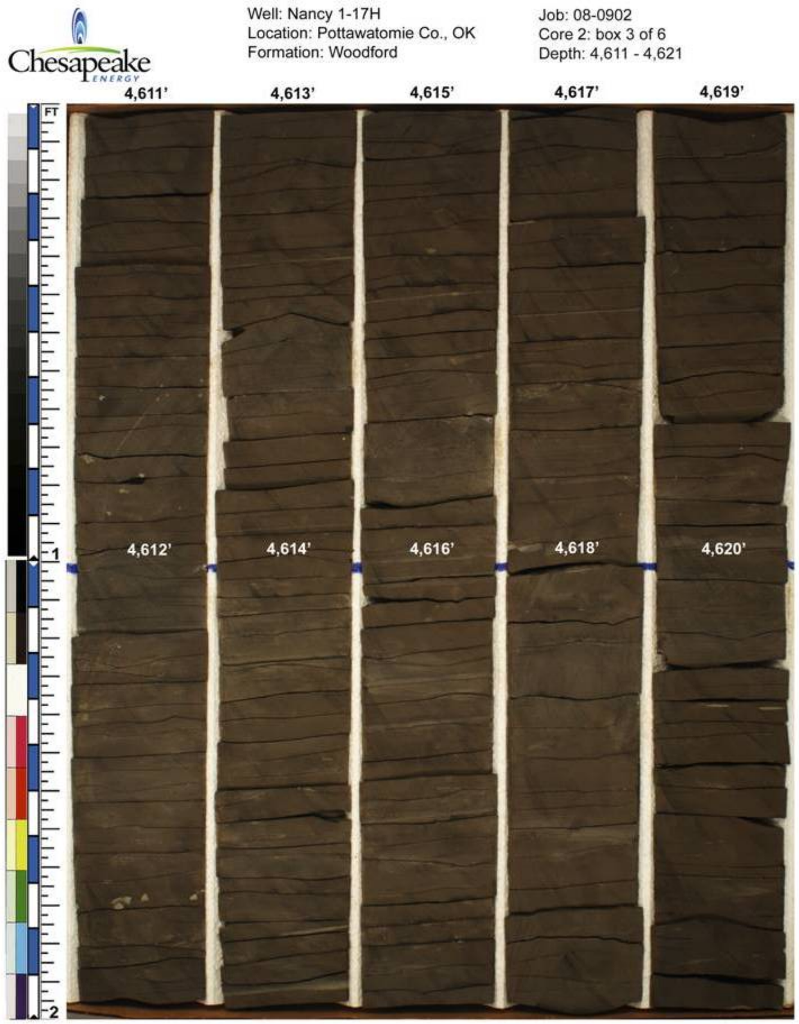

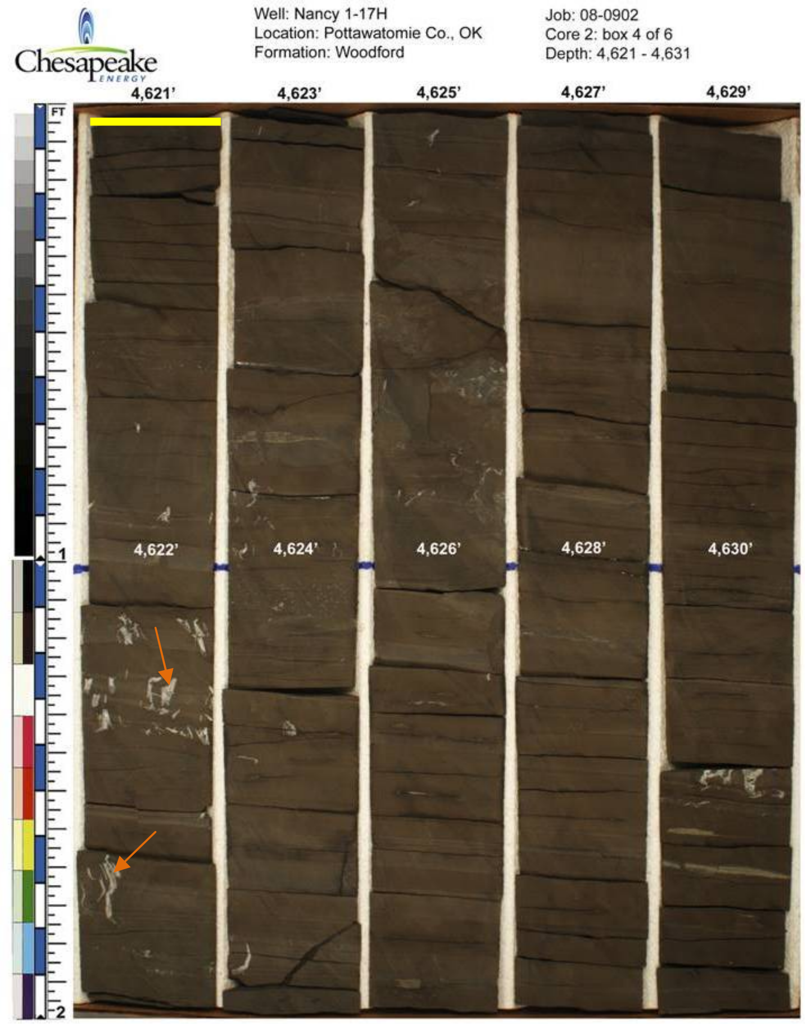

Appendix II. Nancy 1-17 H core images: 4,611' – 4,631' (Woodford Shale, contact between S1 and S2 indicated by yellow line, dissolution features indicated by orange arrows)

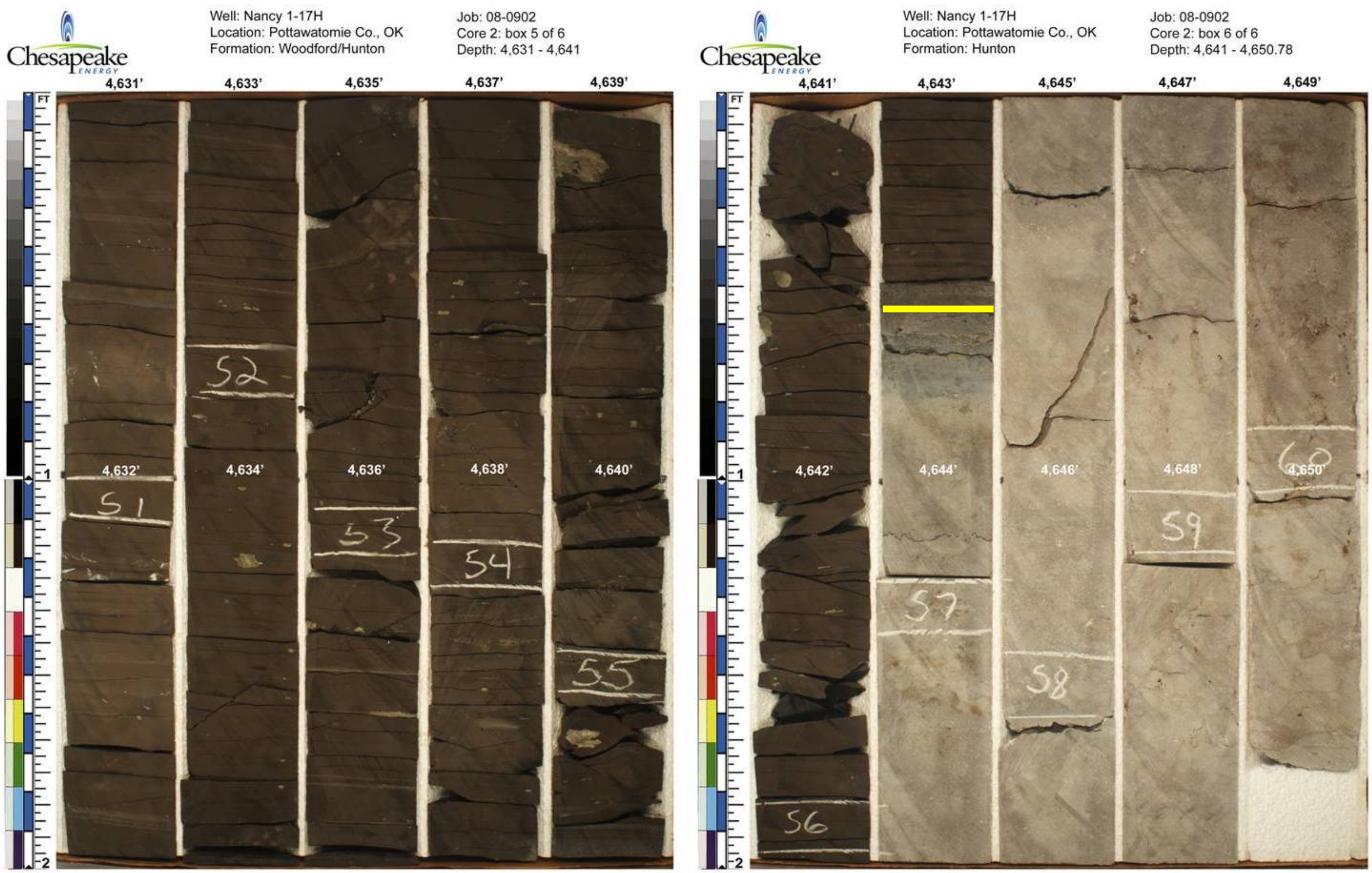

Appendix II. Nancy 1-17 H core images: 4,631' – 4,650.78'
Contact between Woodford Shale S2 and underlying Hunton Group indicated by yellow line

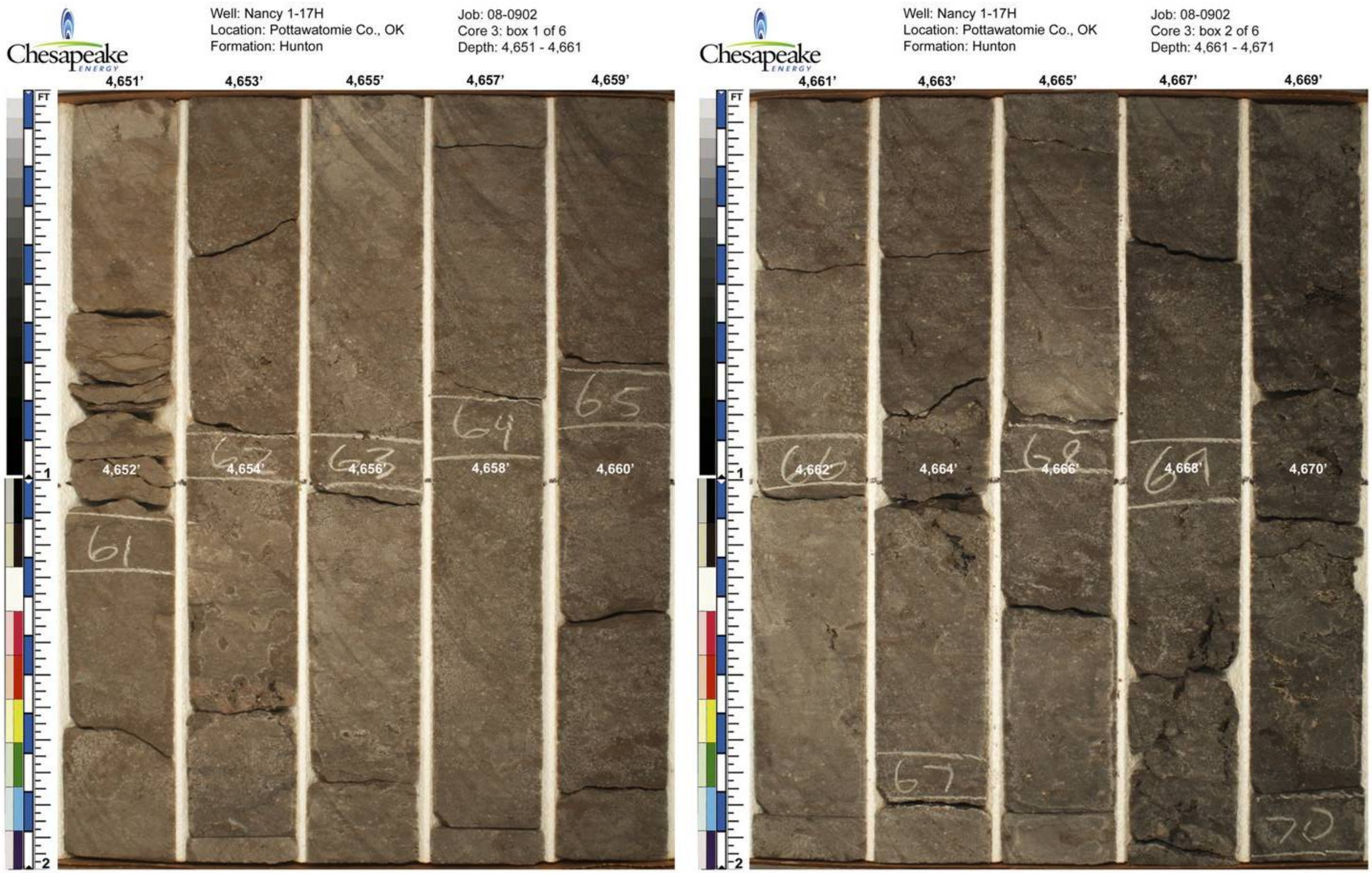

Appendix II. Nancy 1-17 H core images: 4,651' – 4,671' (Hunton Group)

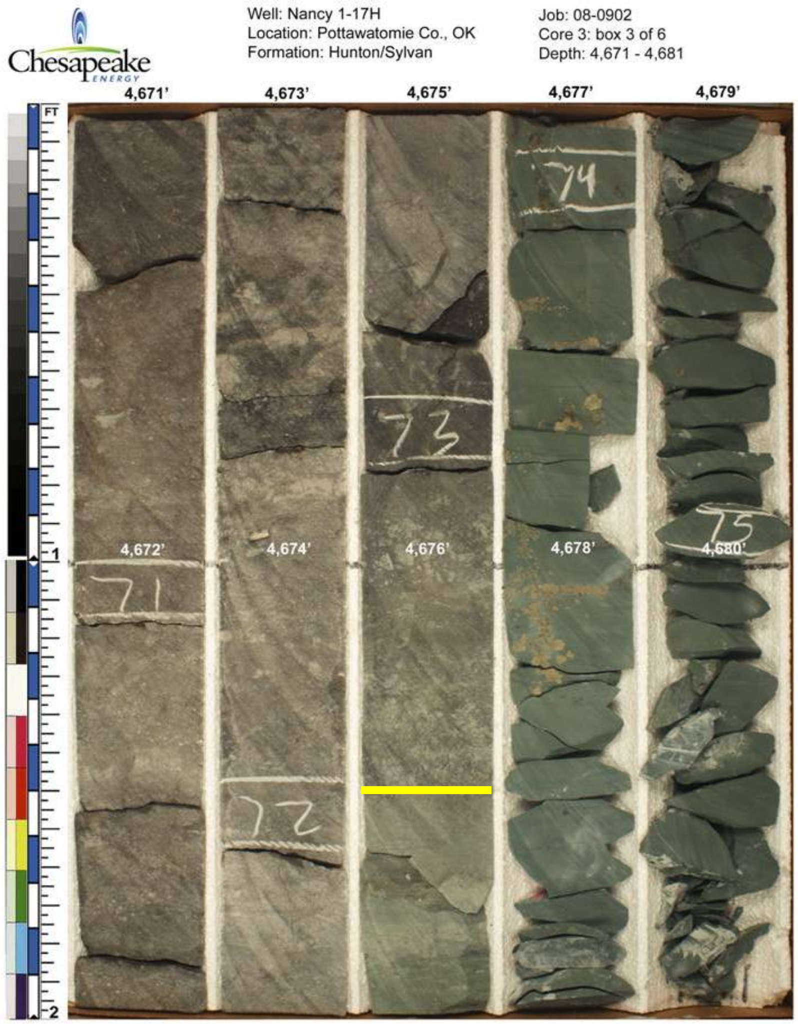

Appendix II. Nancy 1-17 H core images: 4,671' – 4,691'
Contact between Hunton Group and underlying Sylvan Shale indicated by yellow line

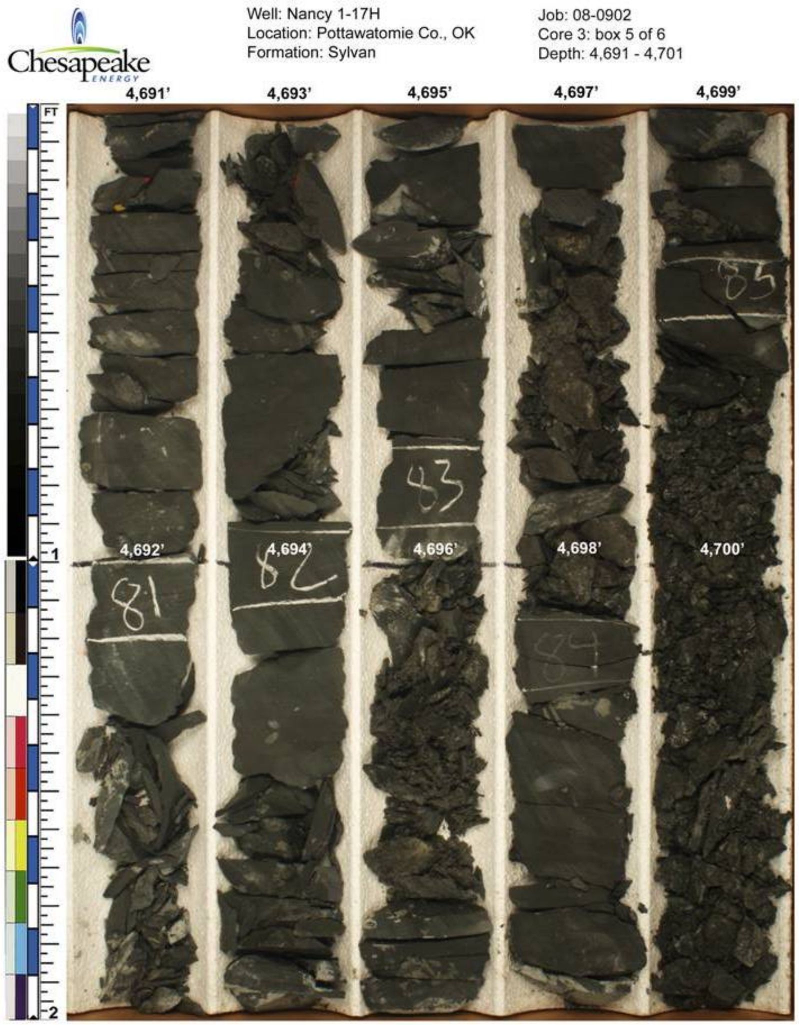

Appendix II. Nancy 1-17 H core images: 4,691' – 4,706' (Sylvan Shale)

VITA

Britni Paige Watson

Candidate for the Degree of

Master of Science

Thesis: INTERNAL STRATIGRAPHY, COMPOSITION, AND DEPOSITIONAL SETTING OF THE WOODFORD SHALE IN SOUTHERN SEMINOLE COUNTY, OKLAHOMA

Major Field: Geology

Biographical:

Personal Data: Born in Tahlequah, Oklahoma, on January 10, 1983, the daughter of John and Linda Higginbotham. Married Robert Lee Watson, III, on October 15, 2005.

Education: Graduated from Hugo High School, Hugo, Oklahoma in May 2001; received Bachelor of Science degree in Geology from Oklahoma State University, Stillwater, Oklahoma, in December 2005. Completed requirements for the Master of Science degree with a major in Geology at Oklahoma State University in December 2008.

Experience: Interned for Chesapeake Energy in Oklahoma City, Oklahoma, May 2007 to present; employed as a teaching assistant for two years by Oklahoma State University, teaching laboratories for introductory geology.

Professional Memberships: American Association of Petroleum Geologists, Society of Exploration Geophysicists

Name: Britni Paige Watson
Date of Degree: December, 2008

Institution: Oklahoma State University
Location: Stillwater, Oklahoma

Title of Study: INTERNAL STRATIGRAPHY, COMPOSITION, AND DEPOSITIONAL SETTING OF THE WOODFORD SHALE IN SOUTHERN SEMINOLE COUNTY, OKLAHOMA

Pages in Study: 141
Candidate for the Degree of Master of Science

Major Field: Geology

Scope and Methods of Study: A core to log analysis was conducted to examine the relationship between lithology and wire-line log characteristics of the Woodford Shale. Shale cores were analyzed to determine if laterally correlative patterns in wire-line log signatures reflected compositional heterogeneity. Cores were described, sampled and analyzed to determine lithofacies and internal composition. Maps were constructed to determine if paleotopography or syndepositional tectonics affected Woodford Shale thickness. The composition of the Woodford Shale in the study area was compared to compositions and interpretations of the shale from studies conducted in the Ozark Uplift of Missouri and Oklahoma, and the Arbuckle Mountains, Lawrence Uplift and Criner Hills Uplift of southern Oklahoma.

Findings and Conclusions: Four (4) laterally correlative subunits were established for the Woodford Shale. These subunits have distinct wire-line log signatures and were traceable across and beyond the study area. Thinning and thickening of the Woodford Shale occurs mostly at the expense of the lower subunits and reflects localized and regional paleotopography. Subunit composition, in particular the relative abundances of silt, chert, TOC and carbonate, may serve as an indicator of sea level. The compositional reflection of sea level was mirrored by changes in spectral gamma-ray measurements. Interpreted zones of relatively high sea level are rich in uranium and have higher U/Th ratios. Intervals interpreted as representing relatively lower sea level are rich in carbonate and silt; consequently these zones have lower uranium and U/Th ratios. A depositional model was developed for the Woodford Shale that places the Woodford Shale in southern Seminole County in a mid-shelf setting between the proposed inner shelf of the Noel Shale in the Ozarks and the distal shelf/slope of the Arbuckle Mountain and Criner Hills Uplifts

ADVISER'S APPROVAL: Dr. Jim Puckette